

# Augmented Reality to Support Helicopter Pilots Hovering in Brownout Conditions

N. V. Meima

28 December 2020



# **Augmented Reality to Support Helicopter Pilots Hovering in Brownout Conditions**

MASTER OF SCIENCE THESIS

For obtaining the degree of Master of Science in Aerospace Engineering  
at Delft University of Technology

N. V. Meima

28 December 2020



**Delft University of Technology**

Copyright © N. V. Meima  
All rights reserved.

DELFT UNIVERSITY OF TECHNOLOGY  
DEPARTMENT OF  
CONTROL AND SIMULATION

The undersigned hereby certify that they have read and recommend to the Faculty of Aerospace Engineering for acceptance a thesis entitled “**Augmented Reality to Support Helicopter Pilots Hovering in Brownout Conditions**” by **N. V. Meima** in partial fulfillment of the requirements for the degree of **Master of Science**.

Dated: 28 December 2020

Readers:

---

dr.ir. C. Borst

---

prof.dr.ir. M. Mulder

---

D. Friesen, MSc.

---

dr. O. A. Sharpanskykh



---

# Acronyms

<b>ADS-33</b>	Aeronautical Design Standard 33E-PRF
<b>AR</b>	augmented reality
<b>BOSS</b>	BrownOut Symbology System
<b>DeViLA</b>	Degraded Vision Landing Aid
<b>DLR</b>	Deutsches Zentrum für Luft- und Raumfahrt
<b>DUECA</b>	Delft University Environment for Communication and Activation
<b>DVE</b>	degraded visual environments
<b>EFIS</b>	electronic flight instrument system
<b>FAA</b>	Federal Aviation Agency
<b>FOV</b>	field of view
<b>FPM</b>	flight path marker
<b>GOFR</b>	global optical flow rate
<b>GVE</b>	good visual environments
<b>HDD</b>	head-down display
<b>HMD</b>	helmet-mounted display
<b>HUD</b>	head-up display
<b>ICE</b>	Integrated Cueing Environment
<b>IGE</b>	in ground effect
<b>LIDAR</b>	laser detection and ranging
<b>MTE</b>	mission task element
<b>OGE</b>	out of ground effect
<b>OSG</b>	OpenSceneGraph
<b>OTW</b>	out-the-window
<b>PFD</b>	primary flight display
<b>PHS</b>	Precision Hover Symbology
<b>RMS</b>	root-mean-square
<b>RMSE</b>	Rating Scale Mental Effort
<b>RPM</b>	revolutions per minute
<b>SA</b>	situational awareness

<b>SART</b>	Situation Awareness Rating Scale
<b>SCAS</b>	stability and control augmentation system
<b>SD</b>	spatial disorientation
<b>SRS</b>	SIMONA Research Simulator
<b>TTC</b>	time-to-contact
<b>TTP</b>	time-to-passage
<b>UCE</b>	usable cue environment
<b>VA</b>	visual acuity
<b>VCCM</b>	Visual Cue Control Model
<b>VCR</b>	visual cue rating
<b>VTOL</b>	vertical takeoff and landing

---

# List of Symbols

## Greek Symbols

$\alpha$	Angle of attack [rad]
$\delta$	Depression angle [rad]
$\Lambda$	Non-linear visual cue
$\lambda$	Linearized visual cue
$\Omega$	Blade angular velocity [rad/s]
$\omega$	Frequency [rad/s]
$\omega_c$	Crossover frequency [rad/s]
$\phi$	Roll angle [rad]
$\psi$	Yaw angle [rad]
$\rho$	Density [kg/m <sup>3</sup> ]
$\tau_e$	Effective time-delay [s]
$\tau$	Time-to-contact [s]
$\theta$	Pitch angle [rad]

## Roman Symbols

$A$	Blade area [m <sup>2</sup> ]
$A$	Effective size parameter [ft]
$C_P$	Power coefficient [-]
$C_T$	Thrust force coefficient [-]
$D$	Drag force [N]
$e_r$	Edge rate [1/s]

$I_h$	Horizontal image coordinate
$I_v$	Vertical image coordinate
$k$	Proportionality constant [1/s]
$L$	Focal length [m]
$L$	Lift force [N]
$p$	Roll rate [rad/s]
$q$	Pitch rate [rad/s]
$R$	Blade radius [m]
$R$	Range [ft]
$r$	Yaw rate [rad/s]
$S$	Splay angle [rad]
$s$	Distance [m]
$T$	Thrust force [N]
$T_x$	Edge separation [m]
$u$	Longitudinal velocity [m/s]
$v_i$	Induced velocity [m/s]
$v$	Lateral velocity [m/s]
$w$	Vertical velocity [m/s]
$x$	Longitudinal position [m]
$Y_c$	Controlled dynamics transfer function
$Y_{OL}$	Open-loop transfer function
$Y_p$	Pilot model transfer function
$y$	Lateral position [m]
$z$	Altitude [m]

---

# Contents

<b>Acronyms</b>	<b>v</b>
<b>List of Symbols</b>	<b>vii</b>
<b>List of Figures</b>	<b>xv</b>
<b>List of Tables</b>	<b>xvii</b>
<b>1 Introduction</b>	<b>1</b>
1-1 Problem statement . . . . .	2
1-2 Research objective and approach . . . . .	3
1-3 Report outline . . . . .	3
<b>I Paper</b>	<b>5</b>
<b>II Literature Study</b>	<b>19</b>
<b>2 Brownout</b>	<b>21</b>
2-1 Characteristics . . . . .	22
2-1-1 Formation and development . . . . .	22
2-1-2 Mitigation strategies . . . . .	23
2-2 Simulating the effect . . . . .	24
2-3 Pilot situational awareness . . . . .	25
2-3-1 False motion cues . . . . .	25
2-3-2 Usable cue environment . . . . .	26

<b>3</b>	<b>Hover Maneuver</b>	<b>29</b>
3-1	Control strategy . . . . .	29
3-2	Characteristics . . . . .	31
3-2-1	Ground effect . . . . .	31
3-2-2	Test course . . . . .	32
3-3	Current hover support displays . . . . .	35
<b>4</b>	<b>Human Vision</b>	<b>41</b>
4-1	Visual system . . . . .	42
4-2	Visual motion perception . . . . .	43
4-2-1	Optical flow . . . . .	44
4-2-2	Global optical flow rate . . . . .	45
4-2-3	Optical splay . . . . .	46
4-2-4	Optical depression . . . . .	47
4-2-5	Edge rate . . . . .	48
4-2-6	Temporal cues . . . . .	49
<b>5</b>	<b>Display Design</b>	<b>51</b>
5-1	Display elements . . . . .	51
5-1-1	Flight path marker . . . . .	51
5-1-2	Artificial horizon line . . . . .	52
5-1-3	Ground texture . . . . .	53
5-1-4	Miscellaneous conformal symbology . . . . .	54
5-2	Display design considerations . . . . .	55
5-2-1	Cognitive tunneling . . . . .	55
5-2-2	Visual clutter . . . . .	56
<b>6</b>	<b>Identification of Visual Cue Usage</b>	<b>57</b>
6-1	Crossover model . . . . .	57
6-2	Visual cue control model . . . . .	58
<b>7</b>	<b>Research Proposal</b>	<b>61</b>
7-1	Configuration of proposed displays . . . . .	61
7-2	Experimental set-up . . . . .	63
7-3	Results, outcome and relevance . . . . .	67
	<b>Bibliography</b>	<b>69</b>
<b>III</b>	<b>Appendices</b>	<b>75</b>
<b>A</b>	<b>Software Architecture</b>	<b>77</b>
A-1	DUECA Architecture . . . . .	77
A-2	OpenSceneGraph Implementation . . . . .	80

<b>B Experiment Briefing</b>	<b>83</b>
<b>C Consent Forms</b>	<b>91</b>
<b>D Experiment Questionnaires</b>	<b>95</b>
D-1 RSME . . . . .	95
D-2 SART . . . . .	96
D-3 Pilot opinion . . . . .	97
<b>E Additional Results</b>	<b>103</b>
E-1 Time trajectories surge motion . . . . .	103
E-2 Ground tracks . . . . .	116
E-2-1 Non-linear model . . . . .	116
E-2-2 Linear model . . . . .	123
E-3 Boxplots . . . . .	130



---

## List of Figures

2-1	Aerial view of a brownout forming around a landing helicopter . . . . .	21
2-2	Rotor downwash in ground effect . . . . .	22
2-3	Schematic of the physics involved in brownout cloud development . . . . .	23
2-4	Usable cue environment . . . . .	27
2-5	Visual cue rating scale . . . . .	27
3-1	Longitudinal control diagram . . . . .	30
3-2	Deceleration and ground speed profiles when approaching a hover target . . . . .	31
3-3	Influence of ground effect on rotor drag . . . . .	32
3-4	Top view of the ADS-33 hover course . . . . .	33
3-5	Side view of the ADS-33 hover course . . . . .	33
3-6	Different symbology sets evaluated by DLR . . . . .	36
3-7	Precision Hover Symbology (PHS) display developed at TU Munich . . . . .	36
3-8	Virtual landing pad on a HUD . . . . .	37
3-9	Synthetic cue display for longitudinal motion during hover . . . . .	38
3-10	Lateral drift indication on landing display by DLR . . . . .	38
3-11	Symbology sets evaluated for use in Integrated Cueing Environment (ICE) . . . . .	39
3-12	SFERION 3D landing symbology by Airbus . . . . .	40
4-1	Dynamic model of the human cognitive system . . . . .	41
4-2	Fundamental aspects of the anatomy of the human eye . . . . .	42
4-3	Static resolution and motion sensitivity of different regions of the eye . . . . .	43

4-4	Optic flow patterns arising in different flight conditions . . . . .	44
4-5	Schematic drawing of a moving observer relative to a plane . . . . .	45
4-6	Schematic drawing of helicopter in forward flight . . . . .	46
4-7	Effects of changing altitude on optical splay . . . . .	47
4-8	Effects of changing altitude on optical depression . . . . .	48
4-9	Control of speed by illusion using edges at exponentially decreasing intervals . . . . .	49
4-10	Optical looming of an object is used in time-to-contact judgments . . . . .	49
4-11	Optical looming for an off-axis approach . . . . .	50
5-1	Basic shape of the flight path marker . . . . .	52
5-2	Different types of ground texture . . . . .	53
5-3	Display to aid hovering above a moving ship deck . . . . .	55
6-1	Control diagram for quasi-linear pilot model . . . . .	58
6-2	Block diagrams illustrating incorporation of Visual Cue Control Model into crossover model . . . . .	60
7-1	Configuration of proposed displays . . . . .	62
7-2	Baseline condition with good visibility . . . . .	63
7-3	Basic instrument panel . . . . .	66
A-1	Software architecture of the DUECA project . . . . .	79
A-2	Basic overview of scene graph structure . . . . .	80
A-3	Detailed overview of the implementation of good visuals . . . . .	80
A-4	Detailed overview of the implementation of displays and brownout . . . . .	81
E-1	Time trajectories of surge motion variables, pilot 1, run 1 . . . . .	104
E-2	Time trajectories of surge motion variables, pilot 1, run 2 . . . . .	105
E-3	Time trajectories of surge motion variables, pilot 1, run 3 . . . . .	106
E-4	Time trajectories of surge motion variables, pilot 1, run 4 . . . . .	107
E-5	Time trajectories of surge motion variables, pilot 1, run 5 . . . . .	108
E-6	Time trajectories of surge motion variables, pilot 1, run 6 . . . . .	109
E-7	Time trajectories of surge motion variables, pilot 2, run 1 . . . . .	110
E-8	Time trajectories of surge motion variables, pilot 2, run 2 . . . . .	111
E-9	Time trajectories of surge motion variables, pilot 2, run 3 . . . . .	112
E-10	Time trajectories of surge motion variables, pilot 2, run 4 . . . . .	113

E-11 Time trajectories of surge motion variables, pilot 2, run 5 . . . . .	114
E-12 Time trajectories of surge motion variables, pilot 2, run 6 . . . . .	115
E-13 Position trajectories during full run (left) and during hover (right), pilot 1, run 1	116
E-14 Position trajectories during full run (left) and during hover (right), pilot 1, run 2	117
E-15 Position trajectories during full run (left) and during hover (right), pilot 1, run 3	117
E-16 Position trajectories during full run (left) and during hover (right), pilot 1, run 4	118
E-17 Position trajectories during full run (left) and during hover (right), pilot 1, run 5	118
E-18 Position trajectories during full run (left) and during hover (right), pilot 1, run 6	119
E-19 Position trajectories during full run (left) and during hover (right), pilot 2, run 1	119
E-20 Position trajectories during full run (left) and during hover (right), pilot 2, run 2	120
E-21 Position trajectories during full run (left) and during hover (right), pilot 2, run 3	120
E-22 Position trajectories during full run (left) and during hover (right), pilot 2, run 4	121
E-23 Position trajectories during full run (left) and during hover (right), pilot 2, run 5	121
E-24 Position trajectories during full run (left) and during hover (right), pilot 2, run 6	122
E-25 Position trajectories during full run (left) and during hover (right), pilot 1, run 1	123
E-26 Position trajectories during full run (left) and during hover (right), pilot 1, run 2	124
E-27 Position trajectories during full run (left) and during hover (right), pilot 1, run 3	124
E-28 Position trajectories during full run (left) and during hover (right), pilot 1, run 4	125
E-29 Position trajectories during full run (left) and during hover (right), pilot 1, run 5	125
E-30 Position trajectories during full run (left) and during hover (right), pilot 1, run 6	126
E-31 Position trajectories during full run (left) and during hover (right), pilot 2, run 1	126
E-32 Position trajectories during full run (left) and during hover (right), pilot 2, run 2	127
E-33 Position trajectories during full run (left) and during hover (right), pilot 2, run 3	127
E-34 Position trajectories during full run (left) and during hover (right), pilot 2, run 4	128
E-35 Position trajectories during full run (left) and during hover (right), pilot 2, run 5	128
E-36 Position trajectories during full run (left) and during hover (right), pilot 2, run 6	129
E-37 Boxplots of velocities during approach (left) and hover (right) . . . . .	130
E-38 Boxplots of attitudes during approach (left) and hover (right) . . . . .	131
E-39 Boxplots of rotational velocities during approach (left) and hover (right) . . . . .	132



---

## List of Tables

2-1	Required response types per UCE level, for hover and low speed . . . . .	28
3-1	Hover performance specification according to the ADS-33 . . . . .	34
5-1	Optical activity as a function of ground texture and motion . . . . .	53
7-1	Available visual cues in each of the displays . . . . .	62
7-2	Experiment variables . . . . .	64
7-3	Experiment conditions . . . . .	65
7-4	Adequate performance bounds from the ADS-33 . . . . .	65
7-5	Hypotheses . . . . .	67
B-1	Experiment conditions . . . . .	85
B-2	Misery Scale . . . . .	86
B-3	Adequate performance bounds . . . . .	87



---

# Chapter 1

---

## Introduction

The safety of helicopter flight remains subpar compared to fixed-wing flight, especially in degraded visual environments (DVE). In particular, brownout or whiteout conditions are frequently the cause of rotorcraft accidents. In such conditions, the downwash from the rotor blades of a low-flying helicopter causes loose particles in the environment like snow (whiteout), sand or dust (brownout) to be stirred up, thereby obscuring the out-the-window (OTW) view from the cockpit [1]. Furthermore, the optical flow that arises due to the (rotational) motion of the particles can give the pilot incorrect motion cues, significantly impairing their situational awareness (SA) [2].

A flight maneuver that, when performed in sandy or snowy environments, can cause these phenomena to occur is the hover maneuver. This maneuver is frequently applied, as it is typically the first step after liftoff and the final step before touchdown. It is particularly difficult to safely perform in a brownout, as it requires constant pilot attention and control input. Moreover, for good visual environments (GVE), pilots are instructed to make use of outside visual references to maintain a stable point above which to hover [3], hence when OTW information is lost they need to adjust their normal control strategy.

Evidently, this can lead to perilous situations as is supported by a study of 375 rotorcraft losses, conducted for the U.S. Department of Defense, which found that 55% of combat non-hostile losses of rotorcraft during low-speed or hover occurred due to flight in DVE [4]. According to a NATO report, approximately 75% of helicopter mishaps that took place since NATO started operating in dry climates such as Afghanistan and Africa can be attributed to brownout conditions [5].

With the emergence of affordable and high-performance head-up display (HUD) and helmet-mounted display (HMD) on the one hand, and the continuing developments in environmental sensing technology and increased on-board storage capacity for terrain databases on the other hand, the use of augmented reality (AR) to compensate for the loss of OTW information has become a promising means to mitigate the difficulties associated with flying in brownout conditions. However, present hover displays contain a lot of different elements, often leading to cluttered displays. Such visual clutter can in fact deteriorate pilot performance, therefore research is needed into what information is really necessary.

## 1-1 Problem statement

The main research question that must be answered is formulated as follows:

**What visual cues are *minimally* needed for helicopter pilots to be able to successfully perform a hover maneuver in a brownout, and how can this information be portrayed effectively on a HMD?**

The following sub-questions are derived from the main research question:

1. *What visual cues and control strategy do pilots use when performing a hover maneuver in GVE?*
  - (a) What knowledge of aircraft states and surrounding environment is required in order to perform a hover maneuver?
  - (b) What visual cues provide the necessary information about the relevant aircraft states?
  - (c) What control behavior do pilots employ, i.e., how do the trajectories of the aircraft states develop during (an approach to) hover?
  
2. *What visual information can be provided to reinforce the natural control strategy (employed in GVE) in brownout conditions?*
  - (a) What information do pilots currently use when hovering in a brownout?
  - (b) What are the differences in terms of available visual cues between brownout conditions and GVE?
  - (c) How do these differences in available information affect the visual perception of ego-motion?
  - (d) What visual cues can be provided in a brownout to counteract these differences?
  - (e) What is the current state-of-the-art in hover aid displays and how do these help pilots to perform a hover maneuver in a brownout? What are their limitations?
  
3. *How can the brownout effect be graphically modeled in a representative way?*
  - (a) What physical parameters play a role in the development of a brownout cloud?
  - (b) How does the motion of particles in a brownout cloud develop over time?
  - (c) How can the motion of the particles be graphically modeled in a computationally efficient way, suitable for real-time simulation?

## 1-2 Research objective and approach

The objective of the research is to contribute to the development of efficient HUDs or HMDs that improve the hover performance in brownout, by conducting a human-in-the-loop experiment to investigate what visual cues *minimally* need to be provided on such displays.

The following sub-goals are formulated to achieve this objective:

1. Perform an in-depth literature study on what visual cues play a role in the perception and control of ego-motion, with a specific focus on the hover maneuver.
2. Explore the ways in which these cues can be provided by (different combinations of) display elements.
3. Develop a virtual world for the simulator environment in which the experiment will take place, and implement the different combinations of the display elements that should provide the necessary information.
4. Graphically model the brownout phenomenon in a computationally efficient way and implement it in the virtual world.
5. Perform an experiment with varying display configurations, i.e., several scenarios with different combinations of display elements.
6. Analyze the effectiveness of the various display configurations.
7. Report the findings in a scientific paper.

## 1-3 Report outline

The report is outlined as follows. Part I is a scientific paper that describes the findings of the experiment that was conducted in the SIMONA Research Simulator at TU Delft. Part II contains the literature study, in which Chapter 2 introduces the brownout phenomenon, describes its formation and development and investigates methods for simulating the clouds. Then, the hover maneuver is examined in detail in Chapter 3. The natural control strategy of pilots is investigated and current state-of-the-art hover displays are discussed. Chapter 4 focuses on human vision, with a specific focus on environmental information humans use for the perception and control of self-motion. Subsequently, Chapter 5 discusses how the theory of visual perception can be used to develop effective AR displays. That chapter also investigates some other important design considerations that must be made from a human factors perspective. Chapter 6 discusses models that can be used to analyze the effectiveness of perspective displays by identifying what visual cues pilots use. Then, a proposal for a human-in-the-loop experiment is proposed in Chapter 7. Finally, additional results and experiment documents, as well as an overview of the developed software is presented in Part III.



**Part I**

**Paper**



# Evaluation of Augmented Reality Displays for Helicopter Hover Support in Brownout Conditions

N. V. Meima, C. Borst, D. Friesen, M. Mulder

*Faculty of Aerospace Engineering, Delft University of Technology, Delft, The Netherlands*

**Abstract**—Augmented reality displays are a promising means to improve the safety of helicopter hovering in brownout conditions. However, previous research has often combined conformal with non-conformal elements in such displays, potentially leading to visual clutter. In this paper, two purely conformal displays are proposed, and their effectiveness is compared with a baseline condition in good visibility depicting the ADS-33 hover course. The first display contains a grid ground texture and a box indicating the hover target position; the second bears close resemblance to the ADS-33 course. Two pilots participated in a simulator experiment in which the effects of display configuration and vehicle dynamics on hover performance, control activity, pilot workload and situation awareness were examined. Results show that performance similar to that in good visibility can be achieved with the grid display, although workload and situation awareness deteriorated. Performance with the second display was worse, likely due to lack of available optic flow. Linear vehicle dynamics led to lower workload than a non-linear model, but not to better performance. For future research, it is recommended to improve availability of longitudinal positioning cues in the grid display, and to investigate the usefulness of that display also in good visibility.

## I. INTRODUCTION

The safety of helicopter flight remains subpar compared to fixed-wing flight, especially in degraded visual environments (DVE) such as a brownout or whiteout. In such conditions, the downwash from the rotor blades of a low-flying helicopter causes loose particles in the environment like snow (whiteout), sand or dust (brownout) to be stirred up in the air where they may become entrained in the flow [1]. As a result, a brownout cloud develops that partially, or even completely, obscures the out-the-window view of the pilot. Furthermore, the optical flow that arises due to the (rotational) motion of the particles can lead to pilots perceiving incorrect motion cues such asvection, further impairing their situation awareness [2].

Evidently, this can lead to perilous situations, a finding supported by a study of 375 rotorcraft losses, conducted for the U.S. Department of Defense, which found that 55% of combat non-hostile losses of rotorcraft during low-speed or hover occurred due to flight in DVE [3]. According to a NATO report, approximately 75% of helicopter mishaps that took place since the organization began operating in arid climates such as Afghanistan and Africa can be attributed to brownout conditions [4].

Frequently performed at low altitudes before touchdown and after liftoff, the hover maneuver is a flight phase which, in dry climates, can lead to brownout formation. Safely performing a hover in a brownout is particularly difficult, because the maneuver requires constant pilot attention and control input.

Moreover, for good visual environments (GVE), pilots are instructed to make use of outside visual references to maintain a stable point above which to hover [5], hence when out-the-window information is lost they are forced to adjust their normal control strategy. Providing visual support systems, either head-down or head-up, is a promising means to improve the safety and performance of hovering in a brownout.

Early research on such visual augmentations for hover focused on providing two-dimensional information on a head-down display (HDD) [6], [7]. However, more recent studies have demonstrated the inherent limitations of both HDDs as well as two-dimensional symbology, and recommended instead to implement three-dimensional conformal imagery, or augmented reality (AR), in head-up displays (HUDs) or helmet-mounted displays (HMDs) [8], [9]. Although several groups have developed extensive displays with such scene-linked symbology [10]–[14], those interfaces are not purely conformal because they also contain superimposed two-dimensional elements such as flight instruments. Furthermore, these displays include so many different elements that often parts overlap. This visual clutter can have adverse effects on performance [15], and lead to deteriorated awareness of other displays or external events [16]. Also, cognitive tunneling is known to be more substantial for displays with non-conformal elements [17].

Even though experimental evaluation has demonstrated that such displays have a positive effect on hover performance, it remains unclear to what extent each display element is responsible for this. In order to avoid the adverse effects of clutter and tunneling, a hover display ideally contains a minimum number of exclusively conformal elements. Therefore, only those cues that are crucial for the task at hand should be provided. Research is needed to investigate what kind of conformal cues such a display minimally needs.

In this paper, two conformal displays are developed and their effectiveness during hover is investigated. The design of the displays is based on replacing the visual cues that are lost due to brownout, in such way that pilots can accurately perceive all relevant helicopter states using as few display elements as possible. The results of an experiment conducted with two licensed helicopter pilots at the SIMONA Research Simulator of TU Delft are presented.

Both a non-linear and a linearized vehicle model are used during the experiment, in order to investigate whether a linearized version is a suitable replacement for the more realistic non-linear kind. In general, linear models are preferred as the outcome is easier to predict and analyze, but these can

adequately replace non-linear models only if pilot performance and control strategy are comparable between both models. The influence of the developed displays and helicopter dynamics on hover performance, control activity, workload and situation awareness is investigated.

The display design, as well as the theory on visual motion perception it was based on, is discussed in Section II. This is followed by the experiment design in Section III. Results of the experiment and discussion of those results are presented in Section IV and Section V, respectively. Finally, the paper ends with a conclusion.

## II. BACKGROUND

### A. Visual Motion Perception

In a brownout, the visual cues that a pilot normally uses during a hover maneuver are unavailable. In order to provide adequate replacements on an AR display, understanding how the human visual system allows pilots to perceive and control their motion and orientation is crucial. This section briefly describes the role of the global optical flow rate (GOFR), splay and depression angles, and optical edge rate.

Successful performance of the hover maneuver results in near motionless flight over a target location. In order to remain stationary, pilots have to be aware of, and correct for, any deviation away from the target. These deviations are noticeable as changes in the visual field of the pilot.

Movement of the helicopter causes points at different locations in the pilot's field of view to move at different rates. The relative velocities of these points is known as optical flow [18]. All flow in the optic array radiates outward from a single expansion point, which is a visual cue for the direction of motion of the pilot.

The total rate of optical flow moving past the pilot, known as the global optical flow rate (GOFR) [20], is defined as  $\frac{V}{z}$ . If speed  $V$  is kept constant, the GOFR is a reliable cue for altitude  $z$ , and vice versa.

Another visual cue that can encode altitude information is splay angle  $S$ , which is the angle between edges parallel to the direction of motion and a line perpendicular to the horizon [21], such as a looming runway. The splay angle  $S$  can be calculated with Equation (1), where  $y_g$  is the lateral displacement of the observer from the line perpendicular to the horizon and  $z$  is the altitude.

$$S = \tan^{-1} \left( \frac{y_g}{z} \right) \quad (1)$$

The splay angle changes as the observer moves through the environment. The rate of change of the angle provides a cue for the perception of altitude and lateral speed, and can be calculated with Equation (2).

$$\dot{S} = -\left(\frac{\dot{z}}{z}\right) \cos S \sin S + \left(\frac{\dot{y}_g}{z}\right) \cos^2 S \quad (2)$$

Analogous to splay is the depression angle, defined as the angular position of an edge perpendicular to the direction of motion. In Equation (3),  $x_g$  is the longitudinal displacement and  $z$  is the altitude.

$$\delta = \tan^{-1} \left( \frac{x_g}{z} \right) \quad (3)$$

The depression rate in case of rectilinear motion over a flat plane can then be defined [22], see Equation (4). It serves as a cue for altitude if longitudinal position is constant, and vice versa.

$$\dot{\delta} = -\left(\frac{\dot{z}}{z}\right) \cos \delta \sin \delta + \left(\frac{\dot{x}_g}{z}\right) \cos^2 \delta \quad (4)$$

Finally, edge rate is the rate at which discontinuities pass by a reference point in the observer's visual field. It is dependent on (ground) texture density and speed but independent of altitude. Defining the separation between edges on the ground surface as  $T_x$ , the edge rate can be calculated using Equation (5) [23]. If the textures are regularly spaced, the edge rate is directly proportional to speed.

$$e_r = \frac{dx}{dt} \frac{1}{T_x} \quad (5)$$

### B. Display Design

In brownout conditions, the outside view is obscured and the environmental visual cues as explained before are unavailable. Two AR displays are developed to replace those lost visual cues. An often used test course for the hover maneuver is described in the ADS-33 [24], and will also be applied here as a baseline condition to compare the to-be-designed displays with. The developed display configurations are depicted in Figure 1. Table I shows an overview of the cues available in each of the three display configurations.

The ADS-33 setup in the baseline condition (Figure 1a) contains a hover board with reference marker and two sets of cones. The inner rectangle in the hover board indicates vertical and lateral *desired* performance, whereas the outer rectangle corresponds to the *adequate* performance bounds as specified in the ADS-33 [24] (see also Table III). Longitudinal position is conveyed by means of five rows of cones in between the yellow lines. The middle row corresponds to the target longitudinal position, the second and fourth row are indicative of desired performance and the outer rows of adequate performance. The diagonal set of cones are a cue for the yaw angle.

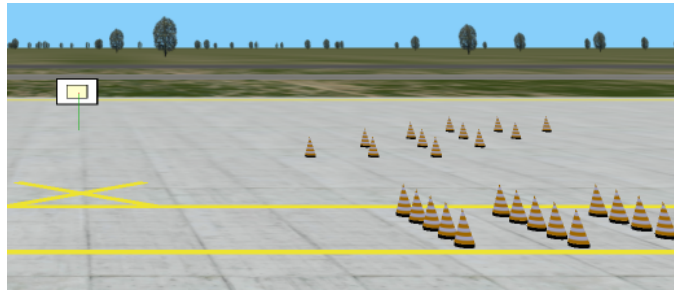
Regarding the first display (Figure 1b, henceforth referred to as Display 1), a straightforward way to implement splay and depression information in a display is by using ground texture [22]. A grid texture contains both types of cues and thus conveys information about movement in all three axes. Therefore, the first proposed display contains a grid surface. Furthermore, the hover target position on this interface is indicated with a hover box, loosely based on [25]. Tick marks are added to the rear vertical edges of the box as a cue for altitude when inside the box; if these coincide with the horizon, the helicopter is flying at target altitude. Finally, an artificial horizon line is added to convey pitch and roll information.

The second display (Figure 1c, hereafter called Display 2), instead, provides similar cues as are available in the ADS-33 hover course. However, the cones are replaced by lines as

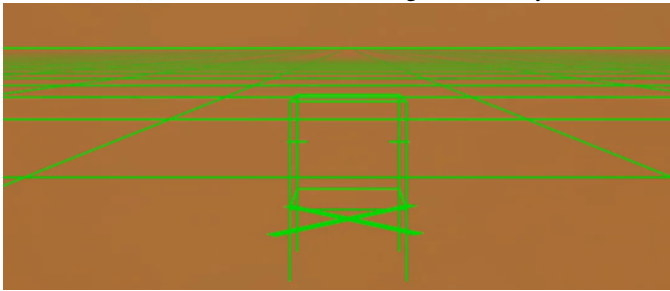
TABLE I: Available visual cues in each of the displays

Outside view (ADS-33)	Display 1	Display 2
$x$ Longitudinal cone position	Depression lines, hover box and cross	Longitudinal lines (cones), hover cross
$u$ Optical flow, edge rate	Depression lines	Hover course (depression) lines
$\theta$ Hover board pitch position	Horizon position	Horizon position, hover board pitch position
$q$ Optical flow	Horizon vertical speed	Horizon vertical speed
$y$ Hover board lateral indicator	Hover box and cross	Hover board lateral indicator
$v$ Optical flow, edge rate	Splay lines	Hover course movement, diagonal lines (cones)
$\phi$ Horizon bank position	Horizon bank position	Horizon bank position
$p$ Optical flow	Horizon rotational speed	Horizon rotational speed
$z$ Hover board	Splay and depression lines, hover box and ticks	Hover board and reference marker
$w$ Optical flow, edge rate	Splay and depression lines	Hover course (depression) lines
$\psi$ Diagonal cones and hover board yaw position	Hover box position, grid lines	Diagonal lines and hover board yaw position
$r$ Optical flow	Grid lines	Diagonal lines and hover board rotational speed

these are expected to be visible more clearly in a HUD implementation, especially when overlaid on a simulated brownout. The cross in front of the box, also present in the other display configurations, must be visible during hover; otherwise the longitudinal target position is overshoot. This display also contains a horizon line for pitch and roll reference.



(a) Baseline condition with good visibility



(b) Display 1: grid and hover box



(c) Display 2: geometric ADS-33

Fig. 1: Configuration of proposed displays

### III. EXPERIMENT

#### A. Apparatus

The experiment was conducted in the SIMONA Research Simulator (SRS) at TU Delft [26], shown in Figure 2. During the experiment, the simulator was set up in helicopter configuration, equipped with pedals, a cyclic stick and a collective lever. The out-the-window visual, produced by a collimated system with three LCD projectors with each a resolution of  $1280 \times 1024$  and a refresh rate of 60 Hz, did not include a chin bubble and was therefore more limited than in real helicopters. The field of view of  $180^\circ \times 40^\circ$  was similar to that available to pilots in cockpits of fixed-wing aircraft (see Figure 2, right).

The motion system of the simulator was not used. As the experiment focused on investigating whether the developed AR displays alone contained sufficient information for pilots to achieve satisfactory hover performance, it was important to isolate the effects of the visual system as much as possible. If motion cueing would be involved as well, the information of the visual and vestibular system would be combined into an integrated perception of motion and orientation, thereby reducing the pilot's reliance on and attention for the displays.

#### B. Participants

Two helicopter pilots with a Commercial Pilot License (CPL) participated voluntarily in the experiment. Participants had a similar level of experience, with number of flight hours ranging from 200 to 225.



Fig. 2: SIMONA Research Simulator

### C. Control Task

The task (which was the same as in [8]) as well as the performance boundaries were based on the hover maneuver described in the ADS-33 [24]. Initial positions were quasi-randomized (standard deviation 10 m) around the point 100 m directly in front of the hover target, which was at a height of 10 ft. The pilots were instructed to approach the target location with the initial forward speed of 10 m/s, decelerate so as to come to a stop precisely at the hover point and then maintain a stabilized hover for 30 seconds. Pilots were encouraged to perform a smooth transition, avoiding decelerating well in advance and then slowly moving toward the target.

### D. Independent Variables

The independent variables in the experiment were *display configuration* and *vehicle dynamics*. The two developed displays were provided, one at a time, as overlays on the out-the-window view of the pilot, which was obscured by a simulated brownout cloud. A condition with good visibility and no hover display, but with the ADS-33 hover course clearly visible, served as a baseline for comparison. Pilots flew these display configurations with both a non-linear and a linear helicopter model, resulting in a total of six experiment conditions (Table II). The order of conditions was balanced between subjects. Each condition was repeated six times, resulting in a total of 36 experiment runs per pilot (excluding warm-up and acclimatization runs).

1) *Visibility and display*: The hover course described in the ADS-33 [24] served as the scenery for the good visibility conditions (see Figure 1a). In the remaining conditions, a simulated brownout cloud obscured the outside view and one of the displays was superimposed on the cloud. Due to the random nature of the brownout simulation, the outside scenery was removed entirely in these conditions in order to avoid it being visible to a varying extent between runs.

The outside scenery, brownout simulation, and hover displays were developed using the open-source 3D graphics library OpenSceneGraph (OSG) in C++. A simple brownout simulation was implemented using a particle system in OSG, similar to the approach in [27]. This system was configured to form a cloud by generating hundreds of sand-colored particles at every time step, each particle with random initial position, rotation, velocity, rotational velocity, lifetime, and color settings (each within a specified range). All generated particles were subject to a simple upward acceleration.

2) *Vehicle dynamics*: Two distinct vehicle dynamics were employed in the experiment. The first was a non-linear six-degree-of-freedom Messerschmitt-Bölkow-Blohm Bo105 helicopter model [28], as was also used in [8]. The alternative was

a linear Bo105 model obtained from [23], with every degree-of-freedom decoupled such that no cross-couplings occurred whatsoever.

Although the non-linear model behaves more realistically, due to the non-linearity it is tedious to use with models such as the crossover model [29] or the Visual Cue Control model [30]. In case performance and control strategy are found to be sufficiently similar between the two models, future experiments might therefore prefer to use the linear model.

### E. Dependent Measures

The control task can be split up in two distinct phases: approach and hover. Where applicable, a separate analysis of the two phases was performed.

Hover performance was measured with the root-mean-square (RMS) error of the helicopter's vertical, longitudinal and lateral position relative to the target location, during 30 seconds after reaching adequate performance for the first time. The boundaries for desired and adequate hover performance as stipulated in the ADS-33 are listed in Table III. The relative time spent within these boundaries also served as a measure for hover performance. The differences in additional track meters traveled and in the duration of the approach phase between the various conditions were used as a metric for performance during approach.

Control activity was measured, separately during approach and hover, as the standard deviations of the longitudinal cyclic, lateral cyclic, collective and pedals. Pilot workload scores were collected after each condition with the Rating Scale Mental Effort (RSME) [31]. Subjective scores of situation awareness were measured with the Situation Awareness Rating Technique (SART) [32].

Finally, pilots were asked to fill out questionnaires about the simulator setup and the experiment conditions. Closed-ended questions were rated on a seven-point scale (1 = low, 7 = high; no descriptors for intermediate values), covering pilot opinions on the helicopter handling qualities with each model, the realism of visuals (both in brownout and good visibility), their confidence in using Display 1 and Display 2 to fulfill the control task, and the usefulness of each display in successful execution of subtasks during the experiment (i.e., holding course and speed, performing a smooth deceleration maneuver, and hovering precisely in place). The participants were encouraged to write down any further comment they had regarding the experiment and displays.

### F. Control Variables

During all conditions and runs, the control task and the simulator setup remained unchanged. Figure 3 shows the head-down basic instrument panel which was available throughout the experiment.

TABLE II: Experiment conditions

Display configuration	Vehicle dynamics	
	non-linear	linear
Good visibility, no HUD augmentation	A	B
Brownout, display 1 (grid and box)	C	D
Brownout, display 2 (ADS-33 on HUD)	E	F

TABLE III: Performance boundaries from the ADS-33

Parameter	Desired	Adequate
Longitudinal deviation	$\pm 3$ ft	$\pm 6$ ft
Lateral deviation	$\pm 3$ ft	$\pm 6$ ft
Altitude deviation	$\pm 2$ ft	$\pm 4$ ft



Fig. 3: Basic instrument panel

### G. Procedure

Before the start of the experiment, participants were familiarized with the questionnaires and informed on the active COVID-19 protocols at the faculty. During the acclimatization period, the pilots performed multiple practice runs for each condition in order to get acquainted with the simulator and the experiment. Every condition started with several warm-up runs, followed by six experiment runs. The RMS deviation from the target location during the 30-second hover phase was communicated to the pilots as a hover performance score when a run was completed. Runs during which the helicopter collided with the ground were immediately abandoned and restarted.

After the first and last run of a condition, physical well-being of the participants was assessed by asking them to rate their discomfort on the Misery Scale [33]. Workload and situational awareness questionnaires were completed after each condition. At the end of the experiment, a pilot opinion questionnaire was distributed to obtain more insight on their subjective experience with the displays and helicopter models.

### H. Data Processing

The control task during the experiment consisted of two distinct phases: the approach phase and the hover phase. To analyze each part individually, the data recordings were separated into two parts. The time step at which the participant entered the adequate performance boundaries (Table III) for the first time during a run was taken as the starting point of the hover phase for that specific run.

Each participant completed the workload (RMSE) and situation awareness (SART) questionnaires once for every experiment condition. These ratings were Z-scored to have a mean of 0 and a standard deviation of 1 for each pilot, in order to compensate for possible subjective differences in scoring.

No statistical tests were performed on the results. With only two participants, such analysis was not expected to provide reliable results.

### I. Hypotheses

Performance is hypothesized to decrease in brownout conditions relative to good visibility. Pilot situation awareness is lower than in clear conditions, due to the lack of available outside cues and the possible false cues generated by the brownout motion. In turn, reduced situation awareness, in

combination with pilots using a novel display, is hypothesized to lead to higher workload and control activity. The effect is expected to be more pronounced in conditions with Display 2 (ADS-33), because the grid ground texture in Display 1 provides relatively more optical flow and edge rate information than the synthetic ADS-33 course.

The non-linear model more realistically simulates the behavior of a real helicopter. Considering that the participants are experienced helicopter pilots, the response of the linear model may be somewhat unexpected for the pilots at first. However, participants are given ample time to get acquainted with all conditions, and, since the target location is directly ahead of the starting point, expected heading changes are minimal during the experiment. This should lower the difference experienced between the models by the pilots. Moreover, linear dynamics are typically considered easier to control than non-linear types. Therefore, control activity and workload are hypothesized to decrease with the linear model, while performance is expected to increase. Due to the lower workload and control activity, also situation awareness increases.

## IV. RESULTS

The effects of display configuration and vehicle dynamics on the dependent measures of the experiment are presented in this section. First, the time trajectories of the input and state variables are analyzed. Then, the measures of performance and control activity are presented. Finally, subjective pilot ratings on situation awareness and workload, and the responses to the opinion questionnaire are provided. No statistical analysis is performed, as only two pilots participated.

### A. Time Trajectories

As a preliminary analysis, the time recordings of the input and state variables are plotted. The hover target was positioned approximately 100 m straight-ahead from the initial location, therefore only the time trajectories of variables involved in longitudinal motion adequately capture both the approach and hover phase. Figure 4 shows the time traces of the variables associated with surge motion (longitudinal cyclic input  $\theta_{1,s}$ , longitudinal position  $x$  and velocity  $u$ , pitch angle  $\theta$  and pitch rate  $q$ ) for one run per condition.

Although the trajectories presented here are of one pilot and one run per condition only, comparable profiles are obtained for the other pilot and runs. Similar trends are noticeable in the position and velocity profiles, indicating that the participants employed a similar strategy regardless of experiment condition. The pilots performed most of the deceleration during the first fifteen seconds in all conditions. However, as evidenced by the longer duration of those runs, it took the pilots considerably more effort to first reach adequate performance with Display 2 (ADS-33) than in the other conditions, despite the comparable decelerating approach.

An explanation for this difference is provided by the ground tracks, see Figure 5. The cluster slightly in front of the target location, clearly visible especially in the linear model curve, suggests that depth perception was worse in these conditions as the pilot was unable to accurately locate the longitudinal location of the target.

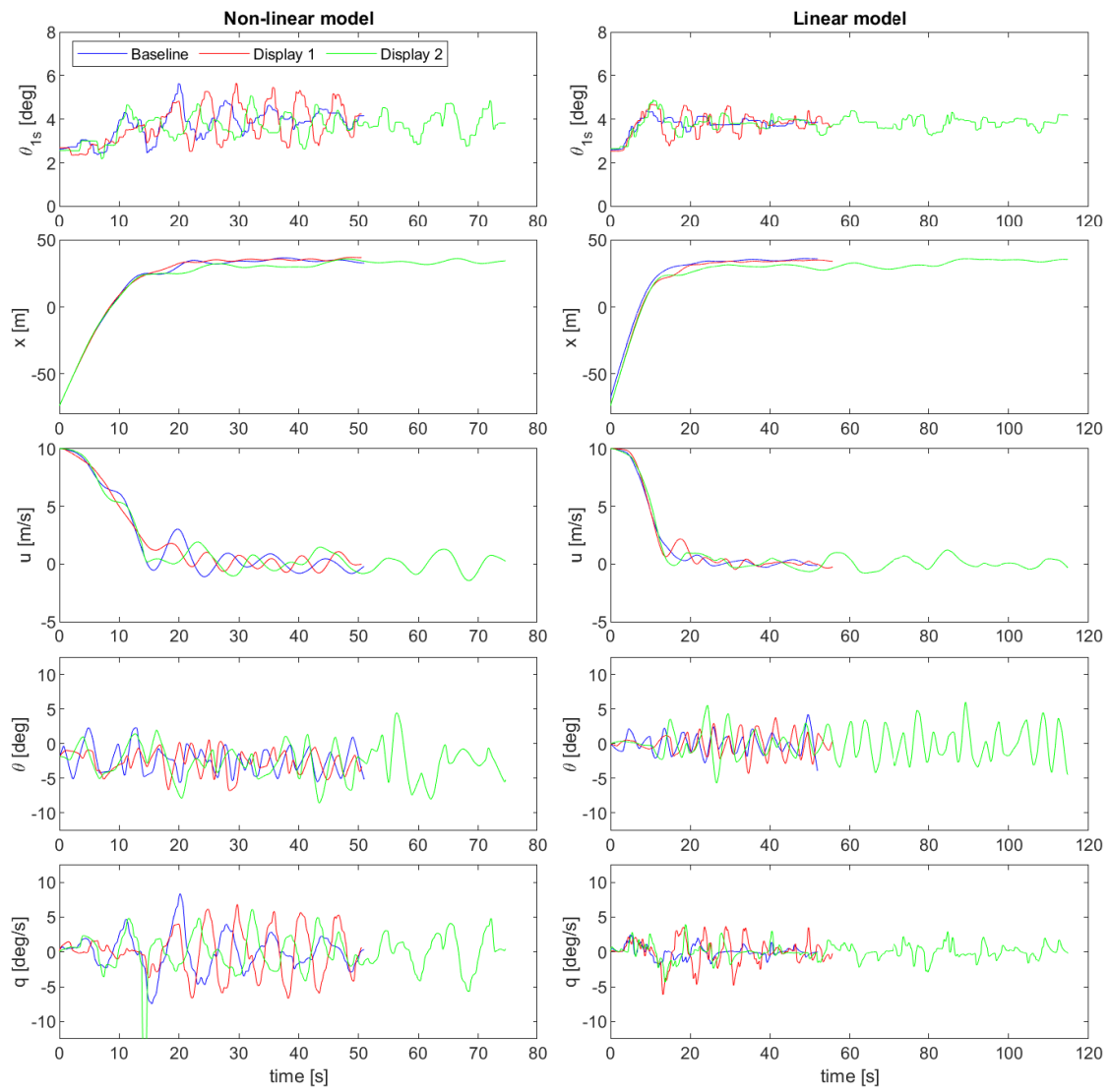


Fig. 4: Time trajectories of surge motion variables, one run per condition

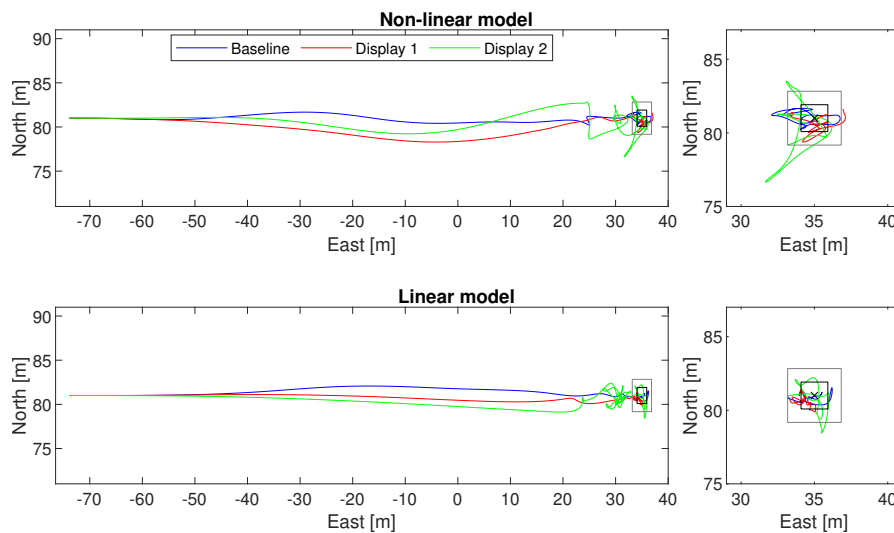


Fig. 5: Ground tracks during full run (left) and during hover (right), one run per condition

## B. Performance

1) *Hover position RMS error*: The RMS distance between the target location and the helicopter position serves as a measure for task performance during the hover phase. Figure 6 shows boxplots of the longitudinal ( $x$ ), lateral ( $y$ ), vertical ( $z$ ), and combined 3D position RMS error. For one run (pilot 2, Display 1, non-linear model, third run), the vertical RMS error was a factor five larger than for the other runs. Therefore, that run was considered an outlier and omitted from further analysis.

For all conditions, the longitudinal RMS error was larger than the lateral and vertical errors. One reason for this larger error is that the approach phase was longitudinal, thus the deceleration maneuver was also predominantly along this axis. As a result of the decelerating approach, some longitudinal oscillatory motion was likely still present. Furthermore, the start of the hover phase was defined as the first time step in which adequate performance was reached. As the optimal trajectory was a straight, purely longitudinal path, in most cases the error in  $x$  at the start of the hover phase corresponded to adequate performance at best, whereas vertical and lateral position were closer to their target values. Finally, another possible reason is that longitudinal cues were the least readily available position cues in each of the displays.

Interestingly, longitudinal performance was better and more consistent with Display 1 (grid and box) than in clear conditions (upper boxplot in Figure 6). Contrary to the hypothesis that performance would decrease in brownout conditions, performance with the grid and box of Display 1 was overall comparable or slightly better than performance in the baseline condition.

The spread of data points in the boxplots is an indication of the level of consistency in performances for a certain condition. Performance was worst for experiment runs with Display 2 (ADS-33); the RMS errors in the four plots not only exhibit the largest spread, but were also higher in those conditions.

Performance is similar between the non-linear and linear vehicle models. No clear influence of vehicle dynamics is noticeable in terms of RMS errors.

2) *Time spent inside boundaries*: In general, pilots were unable to consistently remain within the adequate and desired performance boundaries stipulated in the ADS-33 (see Table III) for the entire 30-second hover phase. Boxplots of the fraction of hover time spent inside these zones, depicted in Figure 7, demonstrate that consistent adequate performance was achieved only in conditions with Display 1. This display, in combination with the linear model, resulted on average in desired performance during approximately two-thirds of the hover time and adequate performance during the entire hover. With Display 1, time spent inside the boundaries increased with the linear model. However, no clear influence of vehicle dynamics was present in the other conditions. Pilots performed better in good visibility (baseline) than with Display 2.

3) *Approach duration and additional track meters*: The time trajectories illustrated that pilots took longer to reach the target within adequate distance in runs with Display 2. Therefore, the approach duration and the additional distance

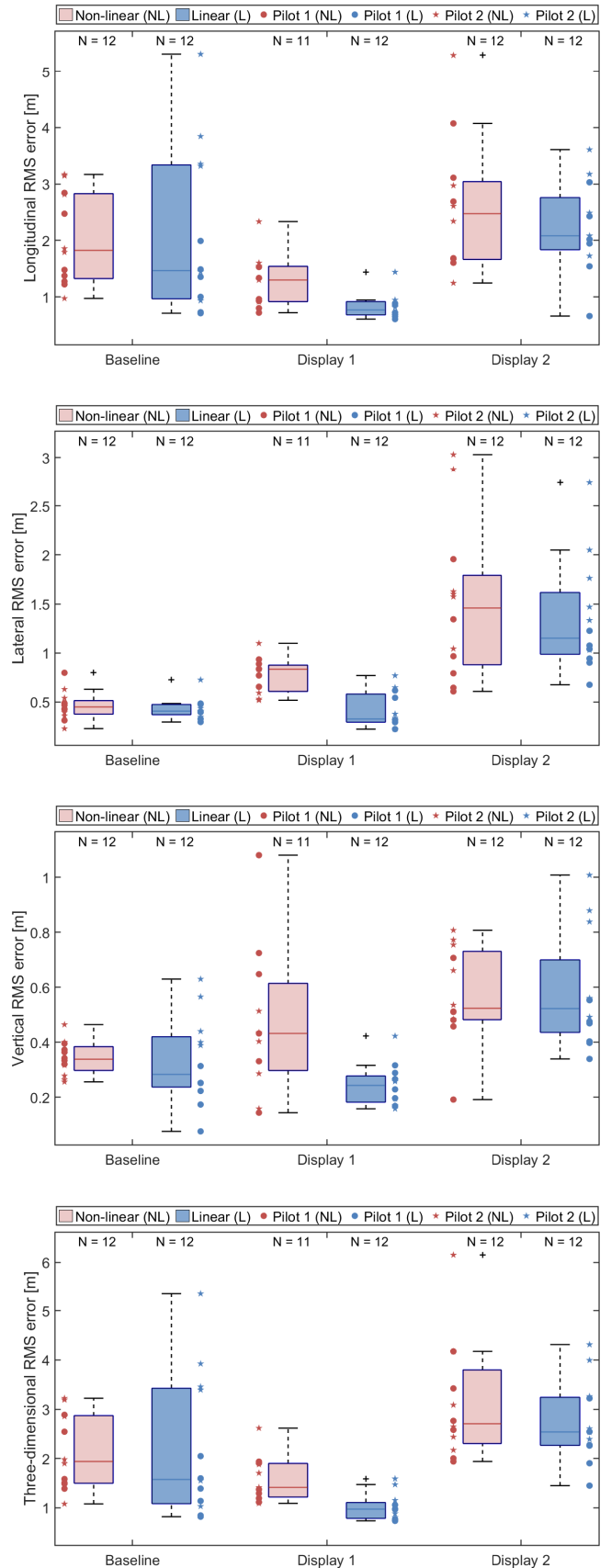


Fig. 6: Boxplots of the RMS error in position

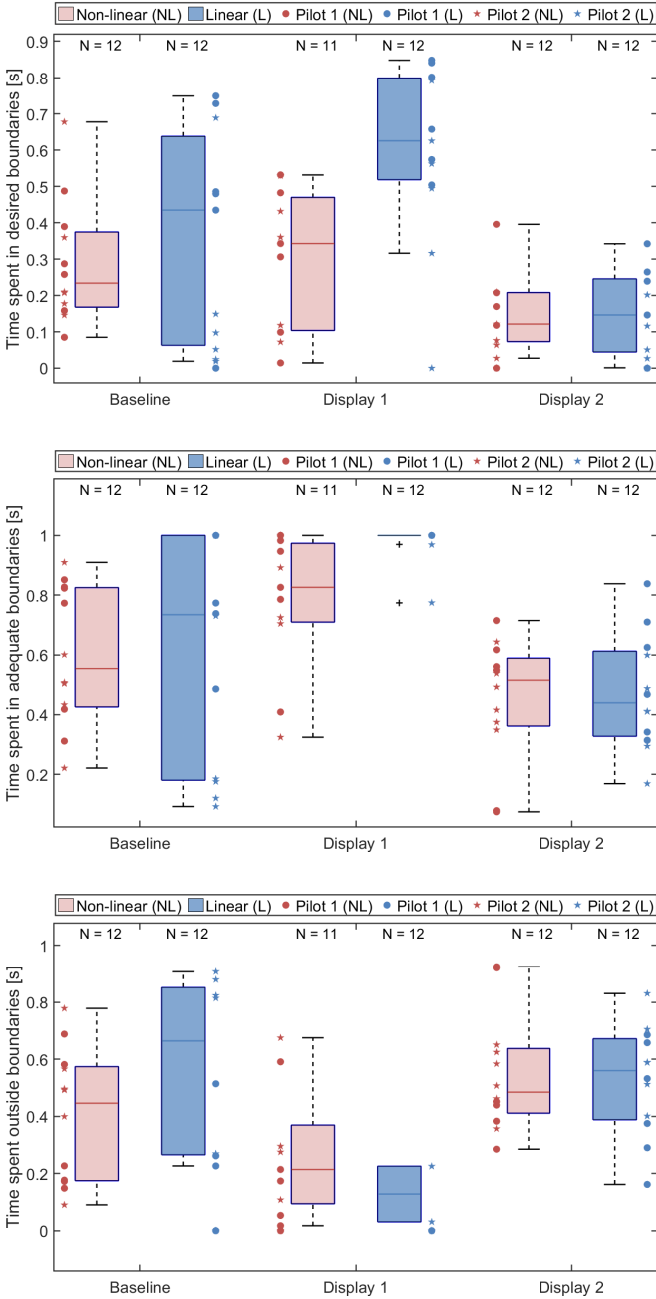


Fig. 7: Boxplots of time spent in desired (top), adequate (middle), and inadequate (bottom) performance boundaries

traveled relative to the shortest path were regarded as indicators of performance during the approach phase.

The average approach time, as shown in the boxplot of Figure 8, was longest with the Display 2 and shortest for the baseline condition. Furthermore, relative extra distance traveled (Figure 9) was considerably larger with Display 2. In terms of this distance metric, similar performance was achieved between conditions with Display 1 and conditions in good visibility. Regarding vehicle dynamics, no clear influence was observed in these metrics.

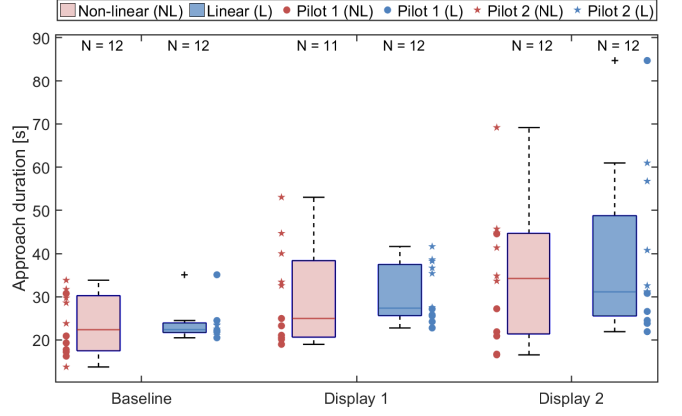


Fig. 8: Boxplot of the approach duration

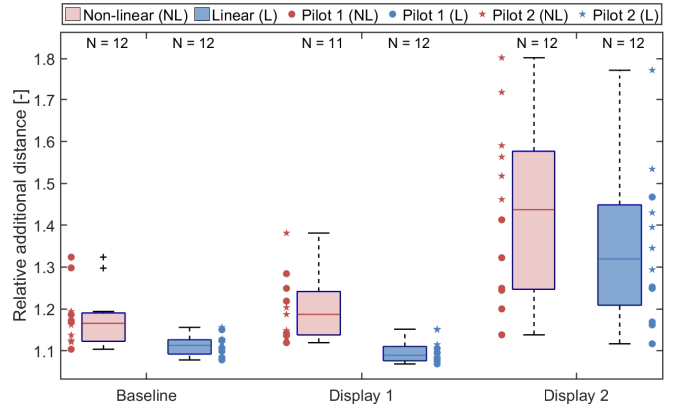


Fig. 9: Boxplot of the additional track meters during approach

### C. Control Activity

1) *Standard deviation of control inputs during hover:* Boxplots of the standard deviations of the four input channels during hover are presented in Figure 10. Regarding longitudinal cyclic, the condition with Display 1 and non-linear dynamics stands out for its much higher measure of control activity than the other conditions. Moreover, a trend of decreasing control activity when switching from non-linear to linear vehicle dynamics is visible.

Whereas the standard deviation of longitudinal cyclic input  $u_{1s}$  exhibits no clear influence of display conditions, in the lateral case control activity is lower in good visibility than with either of the developed displays. Standard deviation of lateral cyclic  $\theta_{1c}$  was comparable between the four brownout conditions, and also between the two vehicle models.

Collective control activity was similar in each of the conditions and appears largely unaffected by both vehicle model and display configuration. Noteworthy, however, is the difference in control activity between the two pilots; for every condition, nearly all data points above the median belong to pilot 2. This implies that the pilots employed a somewhat different strategy during the hover phase, with pilot 2 being more reliant on the collective.

Finally, pedal control activity was higher with the non-linear than the linear model. However, this difference is at least partly explained by recalling that the linear model is a

linearized and decoupled version of the non-linear dynamics. More pedal control activity is required to compensate for the cross-coupling effects present in the non-linear model.

2) *Standard deviation of control inputs during approach:*  
During the approach phase, an unambiguous trend of increased control activity with the non-linear model is visible in the boxplots for each of the input channels, see Figure 11.

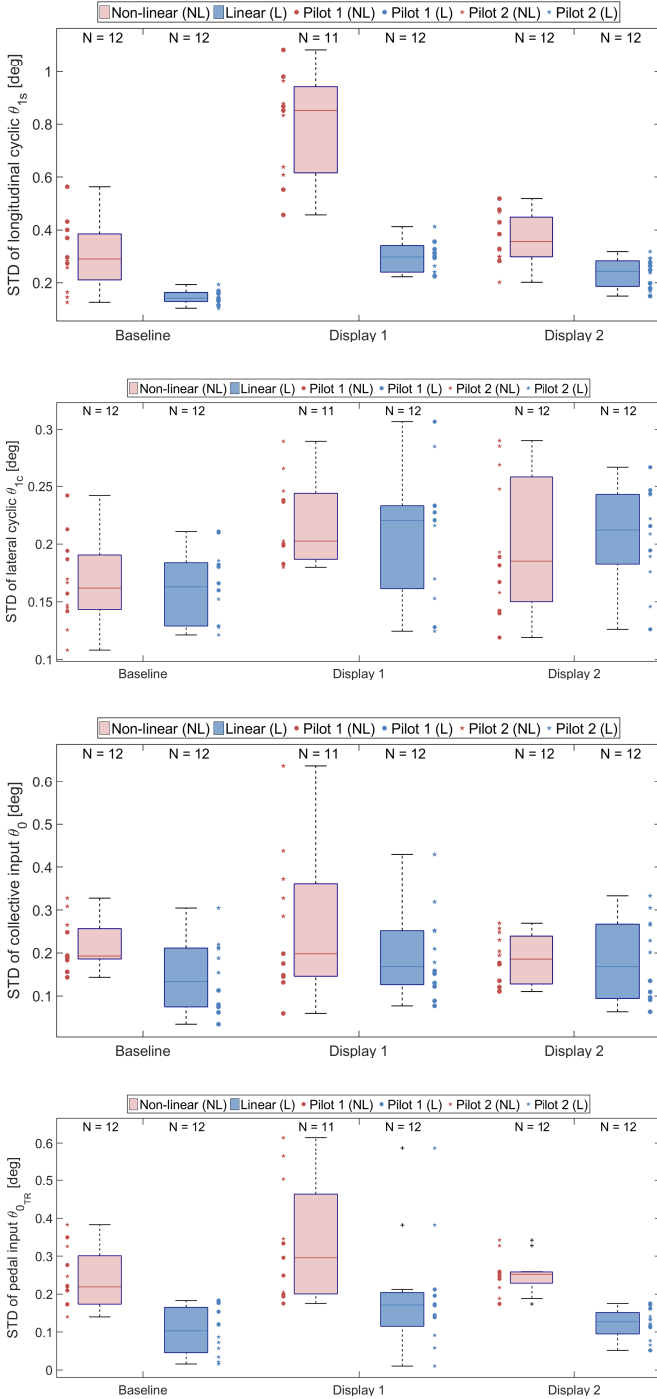


Fig. 10: Boxplots of control input variance during hover; from top to bottom: longitudinal cyclic, lateral cyclic, collective, pedals

However, no difference in control activity can be witnessed between display conditions during the approach phase.

#### D. Workload

Referring to Table IV, pilots experienced higher mental effort in runs with the non-linear model than with the linear model. Furthermore, workload was rated higher in brownout

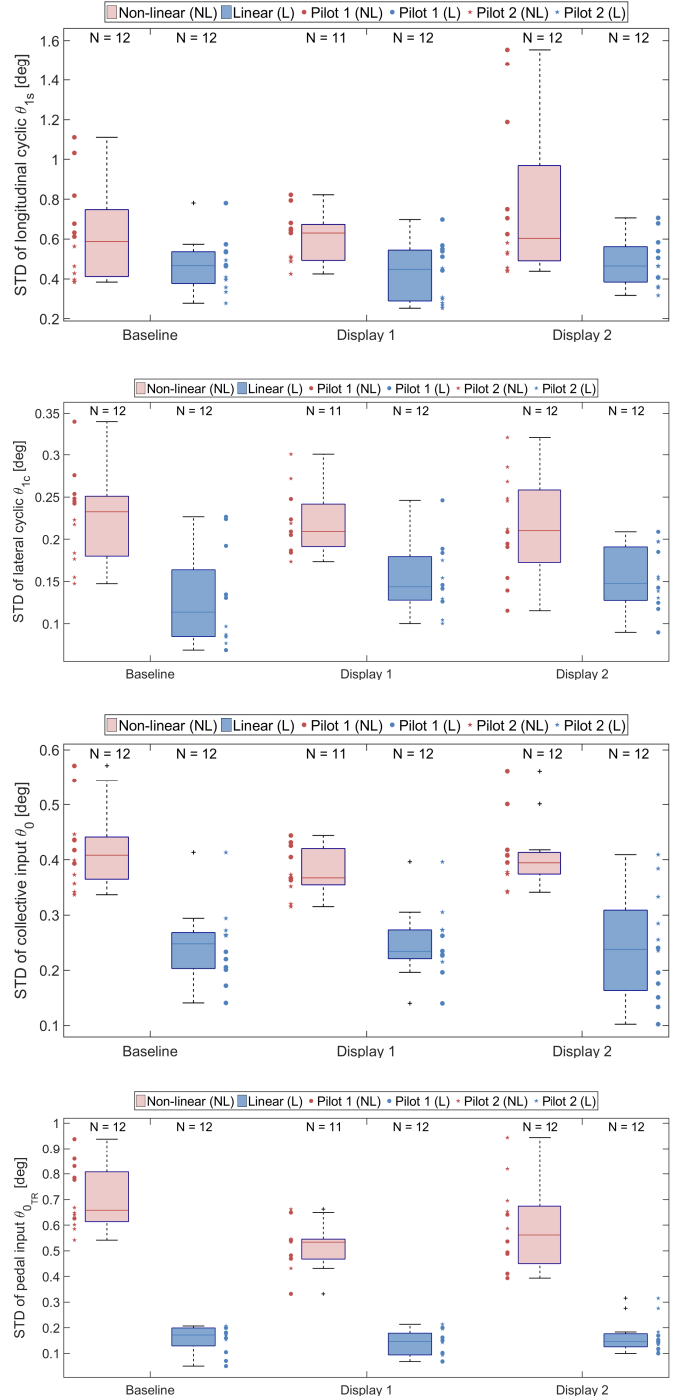


Fig. 11: Boxplots of control input variance during approach; from top to bottom: longitudinal cyclic, lateral cyclic, collective, pedals

conditions than in good visibility. Overall, these findings are in line with the hypotheses. However, a more noticeable difference was expected between Display 1 and 2.

### E. Situation Awareness

The results, shown in Table V, demonstrate that pilot situation awareness was higher in good visibility than with either of the developed displays, as was expected. Furthermore, the linear model led to improved situation awareness compared to the non-linear model, confirming the hypothesis.

### F. Pilot Opinion

The outcome of the pilot opinion questionnaires provides further information on the usefulness of the displays. One pilot reported having difficulty in judging longitudinal position with both types of ADS-33 display (i.e., both good visibility and Display 2), as it was not clear for this participant which longitudinal line (Display 2) or row of cones (baseline condition) to align with. With regards to Display 2, the same pilot further noted having difficulty perceiving altitude except when flying very close to a marker line.

Both pilots pointed out that a slight overshoot when inside the hover box of Display 1 caused them to leave the box and lose reference of the target. Interestingly, concerning his confidence in fulfilling the task, pilot 1 gave a score of 3/7 for Display 1 compared to 6/7 and 5/7 for good visuals and Display 2, respectively, while performance with that display was in fact comparable to the baseline condition.

## V. DISCUSSION

This experiment investigated the effects of two conformal symbology displays and two different vehicle models on hover performance, control activity, workload and situation awareness. As only two pilots were available to participate in the experiment, no statistical analysis was performed. Nevertheless, the presented results provide some useful insight on the differences between the various display configurations and the two vehicle models.

### A. Displays

Interestingly, in terms of hover performance, Display 1 (grid and box) allowed similar and at times even better performance

than in good visibility. Not only did that display configuration have the lowest RMS position error, it was also the only condition that allowed pilots to consistently stay within adequate performance boundaries during hover. These results are in contrast with the hypothesis that performance would decrease in brownout. A possible explanation for these results is that, when hovering at the target location, the cues included in the box and the grid are close-by. Therefore, a small displacement leads to relatively large apparent deviation from the target, allowing the pilots to remain closer to the target than with the ADS-33 hover board. However, a limitation of this display was the lack of far field reference; if pilots moved beyond the box, they lost all reference of target location.

Display 2 (geometric version of the ADS-33) performed worse both during approach and during hover. Pilots reported having difficulty judging their altitude, especially in the approach phase. This was most likely due to the low amount of optic flow available in this interface, as it lacked the ground texture present in good visibility and in the other display.

For all conditions, the RMS error was largest in the  $x$ -axis. This was in part likely due to the longitudinal approach, which caused a relatively large longitudinal error at the start of the hover phase and which may have also led to some remnant oscillations along that axis. However, it is possible as well that longitudinal positioning cues were less readily available than lateral or vertical cues. For Display 2, this outcome is in line with results from an experiment in which a similar ADS-33 overlay was provided on a narrow field-of-view HMD [12].

Considering control behavior, pilots were found to apply a similar decelerating approach with each of the display configurations. This is further supported by the finding that, during the approach phase, control activity was comparable between display conditions. During hover, however, control activity was higher in brownout conditions, especially when considering inputs on the lateral cyclic. In terms of longitudinal control, Display 1 in combination with non-linear dynamics exhibited much larger control activity than other conditions. Again, this may be an effect of the close proximity of the available cues when using this display; deviations may seem larger than they are, leading to increased corrective action. Higher control activity in brownout conditions is in line with the hypothesis, but the difference between the two display configurations is less notable than expected.

Results of the subjective ratings on situation awareness and workload show similar trends. As predicted for brownout conditions, situation awareness decreased and workload increased relatively to the conditions with clear visuals.

### B. Helicopter Dynamics

The helicopter dynamics had a noticeable influence on control activity. Both during approach and hover, the non-linear model required considerably more control activity. In turn, this led the pilots to rate their workload and situation awareness to be higher in conditions with the non-linear model. These findings are in line with the hypothesis. However, it was expected to also see a clear effect of vehicle model on performance measures, but no such influence was detected. This implies that

TABLE IV: Z-scored workload ratings

	Baseline		Display 1		Display 2	
	non-lin.	linear	non-lin.	linear	non-lin.	linear
Pilot 1	-0.81	-1.29	1.61	0.16	0.16	0.16
Pilot 2	-0.72	-1.21	0.52	-0.39	1.60	0.19
Mean	-0.76	-1.25	1.07	-0.11	0.88	0.18

TABLE V: Z-scored situation awareness ratings

	Baseline		Display 1		Display 2	
	non-lin.	linear	non-lin.	linear	non-lin.	linear
Pilot 1	0.91	1.51	-1.1	-0.70	-0.30	-0.30
Pilot 2	-0.05	1.69	-0.92	0.39	-1.06	-0.05
Mean	0.43	1.60	-1.01	-0.16	-0.68	-0.18

vehicle dynamics were not a limiting factor on performance; instead, in order to ameliorate performance, the availability of positioning cues in the display configurations should be improved.

### C. Recommendations

Although no statistical tests were performed, some important trends could be discerned from the results that point to possible improvements in future versions of the visual augmentations.

Longitudinal positioning cues were less readily available than lateral or vertical ones, in each of the displays. Even in good visibility, pilots described experiencing difficulties finding the right information in the ADS-33 course for accurate longitudinal positioning during hover. These issues were further amplified in the geometric ADS-33 version (Display 2), probably due to the lack of ground texture. In good visibility, pilots are instructed to use a point of reference far away in the visual field to stabilize their hover. Such a point of reference was presently not available in Display 1 (once inside the box), therefore it is recommended to adjust this configuration for future research to include one. Several methods are possible; for example by simply adding the reference pole and hover board that are in front of the target in the ADS-33, or by extending the hover box such that it bears resemblance to tunnel-in-the-sky displays, with the end of the tunnel serving as the reference point.

As performance was found to be best in conditions with Display 1 (grid and box), it is worth investigating whether the grid (or even the entire display) would also be beneficial and improve performance in good visibility. The geometric version of the ADS-33 (Display 2) showed worst performance and should be critically evaluated. An updated version of that display should *at least* contain additional ground texture. It may be worth researching first how the ADS-33 in good visibility can be usefully augmented, before revisiting the geometric ADS-33 design of Display 2.

A clear limitation of this experiment was the small number of test subjects. Future experiments should aim at a higher number of participants, such that a statistical analysis can be performed.

## VI. CONCLUSION

This paper investigated the effectiveness of two display configurations for hover support in brownout conditions and the influence of helicopter dynamics.

The results of a small-scale simulator experiment indicate that a display design with a grid ground texture and hover box was the best performing configuration, although it lacked visual reference in the far field. In terms of dynamics, decreased control activity and workload was registered with the linear model relative to the non-linear model. However, this did not lead to notably better performance.

Based on these results, it is recommended to adjust the grid and box display such that it contains a reference point in the far field which pilots can use during hover. Results further indicate that a grid texture may be a beneficial addition in good visibility too.

## REFERENCES

- [1] M. Syal and J. G. Leishman, "Modeling of bombardment ejections in the rotorcraft brownout problem," *AIAA Journal*, vol. 51, no. 4, pp. 849–866, 2013.
- [2] A. J. Benson and J. R. R. Stott, "Spatial Disorientation in Flight," in *Ernsting's Aviation Medicine* (D. J. Rainford and D. P. Gradwell, eds.), ch. 28, pp. 433–458, London, United Kingdom: Hodder Arnold, 4 ed., 2006.
- [3] M. Couch and D. Lindell, "Study on Rotorcraft Safety and Survivability," in *Proceedings of the 66th American Helicopter Society Forum*, (Phoenix, AZ, United States), May 10–13, 2010.
- [4] Task Group HFM-162, "Rotary-Wing Brownout Mitigation: Technologies and Training," tech. rep., (RTO-TR-HFM-162), Brussels, Belgium: NATO, 2012.
- [5] Federal Aviation Administration, "Basic Flight Maneuvers," in *Helicopter Flying Handbook*, ch. 9, pp. 9.1–9.20, Oklahoma City, OK, United States: U.S. Department of Transportation, FAA-H-8083-21B ed., 2019.
- [6] R. A. Hess and P. J. Gorder, "Design and evaluation of a cockpit display for hovering flight," *Journal of Guidance, Control, and Dynamics*, vol. 13, no. 3, pp. 450–457, 1990.
- [7] M. M. Eshow and J. A. Schroeder, "Improvements in Hover Display Dynamics for a Combat Helicopter," *Journal of the American Helicopter Society*, vol. 38, no. 1, pp. 17–28, 1993.
- [8] D. Friesen, M. D. Pavel, C. Borst, P. Masarati, and M. Mulder, "Pilot Model Development and Human Manual Control Considerations for Helicopter Hover Displays," in *45th European Rotorcraft Forum*, (Warsaw, Poland), September 17–19, 2019.
- [9] H.-U. Doehler, P. M. Knabl, S. Schmerwitz, T. W. Eger, and O. Klein, "Evaluation of DVE Landing Display Formats," in *Proceedings of SPIE 8360, Airborne Intelligence, Surveillance, Reconnaissance (ISR) Systems and Applications IX*, (Baltimore, MD, United States), April 23–27, 2012.
- [10] K. A. Feltman, I. Curry, K. Bernhardt, A. Hayes, S. Kirby, B. Davis, J. Sapp, D. Durbin, and G. Hartnett, "Integrated Cueing Environment: Simulation Event Four," tech. rep., (ARL-TR-8538), Fort Rucker, AL, United States: U.S. Army Aeromedical Research Laboratory, 2018.
- [11] N. A. Stanton, K. L. Plant, A. P. Roberts, C. K. Allison, and C. Harvey, "The virtual landing pad: facilitating rotary-wing landing operations in degraded visual environments," *Cognition, Technology and Work*, vol. 20, no. 2, pp. 219–232, 2018.
- [12] F. X. Viertler, *Visual Augmentation for Rotorcraft Pilots in Degraded Visual Environment*. Ph.D. dissertation, Fakultät für Maschinenwesen, Technische Universität München, Munich, Germany, 2017.
- [13] H.-U. Doehler, S. Schmerwitz, and T. Lueken, "Visual-conformal display format for helicopter guidance," in *Proceedings of SPIE 9087, Degraded Visual Environments: Enhanced, Synthetic, and External Vision Solutions 2014*, (Baltimore, MD, United States), May 5–9, 2014.
- [14] T. Münsterer, M. Kress, and S. Klasen, "Sensor based 3D conformal cueing for safe and reliable HC operation specifically for landing in DVE," in *Proceedings of SPIE 8737, Degraded Visual Environments: Enhanced, Synthetic, and External Vision Solutions 2013*, (Baltimore, MD, United States), April 29–May 3, 2013.
- [15] M. T. Curtis, F. Jentsch, and J. A. Wise, "Aviation Displays," in *Human Factors in Aviation*, pp. 439–478, Burlington, MA, United States: Elsevier, 2010.
- [16] J. Crawford and A. Neal, "A Review of the Perceptual and Cognitive Issues Associated With the Use of Head-Up Displays in Commercial Aviation," *The International Journal of Aviation Psychology*, vol. 16, no. 1, pp. 1–19, 2006.
- [17] L. J. Prinzel and M. Risser, "Head-Up Displays and Attention Capture," tech. rep., (NASA TM-2004-213000), Hampton, VA, United States: NASA Langley Research Center, 2004.
- [18] J. J. Gibson, *The Perception of the Visual World*. Cambridge, MA, United States: The Riverside Press, 1950.
- [19] J. J. Gibson, P. Olum, and F. Rosenblatt, "Parallax and perspective during aircraft landings," *American Journal of Psychology*, vol. 68, no. 3, pp. 372–385, 1955.
- [20] J. F. Larish and J. M. Flach, "Sources of Optical Information Useful for Perception of Speed of Rectilinear Self-Motion," *Journal of Experimental Psychology: Human Perception and Performance*, vol. 16, no. 2, pp. 295–302, 1990.
- [21] R. Warren, "Optical transformation during movement: Review of the optical concomitants of egomotion," tech. rep., (AFOSR-TR-82-1028), Columbus, OH, United States: Ohio State University, Department of Psychology, Aviation Psychology Laboratory, 1982.

- [22] J. M. Flach, R. Warren, S. A. Garness, L. Kelly, and T. Stanard, "Perception and Control of Altitude: Splay and Depression Angles," *Journal of Experimental Psychology: Human Perception and Performance*, vol. 23, no. 6, pp. 1764–1782, 1997.
- [23] G. D. Padfield, *Helicopter Flight Dynamics: The Theory and Application of Flying Qualities and Simulation Modelling*. Oxford, United Kingdom: Blackwell Publishing, 2 ed., 2007.
- [24] B. J. Baskett, "Aeronautical Design Standard, Performance Specification: Handling Qualities Requirements for Military Rotorcraft," tech. rep., (ADS-33E-PRF), Redstone Arsenal, AL, United States: U.S. Army Aviation and Missile Command, 2000.
- [25] M. Negrin, A. J. Grunwald, and A. Rosen, "Superimposed Perspective Visual Cues for Helicopter Hovering Above a Moving Ship Deck," *Journal of Guidance, Control, and Dynamics*, vol. 14, no. 3, pp. 652–660, 1991.
- [26] O. Stroosma, M. M. van Paassen, and M. Mulder, "Using the SIMONA Research Simulator for Human-Machine Interaction Research," in *AIAA Modeling and Simulation Technologies Conference and Exhibit*, (Austin, TX, United States), pp. 1–8, August 11–14, 2003.
- [27] T. Gerlach, "Visualisation of the brownout phenomenon, integration and test on a helicopter flight simulator," *The Aeronautical Journal*, vol. 115, no. 1163, pp. 57–63, 2011.
- [28] I. Miletović, D. M. Pool, O. Stroosma, M. D. Pavel, M. Wentink, and M. Mulder, "The Use of Pilot Ratings in Rotorcraft Flight Simulation Fidelity Assessment," in *Proceedings of the 73rd American Helicopter Society Forum*, (Fort Worth, TX, United States), May 9–11, 2017.
- [29] D. T. McRuer and H. R. Jex, "A Review of Quasi-Linear Pilot Models," *IEEE Transactions on Human Factors in Electronics*, vol. HFE-8, no. 3, pp. 231–249, 1967.
- [30] B. T. Sweet, *The Identification and Modeling of Visual Cue Usage in Manual Control Task Experiments*. Ph.D. dissertation, Department of Aeronautics and Astronautics, Stanford University, Stanford, CA, United States, 1999.
- [31] D. de Waard, *The Measurement of Drivers' Mental Workload*. Ph.D. dissertation, Rijksuniversiteit Groningen, Groningen, Netherlands, 1996.
- [32] M. T. Curtis, F. Jentsch, and J. A. Wise, "Situational Awareness Rating Technique (SART): The development of a tool for aircrew systems design," in *Situational Awareness in Aerospace Operations*, pp. 3.1–3.17, Neuilly-Sur-Seine, France: NATO Advisory Group for Aerospace Research and Development, 1990.
- [33] J. E. Bos, S. N. MacKinnon, and A. Patterson, "Motion Sickness Symptoms in a Ship Motion Simulator: Effects of Inside, Outside, and No View," *Aviation Space and Environmental Medicine*, vol. 76, no. 12, pp. 1111–1118, 2005.

## **Part II**

# **Literature Study**

**This part has already been graded as part of the course AE4020.**



---

## Chapter 2

---

# Brownout

Brownout is a phenomenon that occurs when the rotor wake of a low-flying helicopter stirs up loose particles in the environment, typically in dry climates. It results in a condition that is difficult to fly in as the sand or dust cloud causes the OTW view of the pilot to be (partially) obscured, see Figure 2-1. In this chapter, the development and simulation of such clouds is discussed, as well as the effects this condition has on the situational awareness of the pilot.



**Figure 2-1:** Aerial view of a brownout forming around a landing helicopter (photo credit: U.S. Army<sup>†</sup>)

---

<sup>†</sup>Retrieved from: <https://api.army.mil/e2/c/images/2015/02/25/383009/original.jpg>

## 2-1 Characteristics

In order to be able to realistically simulate a brownout, it is essential to have a thorough understanding of the factors that play a role in its development. Besides gaining insight in its formation, also being aware of previous attempts at mitigating the risks associated with flying in such conditions is important; both topics are covered in this section.

### 2-1-1 Formation and development

The rapid rotation of the rotor blades is what allows a helicopter to generate lift. The pilot is able to control the amount of lift generated using the collective, which adjusts the pitch angle of all blades relative to the incoming air. As the blades are rotating, the incoming air is deflected downwards; this effect is known as downwash. Due to the quick rotation of the rotary wings, each blade in fact experiences a reduced angle of attack due to the downwash effect caused by the previous blade.

In flight at high altitudes this downwash effect typically does not have any adverse effects, and the air that is accelerated downwards quickly dissipates into the ambient air; this is known as the out of ground effect (OGE). At lower altitudes, on the other hand, the downwash cannot escape as easily and this leads to the so-called in ground effect (IGE). As shown in Figure 2-2, the vertical velocity of the downwash becomes zero at the ground. This results in a mass of air that is effectively trapped between the ground and the helicopter, thereby reducing the amount of incoming air that is able to flow through the rotor blades [6]. The interaction of the rotor wake with the surface can give rise to considerable ground vortices (see also Figure 2-3). Empirical evidence indicates that IGE becomes substantial at altitudes approximately equal to the rotor diameter and below [7].

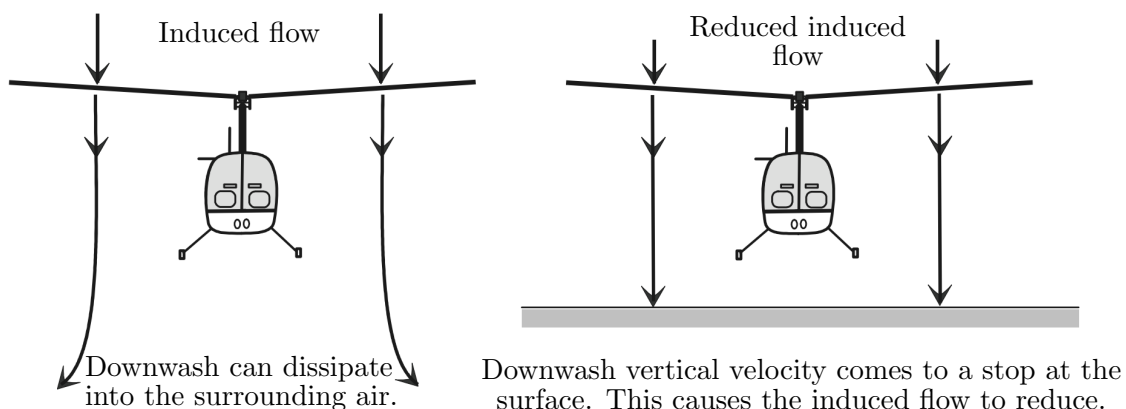


**Figure 2-2:** Rotor downwash in ground effect [6, p. 62]

In arid climates, where there is loose sediment on the ground such as dust or sand, the aerodynamic forces arising from the IGE can drive particles from the ground into the air. The resulting particle cloud is known as brownout if it consists of sand or dust; in the case of snow, the phenomenon is referred to as whiteout. Figure 2-3 shows a schematic of the development of such a brownout cloud.

In order for a particle to be ejected into the air, the aerodynamic force exerted on it must be larger than the gravitational and cohesive forces that keep it in place on the ground. A particle may be lifted from the surface through resonance, by rolling and bouncing off rough edges, or by an ejection event in the ground vortices [8]. Smaller particles are entrained in the flow and become part of the brownout cloud, i.e., they go into suspension. Larger particles, however, descend back to the ground where they will bounce along the surface under the influence of aerodynamic forces, a process known as saltation [9]. The resulting collisions with particles on the ground cause further sediment uplift, thereby expanding the brownout cloud as more of the smaller particles are being entrained in it.

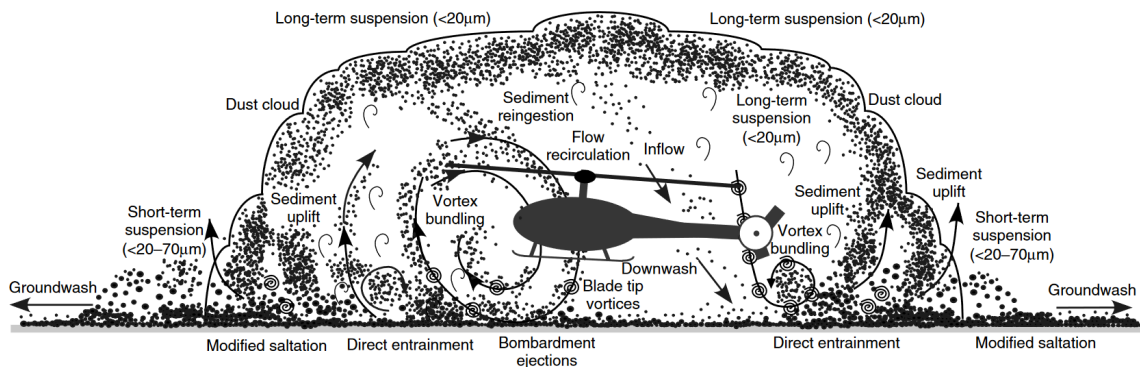


**Figure 2-3:** Schematic of the physics involved in brownout cloud development [10]

Several factors influence the severity of a brownout cloud. From the preceding discussion, it follows that the aerodynamic effects of the blade rotation appear to play a major role in the development and evolution of the brownout phenomenon. Hence, the helicopter design determines at least to some extent the severity of the brownout. Number of main rotors [9], blade twist [11], and disk loading (ratio of thrust over rotor disk area) [12] are among the design parameters that affect the cloud development. Other examples include the weight of the helicopter, number of blades, blade chord length, rotational speed of the rotor, and rotor tip speed. However, it is difficult to isolate and study each of these parameters and their effects on the brownout formation individually, as they have many aerodynamic interdependencies [13]. Thus, much remains unknown about the exact effect each of these parameters has on the resulting brownout formation.

Besides the helicopter design, environmental factors also play a role. The forming of a brownout depends on the existence of loose dust or sand particles on the surface, hence when the soil is more humid the resulting cloud – if at all present – will be much less severe. Likewise, wind around the helicopter interferes with the airflow and this affects the aerodynamic forces that shape the particle cloud. Different distributions of particle sizes also lead to different brownout conditions, in a way that is not yet well-understood [1].

### 2-1-2 Mitigation strategies

Several research studies have focused on attempting to postpone the onset of brownout cloud development or reduce the severity of the phenomenon by adjusting certain helicopter design parameters [13, 14, 15, 16]. This parameter tweaking typically involves the rotor blade designs,

as the aerodynamic effects of the blade rotation seem to be of major importance in the development and evolution of brownouts, as discussed in the previous subsection. As the exact influence of each design parameter is still unknown and their effects are difficult to investigate individually due to their interdependent aerodynamic relations [13], it is not possible to rely solely on rotorcraft design optimization for reducing the severity of brownout clouds, nor will such optimization eliminate all the risks associated with flying in brownout conditions.

Other solutions that mitigate the brownout effects may involve optimization of flight trajectories. The optimization-based methodology proposed by Tritschler et al. [10], which focuses on the aerodynamic interaction of the rotor wake with the ground, was found to generate flight paths that result in less severe brownout development. Furthermore, time spent in a brownout during the optimized approach profiles was shorter than during approaches normally flown, because they typically involve more aggressive strategies than applied naturally by the pilot.

Brownout mitigation strategies, however, are still in their infancy and both the helicopter design techniques as well as the methods involving trajectory optimization need to be further investigated before they can be widely applied. No such strategy will manage to completely remove the dangers associated with flight in brownout conditions, hence additional pilot support systems are still needed to improve the safety of helicopter flight in DVE.

Such support systems might involve haptic cueing, an example of which is the FlyTact display developed by TNO and the Royal Netherlands Air Force [17]. The FlyTact display is effectively a vest containing many tactors that can provide information on altitude and ground speed to the wearer (i.e., the pilot), by giving physical stimuli in the form of vibrations at different locations on the body. A test pilot wearing the vest was able to perform a landing maneuver in a brownout more accurately and with lower mental effort. Despite the promising results, the researchers also note that several aspects of these haptic aids require further investigation, such as the positioning of the tactors on the body and mitigation of the adverse effects of overstimulation.

The most researched means to achieve increased levels of safety while flying in a brownout are visual support systems. The earliest of these studies investigated using a head-down display (HDD), while more recent research tends to focus on synthetic vision systems or AR displayed on HMDs as a way of providing the pilot with visual information about the environment. These types of displays, specifically those for supporting the hover maneuver in brownouts, are covered in Section 3-3.

## 2-2 Simulating the effect

As described in the previous section, the environmental factors and helicopter design parameters that influence the development of brownout clouds are not completely understood yet. Therefore, the modeling and simulation of the effect is a difficult task that – at least at present – cannot be achieved perfectly.

Nevertheless, several studies have focused on developing computational models that capture the essence of brownout cloud formation. Examples of said studies apply Navier-Stokes Computational Fluid Dynamics [18], Lagrangian methods [19], or a combination of both [9] to simulate the evolution of the clouds. Despite having shown to provide realistic brownout

predictions, these techniques require many calculations to be completed at every time step, making the full versions of these models unsuitable for use in real-time simulation in which computational speed is a crucial factor [20]. They are, however, highly useful in investigating the (relative) influence of various factors on brownouts and in gaining a better overall understanding of the phenomenon.

Considering that the to-be-designed brownout simulation will not be used for the latter purpose, and in fact will only be visible on the OTW view of the pilots in a flight simulator, such elaborate modeling of the phenomenon is excessive. Instead, the simulation merely needs to resemble a brownout from the pilot's perspective. This does mean, though, that sufficient particle (rotational) motion should be present in the simulated cloud, in order for it to be realistic enough to trick pilots into believing they are flying in a brownout (and ideally are experiencing the false motion cue ofvection, see Section 2-3-1). Developing such a simulation to a satisfactory level, without resorting to complicated physical modeling, is possible using dynamic particle systems in the open-source 3D graphics library OpenSceneGraph (OSG), as shown by a research group at the Deutsches Zentrum für Luft- und Raumfahrt (DLR) [20].

## 2-3 Pilot situational awareness

It is self-evident that the SA of the pilot is negatively affected when the OTW view is obscured. The loss of visual reference and the (rotational) movement of the particles in the pilot's field of view can provide incorrect motion cues, further deteriorating his or her SA. The extent to which visual cues are unavailable due to poor outside visibility can be indicated on a rating scale. Such a tool can be used to determine the necessary steps that must be taken to counteract the adverse effects caused by the loss of visual cues. Both the false motion cues as well as the rating scale are the subjects of the current section.

### 2-3-1 False motion cues

Humans perceive information about their orientation and motion through various sensory systems. The role of the visual system will be covered in detail in Chapter 4. The vestibular system is located in the inner ear and is composed of the otoliths, which detect linear acceleration, and the semicircular canals, which are sensitive to angular acceleration. Another such system is the proprioceptive system, which provides orientational information using sensory receptors across the body. Finally, also the auditory system plays a small role in the perception of orientation. The central nervous system combines information from all these different channels to construct an integrated perception of body position and movement.

When the central nervous system receives conflicting information from different sensory systems, this can lead to spatial disorientation (SD) of the pilot. This kind of sensory mismatch occurs regularly during flight in brownout conditions, causing perilous situations.

One destructive event that can occur in brownouts is known as *dynamic rollover*. It can happen when, just before touch-down, the helicopter enters a turn at a rate below the perception threshold of the vestibular system, which is about  $0.5^\circ/\text{s}^2$  for rotation about the x- and y-axis and approximately  $0.14^\circ/\text{s}^2$  for rotation about the z-axis [21]. Hence, the vestibular system does not notice the lateral drift, nor is it registered visually as the OTW view is blocked by

the brownout. If this drift is large enough, it can cause a roll moment upon first contact with the ground that leads the helicopter to roll over and impact the surface with the rotors [22].

The previous example is in fact closely related to a form of SD known as *the leans*, which often occurs when the pilot has no visual reference of the horizon. When a helicopter enters a rolling motion at a rate undetectable by the semi-circular canals, after some time the pilot will notice this on the instrument panel and exert a corrective control input, bringing the craft back to straight level flight. However, if this control action causes motion that is above the perception threshold, the vestibular system can then actually give the pilot the sensation of leaning to a side rather than flying straight, as it only perceived the latter (corrective) motion and not the initial movement [2].

Another type of SD that can arise due to misinterpreted vestibular inputs in the absence of good visual cues is the so-called *somatogravic illusion*, or pitch-up illusion, in which a linear acceleration along the direction of motion is mistakenly perceived as a pitch-up movement [23]. The opposite can happen too; then, the pilot mistakes a linear deceleration for a pitch-down motion.

A visual illusion that can occur in brownouts is *vection*, which is a false sensation of self-motion when in fact no such movement is present. In GVE it can occur when hovering over water or grass fields, as the influence of the downwash of the blades on the optic flow field in front of the helicopter causes the pilot to perceive it as forward flow, resulting in the sensation of drifting backward [24]. The effect is caused in brownout conditions by the (rotational) movement of the particles in the cloud. Vection can be circular (inducing the sensation of pitch, roll or yaw rotations) and/or linear (incorrectly causing translational motion cues along x-, y- or z-axis), and the perceived self-motion is in the opposite direction of the particle movement [2].

### 2-3-2 Usable cue environment

The Aeronautical Design Standard 33E-PRF (ADS-33), originally developed for the U.S. military, defines requirements for helicopter handling qualities [25]. It stipulates performance specifications, design criteria and flight testing techniques. An example of such a technique, or mission task element (MTE), is the hover maneuver, detailed in Chapter 3. These MTEs are used to investigate whether a specific helicopter has adequate handling qualities in all flight conditions envisaged during operation.

A useful concept introduced in the ADS-33 is the usable cue environment (UCE), shown in Figure 2-4. When pilots fly during the night, in bad weather conditions, or in brownouts or whiteouts, they lose (part of) their outside visual reference. Pilots can indicate the degree to which they lack visual cues in such circumstances on the visual cue rating (VCR) scale, defined in Figure 2-5, which is then used to determine the UCE level. Typical UCE levels during brownout are 2, in mild cases, and 3, in more severe situations.

When UCE levels are higher than 1, the ADS-33 specifies that a stability and control augmentation system (SCAS) must be used to obtain handling qualities similar to those of UCE level 1. The required response types per UCE level as indicated in the ADS-33 are shown in Table 2-1 for hover and low speed. However, the use of such control augmentation comes at the expense of diminished agility and aggressiveness. Instead, another way to improve the safety and handling qualities in DVE is by means of providing a display that compensates for

the lack of outside visual cues, resulting in an improved VCR score and thus a lower UCE level [26].

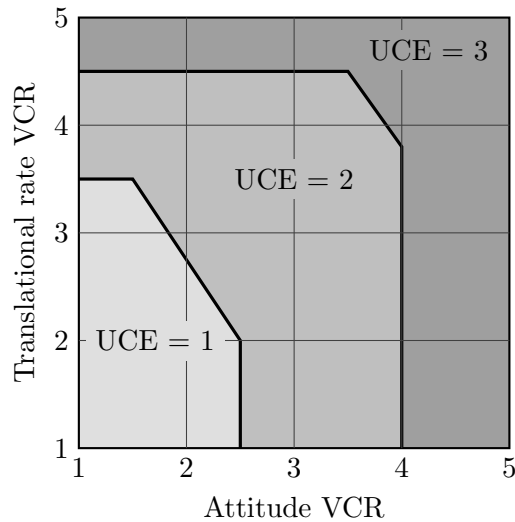
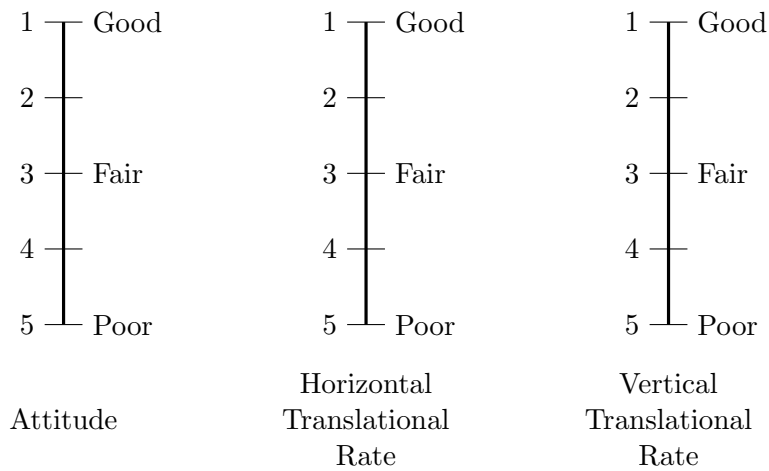


Figure 2-4: Usable cue environment [25]



Pitch, roll, and yaw attitude, and lateral-longitudinal, and vertical translational rates shall be evaluated for stabilization effectiveness according to the following definitions:

- Good: Can make aggressive and precise corrections with confidence and precision is good.
- Fair: Can make limited corrections with confidence and precision is only fair.
- Poor: Only small and gentle corrections are possible, and consistent precision is not attainable.

Figure 2-5: Visual cue rating scale [25]

**Table 2-1:** Required response types per UCE level, for hover and low speed [25]

UCE level	Response type
UCE 1	Rate command
UCE 2	Attitude command, altitude hold (pitch and roll)
	Rate command, direction hold (yaw)
UCE 3	Rate command, height hold (heave)
	Translational rate command
	Rate command, direction hold (yaw)
	Rate command, height hold (heave)
	Position hold (horizontal plane)

---

## Chapter 3

---

# Hover Maneuver

The hover maneuver is unique to helicopters and is one of the abilities that truly sets them apart from fixed wing aircraft. Along with their low-altitude flying and vertical takeoff and landing (VTOL) capabilities, hovering is what allows helicopters to be conveniently used in search and rescue missions, offshore operations and for emergency medical services.

A helicopter is said to hover when it maintains a constant position, altitude, heading and rotor blade revolutions per minute (RPM). The result is an almost motionless flight over a reference point. It is a commonly performed maneuver by helicopter pilots as it is typically the first step after liftoff and the final step before touchdown. As such, the maneuver generally occurs close to the ground surface.

In this chapter, the typical control strategy pilots employ during hover and the knowledge of helicopter states that they require to do so safely and successfully is investigated. Furthermore, a brief introduction to the physics involved in the maneuver is presented and a hover test course from the ADS-33 is introduced. Finally, some previous efforts at using displays to mitigate the risks associated with hovering in brownout conditions are discussed.

### 3-1 Control strategy

As helicopters are typically dynamically unstable, performing a stationary hover (with constant position, altitude, heading and rotor RPM) requires continuous control input from the pilot. Lateral and longitudinal position can be kept constant through use of the (lateral and longitudinal) cyclic, whereas constant altitude is maintained by using the collective. Pilots control heading with the pedals and rotor RPM is handled with the throttle.

When discussing pilot control strategies, it is convenient to draw a (simplified) diagram of the relevant control systems. Such diagrams also promptly indicate the aircraft states the pilot requires information of in order to close the loops, and, as such, be able to hover successfully. Figure 3-1 shows a longitudinal control diagram, where subscripts  $p$  and  $c$  denote the pilot and controlled element, respectively, and subscripts  $i$ ,  $m$ , and  $o$  denote the inner, middle and

outer loop. Analogous diagrams for control of heading and lateral or vertical position can be constructed handily.

Note that assembling these control systems independent of each other is a considerable simplification, as the effects of cross-coupling between different axes is neglected. In real helicopters, a single-axis input often results in a multi-axis response. For example, adjusting pitch angle can lead to a change in roll, or a variation in roll causes a change in yaw. Nevertheless, constructing these diagrams is useful in modeling pilot behavior, analyzing the main control loops involved and for determining what state variables are crucial in hover. Doing so, it follows that the pilot needs knowledge on the position, velocity, attitude and angular velocity in each axis, i.e., the state variables  $x$ ,  $y$ ,  $z$ ,  $u$ ,  $v$ ,  $w$ ,  $\theta$ ,  $\psi$ ,  $\phi$ ,  $p$ ,  $q$ , and  $r$ .

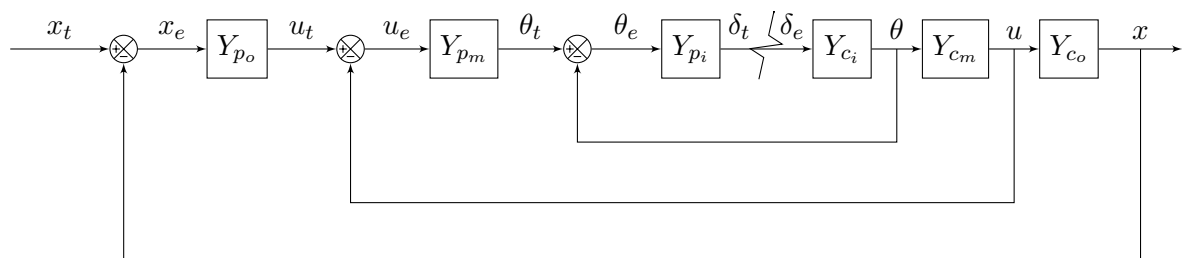


Figure 3-1: Longitudinal control diagram

Performing a hover maneuver solely relying on the airspeed, altitude and attitude indicators in the cockpit is virtually impossible. This is partly due to the fact that it requires substantive mental effort to integrate the data from these various channels during a maneuver that of itself already induces high workload, but also, more importantly, because the information shown on them is not sensitive and accurate enough at low altitudes and velocities [27]. Hence, pilots need to judge their position and attitude visually using reference points in the outside world.

Indeed, in GVE with sufficient visual reference of outside scenery, the Federal Aviation Agency (FAA) instructs pilots to maintain a hover by focusing their visual attention on reference objects some distance ahead of the helicopter in order to notice variations in position and altitude [3]. This point of reference must not be too close, as this might lead to overcontrolling. However, a point very far away is of little use either, as the available motion cues in the visual field become weaker with distance (see also Section 4-2-2).

As such, hovering at a specific target location over nondescript terrain (grass, water, etc.) or in a brownout or other forms of DVE is practically impossible without additional support, either visual or in the form of control augmentation and/or automation. In order to adequately develop a support display for use in such situations, it is helpful to be aware of what typical approach-to-hover profiles look like when executed in GVE.

To acquire aforementioned reference profiles, a mathematical model developed by Heffley may be used, which allows for trajectories of deceleration and ground speed in terms of range, or distance to hover target, to be generated [28]. The model is based on the hypothesis that, as they slow down toward a hover target, helicopter pilots regulate the range rate proportionally to the perceived range. Without resorting to too much detail for the present text, this rate-command behavior is then incorporated into the crossover model (see also Section 6-1), resulting in characteristic deceleration and ground speed profiles as shown in Figure 3-2,

where  $k$  is the proportionality constant, or crossover gain, and length  $A$  is an effective size parameter (used to relate perceived to real range).

In his paper, Heffley describes how  $k$  and  $A$  can be estimated using empirical relationships. The figures below were generated with values of  $k = 0.25/s$  and  $A = 600$  ft. Using these parameters, the maximum value of deceleration as well as the distance from the target at which this peak occurs can be estimated (see Figure 3-2a). The model was shown to closely match trajectories obtained from a flight investigation of 236 visual approaches, conducted by Moen et al. [29], in which the peak values for deceleration occurred approximately 60 m ahead of the target and were measured to be between 0.14g and 0.24g. They further found a significant increase in pitch control activity during the last 120 m, with maximum pitch attitude occurring around the same distance as peak deceleration, its values varying between  $7^\circ$  and  $11.5^\circ$  nose-up relative to the trim pitch.

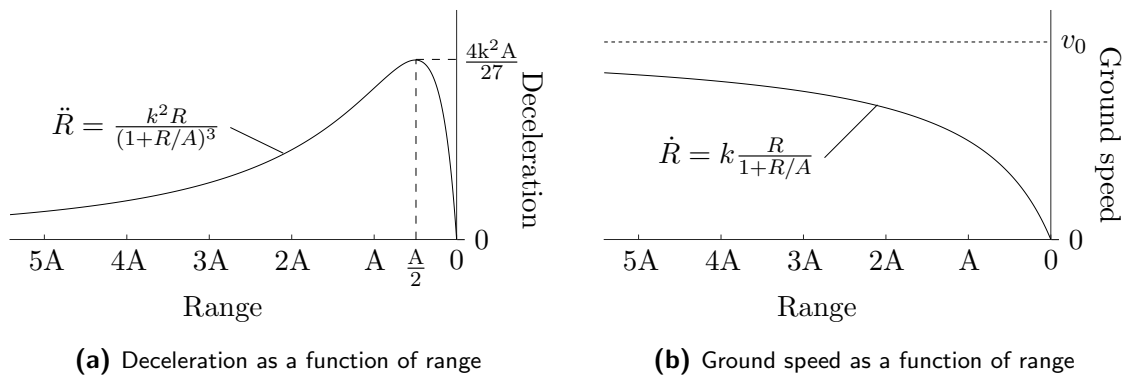


Figure 3-2: Deceleration and ground speed profiles when approaching a hover target

### 3-2 Characteristics

Aiming at improving the safety of performing a hover maneuver in brownout conditions, having a basic understanding of the physics involved in this phase of flight, particularly when performed close to the ground surface, is imperative. At low altitudes, the ground effect comes into play and this also influences the required pilot control action. Furthermore, it is beneficial to be aware of the test courses commonly utilized in research related to the hover maneuver.

#### 3-2-1 Ground effect

The concept of ground effect introduced in Section 2-1-1 also has an influence on the hover maneuver and the power required to achieve it. At altitudes higher than the rotor diameter, the helicopter is hovering out of ground effect (OGE). The vehicle is staying nearly motionless in the same position, hence the forces acting on it are in equilibrium and the total rotor thrust simply balances out the helicopter weight.

As shown before in Figure 2-2, as the helicopter descends to lower altitudes the in ground effect (IGE) starts to play a role, causing the induced flow to decrease. If the blade pitch

angle  $\theta$  is kept constant during this descent, the reduced amount of incoming flow leads to a higher angle of attack  $\alpha$ . In turn, with an increased  $\alpha$  the helicopter generates more rotor thrust and more lift and, as a result, it will start climbing.

In order to maintain a hover after descending to altitudes where the IGE comes into effect, the pilot will have to bring the total thrust force and helicopter weight back in equilibrium by reducing the pitch angle, and thus the angle of attack, by lowering the collective. The effect of this process on the rotor drag is indicated in Figure 3-3. Note how for the same amount of lift, the drag generated is lower when hovering close to the ground. Rotor efficiency rises if the  $L/D$  ratio is improved and the collective lever is lowered [6], hence less power is required to hover IGE than OGE.

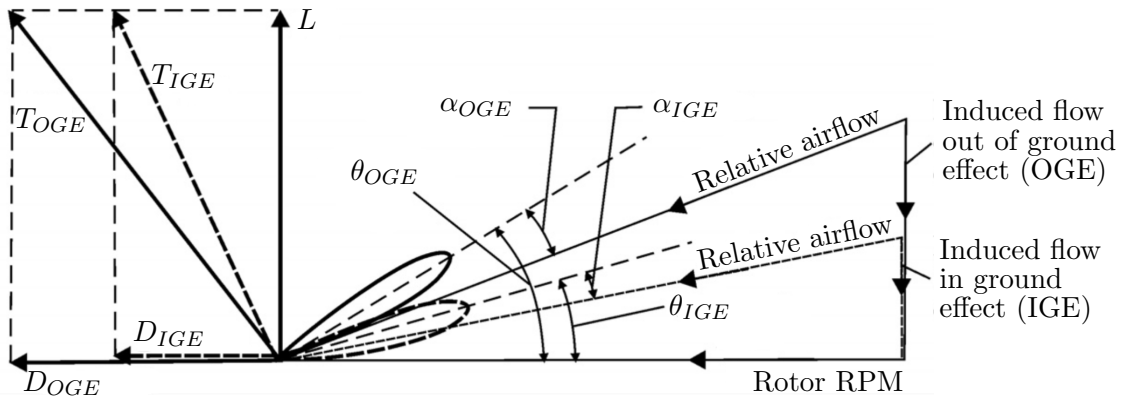


Figure 3-3: Influence of ground effect on rotor drag [30]

The power needed to hover is thrust  $T$  multiplied by induced, or downwash, velocity  $v_i$ , which depends on disk loading  $T/A$  and can be calculated using Equation 3-1 [31].

$$v_i = \sqrt{\frac{T}{A} \frac{1}{2\rho}} \quad (3-1)$$

Analogous to the lift and drag coefficients, these parameters are typically normalized to ease making comparisons between different rotor configurations. The normalized downwash velocity  $\lambda_i$  is obtained by dividing the velocity by the rotor tip speed, i.e., radius  $R$  multiplied by angular velocity  $\Omega$ , whereas the thrust coefficient  $C_T$  is calculated using dynamic pressure times rotor area, comparable to normalization of lift and drag [31]. The normalized power coefficient can then be calculated using Equation 3-2.

$$C_P = C_T \cdot \lambda_i = \frac{T}{\frac{1}{2}\rho(R\Omega)^2(\pi R^2)} \cdot \frac{v_i}{R\Omega} \quad (3-2)$$

### 3-2-2 Test course

Commonly employed test courses in research involving helicopter flight, both in simulation as well as real flight, are those specified in the ADS-33. Introduced before in this text in Section 2-3-2, the ADS-33 stipulates performance specifications, design criteria and flight

testing techniques to ensure adequate helicopter handling qualities in all expected flight conditions [25]. The hover maneuver is one of the mission task elements (MTEs) incorporated in the document, with the course setup as depicted in the figures below.

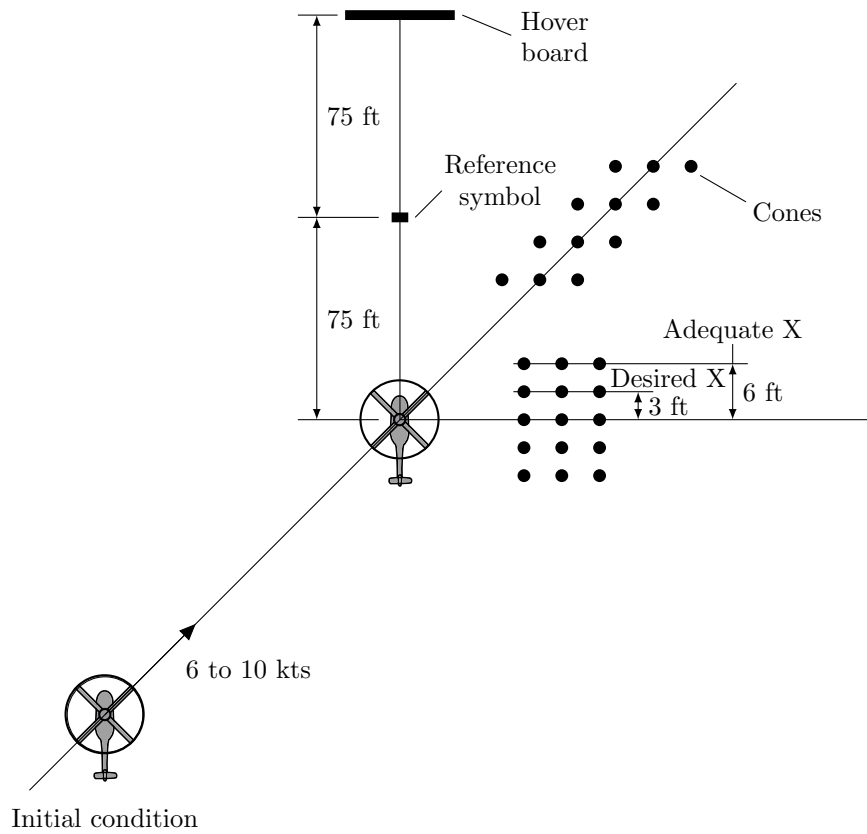


Figure 3-4: Top view of the ADS-33 hover course [25]

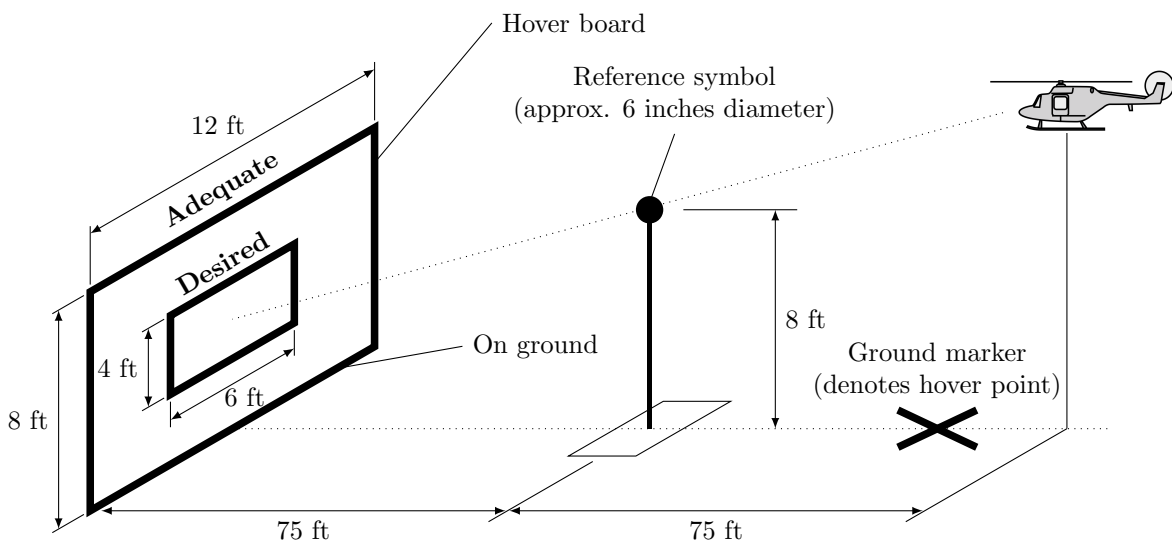


Figure 3-5: Side view of the ADS-33 hover course [25]

**Table 3-1:** Hover performance specification according to the ADS-33 [25]

	Scout/Attack		Cargo/Utility		Externally Slung Load	
	GVE	DVE	GVE	DVE	GVE	DVE
<b>Desired Performance</b>						
• Attain a stabilized hover within X seconds of initiation of deceleration:	3 sec	10 sec	5 sec	10 sec	10 sec	13 sec
• Maintain a stabilized hover for at least:	30 sec	30 sec	30 sec	30 sec	30 sec	30 sec
• Maintain the longitudinal and lateral position within $\pm X$ ft of a point on the ground:	3 ft	3 ft	3 ft	3 ft	3 ft	3 ft
• Maintain altitude within $\pm X$ ft:	2 ft	2 ft	2 ft	2 ft	4 ft	4 ft
• Maintain heading within $\pm X$ ft:	5 deg	5 deg	5 deg	5 deg	5 deg	5 deg
• There shall be no objectionable oscillations in any axis either during the transition to hover or the stabilized hover:	✓*	✓	✓	✓	✓	NA*
<b>Adequate Performance</b>						
• Attain a stabilized hover within X seconds of initiation of deceleration:	8 sec	20 sec	8 sec	15 sec	15 sec	18 sec
• Maintain a stabilized hover for at least:	30 sec	30 sec	30 sec	30 sec	30 sec	30 sec
• Maintain the longitudinal and lateral position within $\pm X$ ft of a point on the ground:	6 ft	8 ft	6 ft	6 ft	6 ft	6 ft
• Maintain altitude within $\pm X$ ft:	4 ft	4 ft	4 ft	4 ft	6 ft	6 ft
• Maintain heading within $\pm X$ ft:	10 deg	10 deg	10 deg	10 deg	10 deg	10 deg

\*Note: ✓ = performance standard applies; NA = performance standard not applicable

The hover task proposed in the ADS-33 instructs an initial altitude below 20 ft with a ground speed of between 6 and 10 knots, at a heading of 45° relative to the target location. Furthermore, it is specified that the transition to hover must be achieved in a smooth maneuver; hence, decelerating considerably well ahead of the target and then slowly approaching the final position is not regarded as satisfactory performance.

Referring to Figures 3-4 and 3-5, the suggested test course contains strategically placed cones and a hover board with reference symbol as cues for three-dimensional position and heading. The separation between the various cones as well as the rectangles drawn on the hover board are proportional to the desired and adequate performance bounds established in the ADS-33, see Table 3-1. Originally developed for the U.S. army, distinctions are made between performance specifications for rotorcraft with various military functions.

### 3-3 Current hover support displays

Early research into hover aid displays, by for example Hess [32] or Eshow [33], predominantly investigated the usefulness of providing information on a HDD. More recent research, however, has shown the limitations of using such HDDs. A study performed in the SIMONA Research Simulator (SRS) at TU Delft concluded that the lack of peripheral cues and optic flow information in such displays as well as the increased demands on the pilot caused an additional time delay that prohibited the pilots from successfully hovering in the absence of OTW information [34].

Therefore, the discussion that follows will focus on displays providing head-up information. Various research groups have been researching synthetic cues on HUDs or HMDs to aid hover performance. Some of these were developed for use in brownout landings and not specifically for hover, but as those displays are generally active during the approach as well and given that pilots typically hover prior to landing, certain features of said displays may prove useful also for hover support.

Several of the HMD solutions that have been developed to allow safe hovering and landing in DVE merely provide overlaid 2D information, often a combination of a bird's-eye view and forward view. Examples of such 2D symbologies are the BrownOut Symbology System (BOSS) developed by the U.S. army (Figure 3-6a), the Degraded Vision Landing Aid (DeV-iLA) by Cassidian (part of former EADS, see Figure 3-6b), and JedEye™ from Elbit Systems (Figure 3-6c).

A research study at DLR evaluated the relative effectiveness of displays with these symbology sets, both as HDD and (monochrome) HMD [35]. They found no significant differences in task load or pilot SA between the various sets, nor did they find evidence that using HMDs led to better task performance than HDDs, despite those being the clear preference of the pilots. The researchers conclude that static 2D formats are not a suitable means for providing guidance data. Moreover, attentional tunneling and cluttering (see also Section 5-2) caused by such 2D overlays are seen as impediments unfavorable to their effectiveness. Therefore, they recommend using 3D conformat imagery in future HMDs, that is, superimposing perspective projections on the pilot's view in a way that is consistent with real world spatial relations (in other words, AR).

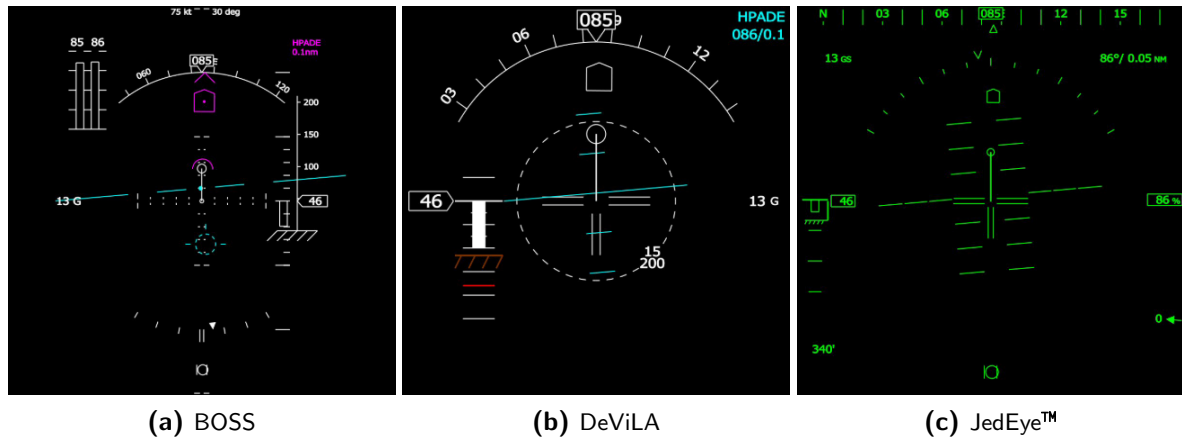


Figure 3-6: Different symbology sets evaluated by Doehler et al. [35]

A display concept that utilizes such conformal imagery, or AR, is the Precision Hover Symbology (PHS) display concept shown in Figure 3-7, developed at the Technical University of Munich [36]. The proposed hover HMD contains elements from the ADS-33 course introduced in Section 3-2-2, albeit somewhat adjusted, such as the hover board with reference marker as well as the heading cones. Two extra hover boards are placed at 30° on either side of the “original”, with extending or retracting triangles on the sides to indicate lateral and vertical drift. Furthermore, a 2D bird’s-eye (i.e., non-conformal) view of the ownship position, to aid horizontal positioning, is superimposed on the other elements. Finally, the display makes use of color-coding to distinguish between synthetic cues and navigation symbols (magenta), terrain visualization (green), database (known) objects (cyan), and unknown objects (red).

Viertler conducted a simulator experiment in which the PHS was presented on a low-cost

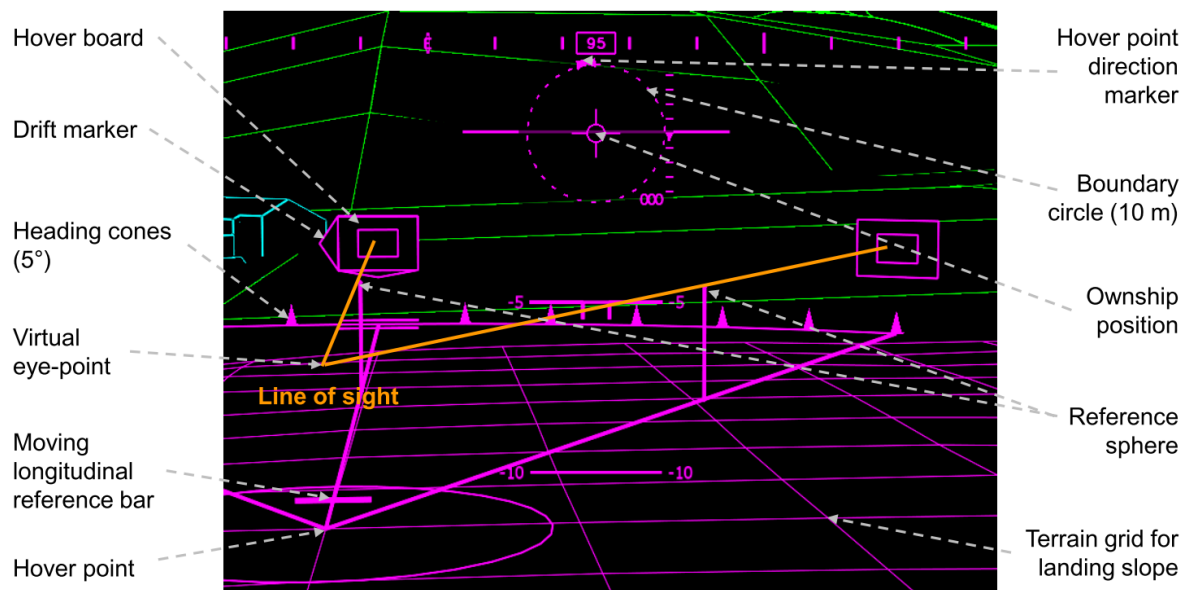


Figure 3-7: PHS display developed at Technical University of Munich [36]

HMD [36]. The results were mixed; the pilot response was generally positive, but in conditions of severe DVE (visibility < 100 m) the display did not provide sufficient assistance to allow precise hover. Particularly along the longitudinal axis the error was substantial, which the researchers argue may be due to the small field of view (FOV) of the HMD and the absence of micro-textures in low visibility. Furthermore, some pilots remarked that the 2D ownship position at times obstructed relevant parts of the conformal scene.

The potential drawbacks of HMDs with limited FOV were also acknowledged by a research group at the University of Southampton, which is why for the development of their virtual landing pad they opted for using a full cockpit HUD instead, anticipating future windshield displays [37]. Their experiment focused on investigating the effect of the HUD on pilot ratings of workload and SA. The results indicate that SA was not significantly different when flying in dense fog with the HUD compared to clear conditions, but pilot workload, both mental and physical, was significantly higher.

Referring to Figure 3-8, their design presents a combination of classic 2D flight instruments and 3D conformal symbology to the pilots. The 3D cues provided are threefold: (1) is a magenta ring that represents the helicopter orientation, when it coincides with the ground-fixed blue ring the helicopter is aligned with the ground; (2) are AR trees (the inner ones 75 ft tall, the outer ones 150 ft) intended to support perception of speed, position and heading; and (3) is a circular landing zone with the center indicating the target location.

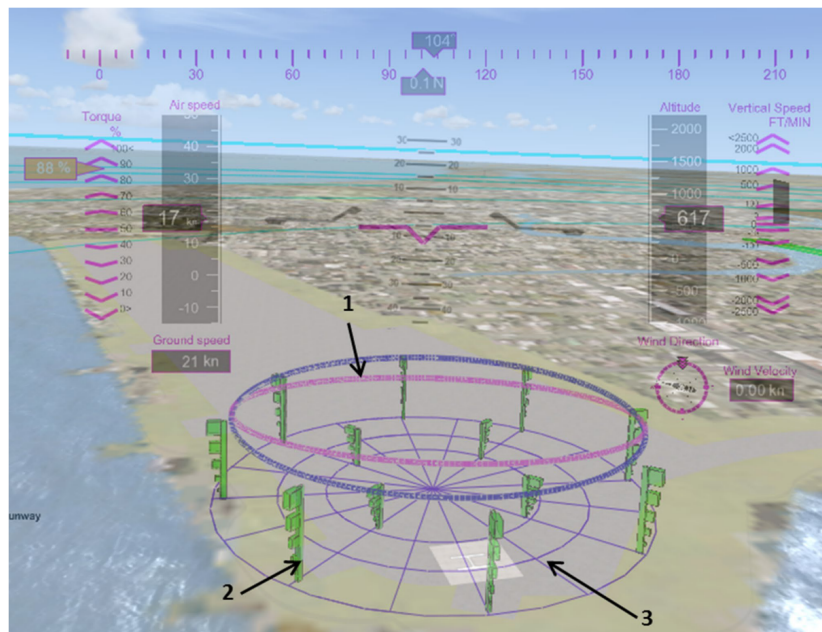


Figure 3-8: Virtual landing pad on a HUD [37]

Using full cockpit HUDs or simply HMDs with larger FOV may potentially allow for improved longitudinal hover performance, but it is nevertheless important to investigate how visual cueing for longitudinal position can be enhanced. An example thereof is the design developed by Bachelder, see Figure 3-9, which provides synthetic cues for control of fore-aft position primarily by adjusting the size of a near frame relative to a constant-size far frame. When the desired hover location is reached, the two frames coincide (center arrows in Figure 3-9a).

Overlaid on a simulated night-vision display (as in Figure 3-9b) together with a horizon line (green) and aircraft attitude indicator (yellow), the design was found to substantially improve hover performance.

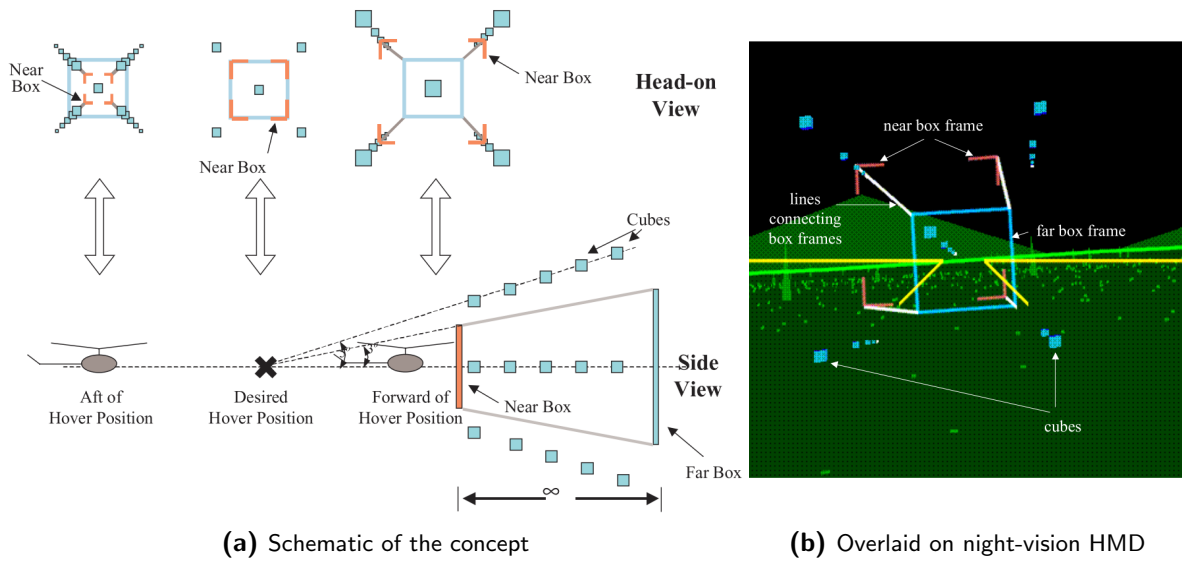


Figure 3-9: Synthetic cue display for longitudinal motion during hover [38]

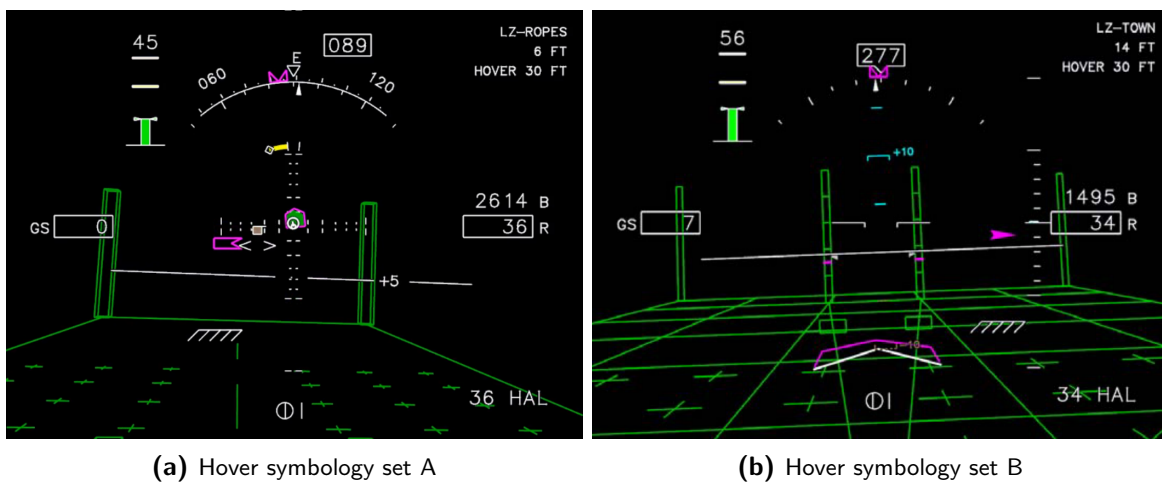


Figure 3-10: Lateral drift indication on landing display by DLR [39]

Pilots need to be aware not only of longitudinal, but also lateral drift. As described in Section 2-3-1, one of the hazards involved with flying in brownouts is when an unnoticed lateral drift occurs prior to touchdown, potentially leading to dynamic rollover. In order to prevent this from happening, DLR has been investigating methods of amplifying sideways drift on HMDs. Following the conclusions of their 2D symbology comparison (Figure 3-6), their

new research focuses on 3D conformal displays. Part of ongoing studies, several configurations have been tested but the principal concept is the same in each, an example of which is shown in Figure 3-10 [39].

The design contains, aside from 2D flight information, a horizon line and a rectangular landing zone with, at the rear end, a dashed line. The pattern of this line moves sideways in the opposite direction of the helicopter; the speed at which it moves correlates with the helicopter's lateral velocity. In an experiment, the researchers compared landing performance with no HMD, a static version of the display, and the dynamic one just described. Highest lateral precision was achieved with the dynamic display, performance approximately a factor of two better than in conditions without the moving pattern.



**Figure 3-11:** Symbology sets evaluated for use in Integrated Cueing Environment (ICE) [40]

As mentioned before, (visual) brownout support systems have also been developed for and by the U.S. army. Since the inception of the first version of aforementioned BOSS (Figure 3-6a), research institutes within the U.S. defense have continued development and the current state of their efforts is the so-called ICE, which combines visual, auditory and tactile cues (using tactors on the seat, belt and pilot's shoulders) tailored to different phases of flight. In terms of visual support, the 2D BOSS is still used but now typically in combination with 3D conformal cueing as well as a synthetic real-time rendering of the environment using laser detection and ranging (LIDAR). One of their more recent studies compares two symbol sets, each adapted for the flight phases en-route, approach, hover and landing [40].

The two sets developed for use during the hover maneuver are shown in Figure 3-11. Each set contains a white line across the screen designating the horizon, and a 3D artificial landing pad, with the poles' height serving as an indication of target altitude for hover. The magenta elements in the displays provide flight path guidance optimized to minimize time spent in brownout conditions. Set A employs a guidance box in the center of the display; pilots maintain their altitude and lateral position by keeping the aircraft icon inside the box. Set B, on the other hand, provides longitudinal guidance in the form of a magenta chevron. The lacking longitudinal guidance in A, and lateral and altitude in the case of set B, was compensated using tactile cueing. Set A was found to be superior in all measures tested, those being performance, biometric, workload, SA, and usability.

Finally, SFERION is the 3D conformal HMD created by Airbus Defense and Space. It combines environmental sensing techniques (LIDAR) and object detection with database information to provide accurate real-time knowledge of the terrain. The conformal imagery depicted on the HMD depends on the flight phase; active during final approach and landing is the symbology shown in Figure 3-12 [41]. During operation it is normally supplemented with 2D flight information.

The conformal part of the design consists of a “doghouse” landing zone, with the 40 m by 40 m grid outlining the measured surface and the triangle indicating preferred heading, and 3D pillars serving as cues for position. The circular landing zone tilts in accordance with the real surroundings, and thus it serves as an indication of the slope of the landing zone. The thicker poles at the corner of the taller columns represent the current height above ground. Furthermore, during the approach five chevrons are displayed on the ground surface for pilot guidance to the landing zone (not shown in figure).

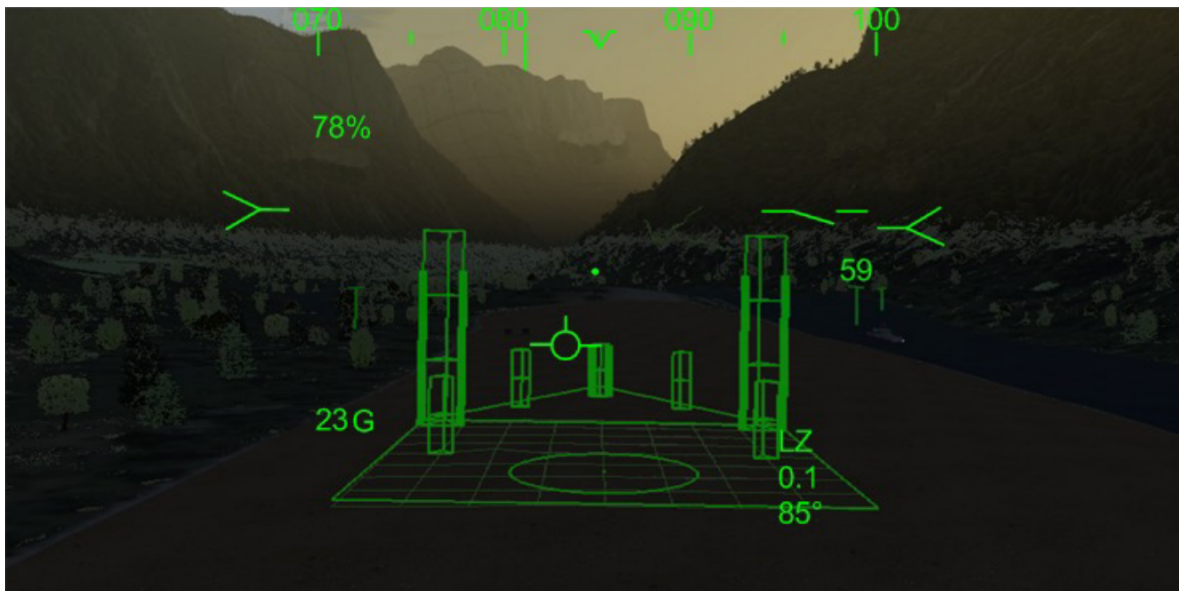


Figure 3-12: SFERION 3D landing symbology by Airbus [41]

---

## Chapter 4

---

# Human Vision

One way to look at human decision-making is as a circular dynamic relationship with the environment, in which humans sense stimuli from their surroundings and decide on the action that needs to be performed based on their perception of the stimulus. The resulting action in turn gives rise to another environmental stimulus, reinitiating the cycle. This process is illustrated in Figure 4-1.

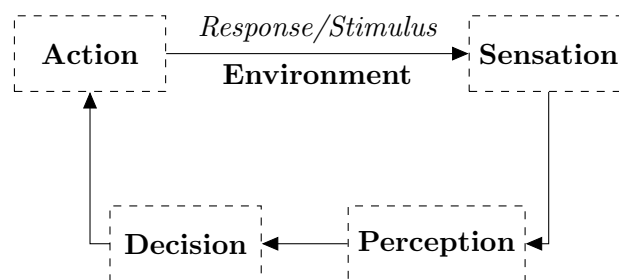


**Figure 4-1:** Dynamic model of the human cognitive system [42, p. 5]

With regards to the control of motion, several sensory systems are involved. As discussed in Section 2-3-1, these are the visual, vestibular, proprioceptive and, to some extent, auditory systems. However, the visual system appears to play a crucial role in human motion perception. Just imagine how hard it would be to ride a bicycle or drive a car with one's eyes closed. Especially when developing hover displays, having a solid knowledge of the visual system, and in particular of its function in the perception of motion, is of paramount importance.

In this chapter, the biological functioning of the human eye and the visual system is introduced in a brief manner, after which the focus lies on what information in the visual field humans use in the perception and control of self-motion.

## 4-1 Visual system

A deep understanding of the remarkable intricacies of the human eye and its physical functioning, though very interesting and worth studying, is out of the scope of the present study. However, it is necessary to have some knowledge of the fundamental aspects of the visual system in order to be able to develop an effective hover support display. These key features are depicted in Figure 4-2.

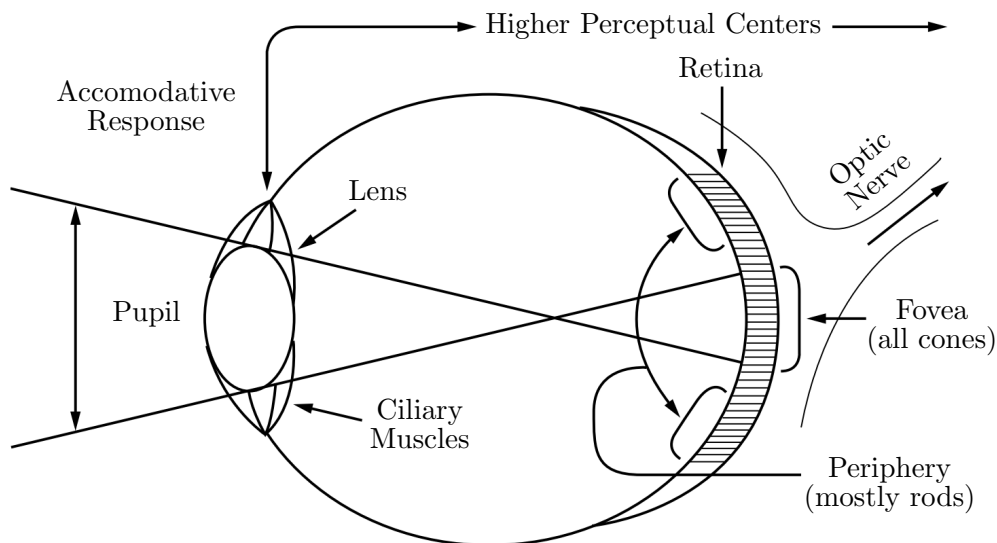


**Figure 4-2:** Fundamental aspects of the anatomy of the human eye [43, p. 46]

Light enters the human eye through the pupil, which controls the amount of light that comes in by constricting (when it is bright) or by dilating (when it is dark). The shape of the lens is modified so as to ensure that the incoming light is in focus on the retina; this process is known as accommodation and is achieved by the ciliary muscles. The light must be focused on the retina, as this is where all the receptors sensitive to light are located.

There are two types of receptors: rods and cones. The cones are predominantly present in the fovea, which is generally considered to be the central two degrees of the visual field [43]. The rods, on the other hand, occur in higher numbers away from the fovea, in the periphery. These two receptors have different functions. The cones allow humans to see colors and have a higher resolution, thus warranting a greater discrimination of detail. The ability to recognize small details is known as visual acuity (VA) and is defined in terms of the angular size of the smallest detectable object. A “normal” VA is 1.0, which is the ability to detect objects separated by 1 minute of arc. The rods, instead, have a higher sensitivity to light than cones and allow humans to discern their environment in dim circumstances.

Following the preceding discussion, a distinction between foveal (sharp) vision and peripheral (blurry) vision can be made. The fovea plays an important role in depth and distance judgments, through both monocular and binocular cues. Examples of monocular cues are shape and size constancy (the appearance on the retina of objects compared to the known shape or size), optical flow (see next section), textural gradient, and occlusion (also known as interposition; objects that are nearby block those behind them) [22]. Binocular cues are

vergence (the rotation of the eyes in opposite directions to project the incoming light on the center of the retina), stereopsis (the integration of the information from both eyes to form one image), and the concept of accommodation discussed priorly [22].

Although the resolution of the rods is lower than that of the cones, peripheral vision does play a role in orientation and in the perception of motion. Figure 4-3 shows how the level of detail of the retinal image quickly reduces further away from the foveal region; the sensitivity to motion, however, remains substantial also in the periphery. The combined action of the foveal and peripheral region allow humans to navigate safely through their environment [43]. Thus, a hover support display that must compensate for the loss of OTW visuals should ideally stimulate both regions of the retina.

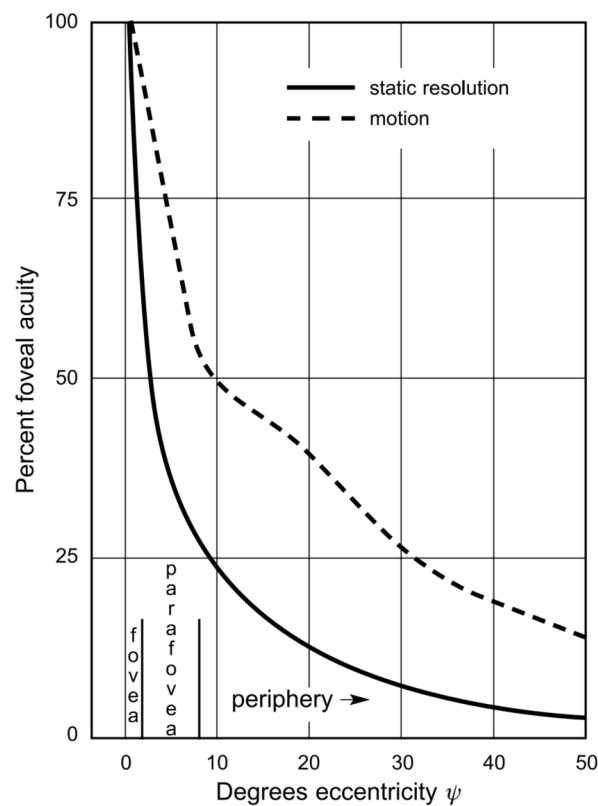


Figure 4-3: Static resolution and motion sensitivity of different regions of the eye [31, p. 528]

## 4-2 Visual motion perception

In order to develop a display that will effectively support pilots when their OTW view is obscured, it is essential to know what properties of the outside environment pilots generally use to control the helicopter. In other words, one must investigate what information plays a role in the visual perception and control of ego-motion.

The foundations of the theory on visual perception were laid by James Gibson [44]. He postulated the idea of optical invariants, which are visual cues that represent certain properties of light rays that have a never changing relationship to the location and heading of the

observer. These visual cues and their relevance to the perception and control of self-motion have since been researched extensively in various empirical studies. Several of these are introduced here.

#### 4-2-1 Optical flow

As an observer moves through the world, (stationary or moving) points throughout the visual field will move with respect to the observer [45]. The relative velocities of these points is known as optical flow [44], which is an important cue for the perception of direction of motion.

All optical flow radiates outward from a single point source known as the center of expansion, see Figure 4-4a. This expansion point serves as a cue for the direction of motion; for example, if it lies below the horizon as in Figure 4-4b, this will result in a collision with the ground unless the observer changes course. When the rate of flow is equal around all sides of the center of expansion, the observer's heading is straight into the ground surface (f.e. a helicopter landing vertically, see Figure 4-4c).

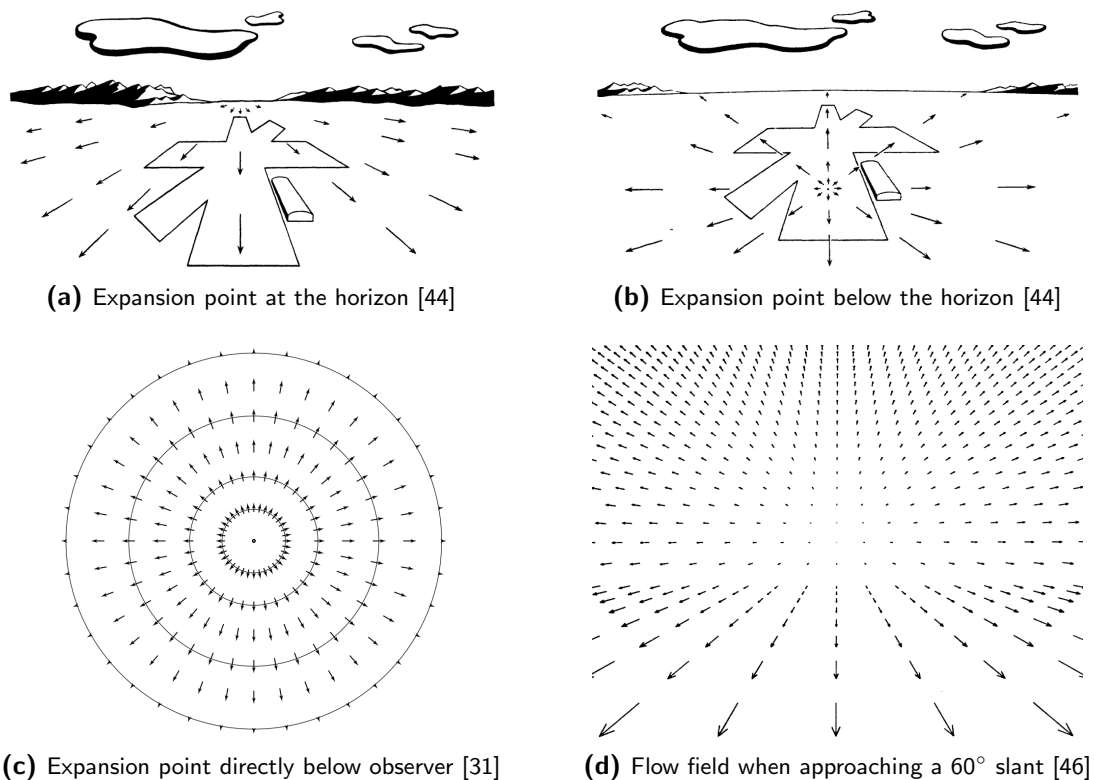


**Figure 4-4:** Optic flow patterns arising in different flight conditions

Research has shown that in linear translation, optical flow information alone is sufficient for observers to accurately judge their heading within  $\pm 1^\circ$  angular accuracy [47]. Control of heading substantially improves as more moving points are added to the visual scene (i.e., increasing the optical texture density) [48].

The optic flow field will be convoluted due to observer eye movements, such as fixating on a point other than the expansion point. However, even when such (rotational) eye movements

are included, optic flow alone serves as an adequate cue for determining heading [49]. In other words, observers are able, solely using optic flow information, to distinguish their heading from their viewing direction [50].

The characteristics of the optic flow field can provide the observer with knowledge of the surrounding environment. If the flow rate around the expansion point is non-uniform, as in Figure 4-4d, this provides information about the slant of the surface relative to the observer's direction of motion [46]. Moreover, as the observer moves, objects in the visual field that are far away move slower than those that are closer. The difference between these velocities, also known as motion parallax [51], serves as a means for the observer to estimate depth variations between various objects in the visual scene [52]. The magnitude of the velocity of a specific object is roughly proportional to the inverse of its depth in the visual field [53].

#### 4-2-2 Global optical flow rate

The global optical flow rate (GOFR) is an extension of the analysis of optical flow rate by Gibson et al. [53], and was first defined by Warren [54]. GOFR is the total rate of optical flow moving past the observer and is a function of both the velocity and altitude of the observer [55].

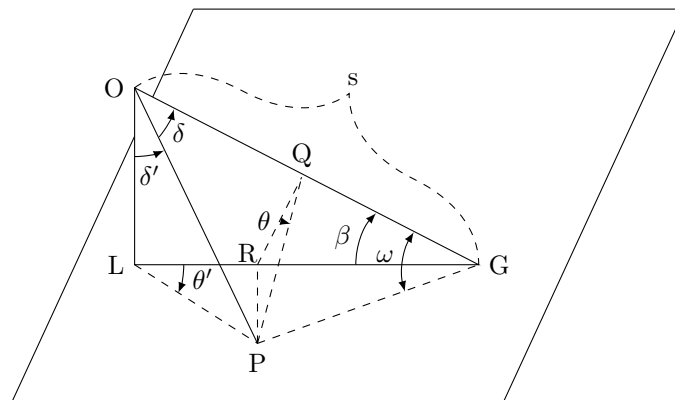


**Figure 4-5:** Schematic drawing of a moving observer relative to a plane [53]

Figure 4-5 shows an observer moving toward a point  $G$ , at a distance  $s$ , on the ground plane. The mathematical model of the flow field developed by Gibson et al. [53] results in the following expression for the optical flow rate for an arbitrary point  $P$  on a surface:

$$\frac{d\delta}{dt} = \frac{V}{s} (\sin \delta \cos \delta + \sin^2 \delta \cos \theta \cot \beta) \quad (4-1)$$

In Equation 4-1, global (through  $\frac{V}{s}$ ) and local (through the trigonometric functions) properties can be distinguished. The local factors show the flow rate of an object depends on its location within the flow field relative to the observer. The global factor, known as GOFR [55], increases with the speed of motion of the observer, and decreases as the distance to the surface increases. Therefore, GOFR serves as a reliable cue for perception of changes in speed *only* when altitude is kept constant, and vice versa. Note how for a helicopter landing vertically, point  $G$  is

directly below the observer and thus  $\beta = 90^\circ$ . Then, the second term in parenthesis in Equation 4-1 drops out and the resulting flow pattern is that of Figure 4-4c.

Research on visual perception typically employs the eye-height scale rather than the absolute values of distance and velocity, as it allows for inferring body-scaled information about the environment during motion [56]. The velocity in eye-height per seconds for an observer at a certain eye-height  $z$  is given by Equation 4-2:

$$\dot{x}_e = \frac{dx}{dt} \frac{1}{z} \quad (4-2)$$

Referring back to the flow patterns in Figure 4-4, note how the magnitude of the flow vectors decrease as the distance from the observer increases. Effectively, this means that the available motion cues in the flow field become weaker the further away from the observer they are. Using the eye-height scale, a threshold in terms of distance from the observer can be defined, beyond which the motion cues are no longer noticeable to the observer.

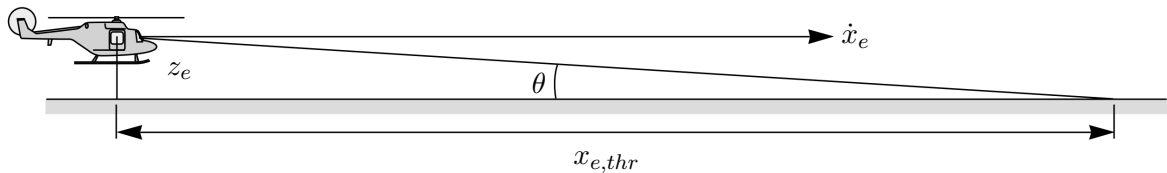


**Figure 4-6:** Schematic drawing of helicopter in forward flight, generalized adaptation from Padfield [31, p. 525]

Taking into consideration only forward motion, the rate of change of elevation angle  $\theta$  in terms of eye-height (see Figure 4-6) can be written as follows [31]:

$$\frac{d\theta}{dt} = \frac{\dot{x}_e}{1 + x_{e,thr}^2} \quad (4-3)$$

Using a value of  $\frac{d\theta}{dt} = 40$  arcmin/s as the threshold for velocity perception, as suggested for complex tasks by Perrone [46], and considering a typical approach-to-hover velocity of 10 m/s at an altitude of 10 m (i.e.,  $\dot{x}_e = 1$  eye-height/s), a rough estimate for the threshold location  $x_{e,thr}$  follows from Equation 4-3 to be 9 – 10 eye-heights away from the observer. The length of the flow vectors (as drawn in Figure 4-4) located further than this threshold will be zero, hence during a(n) (approach-to-)hover maneuver, there are no usable motion cues in the optic flow field beyond this point.

### 4-2-3 Optical splay

The optical splay angle provides information about the altitude of the observer, as first noted by Warren [54]. It is an optical invariant if the observer moves forward at constant speed. The splay angle is the angle between edges parallel to the direction of motion (f.e., the sides of a looming runway) and a line perpendicular to the horizon, see Figure 4-7.

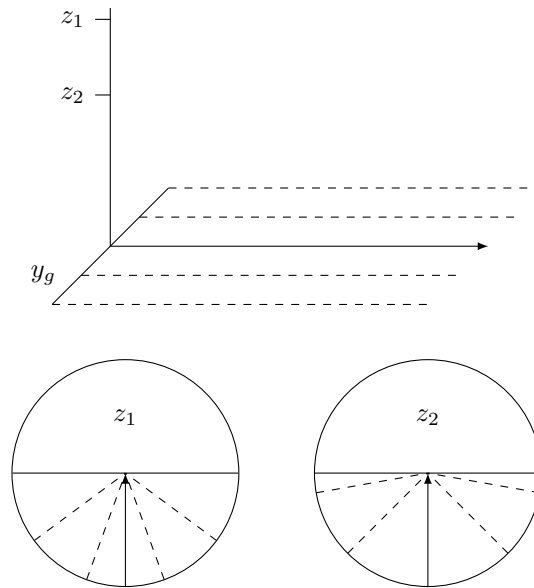


**Figure 4-7:** Effects of changing altitude on optical splay [57]

The splay angle  $S$  can be calculated with Equation 4-4, where  $y_g$  is the lateral displacement of the observer from the line perpendicular to the horizon and  $z$  is the altitude.

$$S = \tan^{-1} \left( \frac{y_g}{z} \right) \quad (4-4)$$

The splay angle will change as the observer moves through the environment. The rate of change of the angle provides a cue for the perception of altitude and lateral speed, and can be calculated with Equation 4-5.

$$\dot{S} = -\left(\frac{\dot{z}}{z}\right) \cos S \sin S + \left(\frac{\dot{y}_g}{z}\right) \cos^2 S \quad (4-5)$$

If the observer flies symmetrically forward, only the left-hand term remains and the direct relation between change in splay and altitude becomes apparent. Conversely, if the observer maintains a constant altitude, the change in splay serves as a clear cue for perceiving the lateral speed. In other words, a non-zero lateral velocity introduces a noise factor (defined by the right-most term in Equation 4-5) when an observer is using the splay angle rate to make altitude judgments and, in turn, a changing altitude causes noise (defined by the first term on the right-hand side) in lateral velocity judgments [57]. This concept of noise in optical activity is further elaborated on in Section 5-1-3.

#### 4-2-4 Optical depression

Optical depression is a cue for altitude and forward speed changes. It arises in a similar fashion as the optical splay, but in this case the edges are perpendicular to the direction of motion instead of parallel, see Figure 4-8.

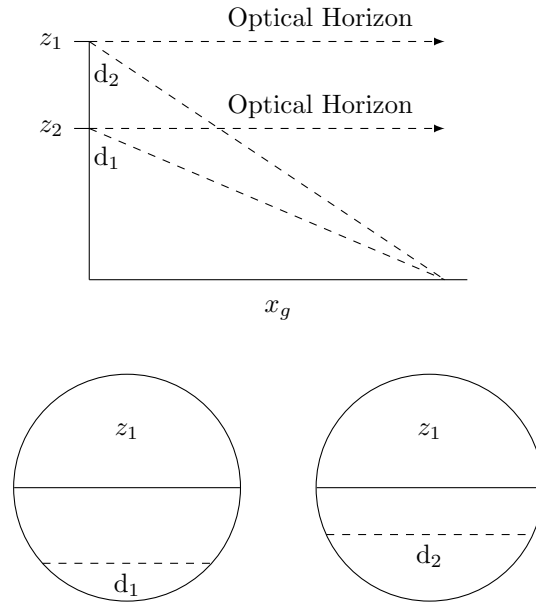


**Figure 4-8:** Effects of changing altitude on optical depression [57]

The depression angle  $\delta$  is defined as the angular position of one of these edges below the horizon [58], see Equation 4-6, where  $x_g$  is the longitudinal displacement and  $z$  is the altitude.

$$\delta = \tan^{-1} \left( \frac{x_g}{z} \right) \quad (4-6)$$

The depression rate in case of rectilinear motion over a flat plane can then be defined [57], see Equation 4-7.

$$\dot{\delta} = - \left( \frac{\dot{z}}{z} \right) \cos \delta \sin \delta + \left( \frac{\dot{x}_g}{z} \right) \cos^2 \delta \quad (4-7)$$

It becomes clear that the rate of change of the depression angle is affected by both altitude and speed. Hence, non-zero fore-aft movement introduces a noise factor into the altitude judgments, and vice versa, similarly to the noise factors present in the splay angle rate (see also Section 5-1-3). Note that the term  $\frac{\dot{x}_g}{z}$  is simply the GOFR.

#### 4-2-5 Edge rate

Another aspect of the optic array that plays a role in the perception of egospeed is the optical edge rate. It was defined by Warren in an extensive review [54] as the rate at which discontinuities, or edges, pass by a fixed reference point in the observer's visual field (such as the frame of the cockpit). It is dependent on (ground) texture density and speed but independent of altitude. Defining the separation between edges on the ground surface as  $T_x$ , the edge rate can be calculated using Equation 4-8 [31].

$$e_r = \frac{dx}{dt} \frac{1}{T_x} \quad (4-8)$$

If the textures are regularly spaced, the edge rate is directly proportional to speed. For example, a helicopter pilot approaching a hover target location with a velocity of 10 m/s over a terrain with textures spaced 10 m apart experiences an edge rate of 1/s.

The importance of optical edge rate in the perception of velocity was famously shown by Denton [59]. In his work, he showed that drawing stripes on roads in front of roundabouts at exponentially decreasing intervals (i.e., increasing edge rate) resulted in lower approach speeds and reduced accident rates. The principle of this method, which Denton termed *control of speed by illusion*, is shown in Figure 4-9.

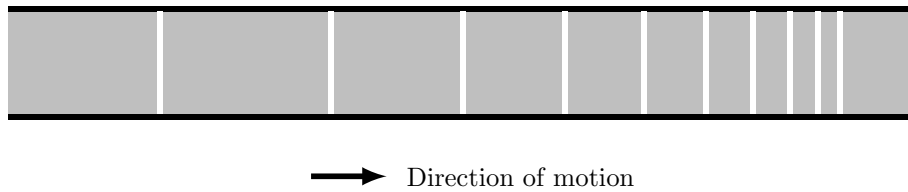


**Figure 4-9:** Control of speed by illusion using edges at exponentially decreasing intervals

#### 4-2-6 Temporal cues

Temporal cues are those that can provide information for the timing of actions with respect to the environment. These types of cues are a product of the optic flow field. The main example, time-to-contact (TTC), described first by Lee [60], is concerned with the “looming” property of objects in the optical flow field (see Figure 4-10). It is based on the hypothesis that not the absolute size, distance, or velocity of an object is relevant for a moving observer aiming to estimate the time to pass or collide with it, but rather the ratio of the object’s size to the rate at which its image on the retina grows. This ratio, known as TTC, is the same as the ratio of distance to the object over approach speed, and is expressed in linear and angular form in Equation 4-9.

$$\tau(t) = \frac{x}{\dot{x}} = \frac{\theta}{\dot{\theta}} \quad (4-9)$$

Using the small-angle approximation  $\theta$  can be expressed as

$$\theta = \arctan\left(\frac{z}{x}\right) \cong \frac{z}{x} \quad (4-10)$$

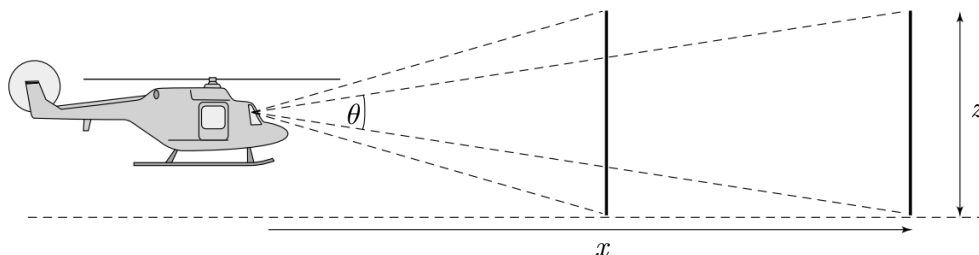


**Figure 4-10:** Optical looming of an object is used in TTC judgments [31, p. 533]

A helicopter pilot trying to avoid collision with an object or, more germane to the topic at hand, aiming to come to a stop at the hover point, may do so by directly controlling the rate of change of the TTC [56]. This optical tau rate is a function of distance to stop (negative by convention), velocity and acceleration, see Equation 4-11.

$$\dot{\tau}(t) = 1 - \frac{x\ddot{x}}{\dot{x}^2} \quad (4-11)$$

Thus, if  $\dot{\tau} < 1$  the aircraft is decelerating, for  $\dot{\tau} > 1$  it is accelerating and  $\dot{\tau} = 1$  means the velocity is constant. In case the pilot applies a constant deceleration, the distance to stop follows from Equation 4-12. In such a situation, it must hold that  $\dot{\tau} = 0.5$  precisely when the pilot reaches the hover target location.

$$x = -\frac{\dot{x}^2}{2\ddot{x}} \quad (4-12)$$

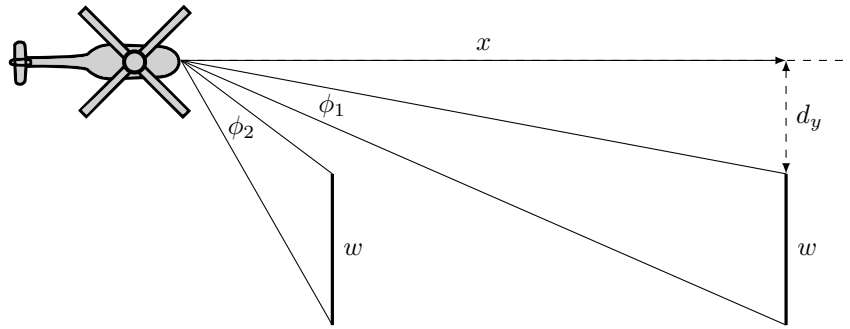


**Figure 4-11:** Optical looming for an off-axis approach

As depicted in Figure 4-11, the optical looming during an off-axis approach is not merely a function of the distance between observer and object, thus Equation 4-10 no longer holds. Instead, for off-axis approaches, the temporal cue is referred to as time-to-passage (TTP), and the angle must be calculated using Equation 4-13 [61].

$$\phi = \cos\left(\frac{d_y}{x}\right) \frac{w}{\sqrt{x^2 + d_y^2}} \quad (4-13)$$

---

## Chapter 5

---

# Display Design

The visual cues that humans use for motion perception, covered in the previous chapter, can be provided synthetically on AR displays. This chapter investigates how these cues may be incorporated in displays, or, in other words, what display elements can encode information about the relevant helicopter states. Furthermore, several important considerations that need to be made from a human factors perspective are presented.

Note that the displayed information is assumed to be perfectly known, bypassing the need to investigate the source of information used to create the display elements. Hence, an in-depth discussion of environmental sensing techniques, such as LIDAR used to generate 3D landing zones in research of the U.S. army [62] or the extremely high frequency radar employed in the brownout landing aid system technology (BLAST) of BAE Systems [63], and subsequent blending with on-board terrain databases, such as in SFERION of Airbus [41], is out of the scope of the current study. Instead, the focus here lies on what information to present and in what form, not on the methods used to obtain said knowledge.

### 5-1 Display elements

Only a short coverage of potential display elements will be provided here. Many were already introduced to some extent when the previous research into hover displays was discussed in Section 3-3. In this section, the main findings from that discussion will be reiterated and combined with the knowledge obtained of the visual cues humans use for motion perception. The first display element that will be covered here is the flight path marker (FPM), followed by the horizon line and ground texture. Finally, other forms of 3D conformal symbology will be explored.

#### 5-1-1 Flight path marker

The FPM has a long history of use in both fixed-wing aircraft as well as helicopters, initially provided on the primary flight display (PFD) and later on HUDs. The symbol depicts the

flight path the aircraft is on, by combining the lateral and longitudinal velocity with the heading and generally also compensating for wind direction. As such, it is basically a symbolic implementation of the expansion point of optic flow, covered in Section 4-2-1. The basic shape of the symbol is shown in Figure 5-1, although it not seldomly appended with additional cues such as speed error or acceleration indicators.

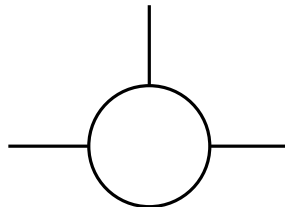


**Figure 5-1:** Basic shape of the FPM

However, the approach-to-hover generally occurs at low speeds and the hover itself is a stationary maneuver, which renders the FPM unsuitable for use during that phase of flight. Therefore, in an evaluation study conducted for the U.S. army, in which different versions of BOSS symbology were compared, the FPM becomes dashed when the helicopter's velocity is below 30 kts and disappears completely below 20 kts [62]. An alternative at low speeds could be to replace the FPM by some kind of hover vector. For example, at speeds below 30 kts, the electronic flight instrument system (EFIS) developed by Cobham Avionics shows a hover aid composed of two concentric circles representing drift velocities (the inner denoting 15 kts, the outer 30 kts), with a superimposed 2D hover vector indicating direction and magnitude of drift [64].

### 5-1-2 Artificial horizon line

The horizon serves as an important cue for roll and pitch attitude in good visual conditions, hence pilot judgment of those angles severely deteriorates when the OTW view is obscured. An artificial horizon in the form of the attitude indicator on the PFD has been in use for decades in helicopters and fixed-wing aircraft alike. Accordingly, a similar feature mimicking the real horizon may be provided in a perspective scene on a HUD or HMD.

The true horizon is not only a function of pitch and roll, but also changes with altitude. However, the attitude indicator, functioning with gyroscopes, is purely dependent on roll and pitch. If the aircraft pitches down, the artificial horizon will move upwards, and if the aircraft pitches up, the horizon will move downwards. Likewise, as the aircraft is rolling in clockwise direction along its longitudinal axis, the artificial horizon displayed will rotate in opposite direction, maintaining alignment with the actual horizon.

When implementing an artificial horizon on an AR display, it would be a good idea to preserve this exclusive relation to pitch and roll and omit the influence of altitude. Not only would that be consistent with pilots' career-long experience with the attitude indicator, but it would also reduce the noise present in the horizon line when used for pitch judgments, since a changing altitude produces the same horizon movement as an altering pitch angle.

### 5-1-3 Ground texture

The use of ground texture on an AR display can be a straight-forward way of providing cues such as optical splay, depression, and edge rate. Flach et al. investigated how the control of altitude in the presence of disturbances (in all three axes) was affected by different surface textures [57]. As portrayed in Figure 5-2, the evaluated texture types were splay, depression, grid (i.e., splay and grid), and dot (small triangles quasi-randomly distributed around the grid intersections).

As mentioned in Sections 4-2-3 and 4-2-4, splay and depression rate are not exclusive cues for altitude, as fore-aft movement affects depression and lateral movement influences splay. Hence, when using such a cue for determining either vertical or horizontal movement, a noise factor is introduced by motion along the axis that is not of interest. Likewise, the optical

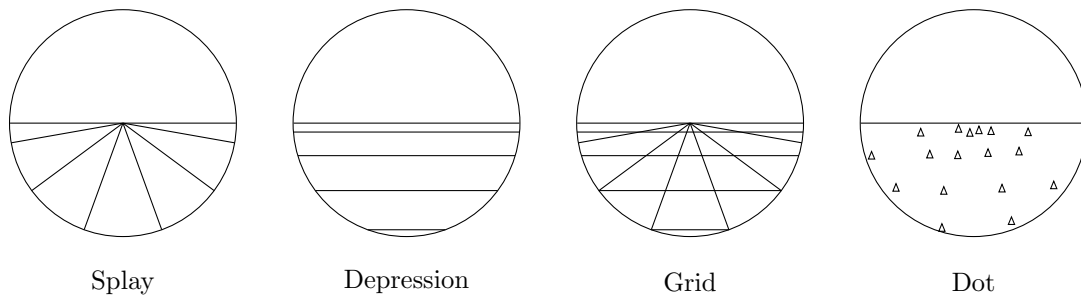


**Figure 5-2:** Different types of ground texture as used in experiment by Flach et. al [57]

**Table 5-1:** Optical activity as a function of ground texture and motion [57]

Texture	Signal		Noise
	Altitude	Fore-aft	Lateral
Grid	$-\left(\frac{\dot{z}}{z}\right) \cos S \sin S$	$\left(\frac{\dot{x}_g}{z}\right) \cos^2 \delta$	$\left(\frac{\dot{y}_g}{z}\right) \cos^2 S$
	$-\left(\frac{\dot{z}}{z}\right) \cos \delta \sin \delta$		
Dot	$-\left(\frac{\dot{z}}{z}\right) \cos S \sin S$	$\left(\frac{\dot{x}_g}{z}\right) \cos^2 \delta$	$\left(\frac{\dot{y}_g}{z}\right) \cos^2 S$
	$-\left(\frac{\dot{z}}{z}\right) \cos \delta \sin \delta$		
Depression	$-\left(\frac{\dot{z}}{z}\right) \cos \delta \sin \delta$	$\left(\frac{\dot{x}_g}{z}\right) \cos^2 \delta$	
Splay	$-\left(\frac{\dot{z}}{z}\right) \cos S \sin S$		$\left(\frac{\dot{y}_g}{z}\right) \cos^2 S$

activity in the dot and grid textures of Figure 5-2 is affected by motion along all three axes. Considering Flach et al. were investigating altitude control, disturbances along the vertical axis were regarded as the signal, and fore-aft and lateral movement were deemed noise. For each of the ground textures, the terms in the splay and depression rates of Equations 4-5 and 4-7 that are considered noise or signal are listed in Table 5-1.

Flach et al. discuss the findings of three experiments. In the first experiment, participants performed a constant altitude tracking task with four different levels of GOFR for each of the ground textures. They found that root-mean-square (RMS) error in altitude increased with increasing GOFR. Furthermore, best altitude RMS error was achieved with the splay configuration, whereas performance with depression lines was worst. Interestingly, this is contrary to the results of a similar experiment by Johnson et al., who found that altitude control was best with depression lines [65]. Performance with grid lines was intermediate, and with dot texture somewhat worse than with the grid.

A second experiment was conducted by Flach et al. in order to investigate whether these contrasting findings may be due to participants using local instead of global sources of information. Therefore, in the follow-up experiment half of the participants were instructed to wear occluding goggles, narrowing their view to cover nearby cues only. However, no significant results were found in terms of viewing condition.

In the experiment, pilots performed the same task as before, with on average similar results for various levels of GOFR; overall lowest RMS error was with splay, followed by grid, dot, and finally depression. Through spectral analysis, the researchers investigated what disturbances led to the largest altitude control exerted by the pilots. Increased control power was found for fore-aft disturbance with the depression lines, whereas for splay the control power increased for lateral disturbances; confirming their signal-to-noise hypothesis indicated in Table 5-1. Noteworthy is the fact that if only the hover condition (i.e., a GOFR of 0 eye-height/s) is considered, depression lines were found to be superior to splay in terms of altitude RMS error.

#### 5-1-4 Miscellaneous conformal symbology

The discussion on current hover displays of Section 3-3 demonstrated that the options in terms of conformal symbology are virtually endless. Aside from the previously discussed ground textures, FPM, and horizon line, the conformal elements in to-be-developed displays may consist of e.g. landing pads, guidance symbols, or explicit cues for state variables, such as the hover board in the ADS-33 course. Therefore, listing the countless possibilities and varieties of such symbology would be both impracticable and superfluous.

Instead, another example of a hover display will be discussed in order to illustrate how conformal symbology other than ground texture can convey splay and depression information too, and at the same time provide explicit cues for certain helicopter states. The display shown in Figure 5-3 was developed to aid pilots hovering above a moving ship [66]. The perspective drawing of the cube and ship deck provide implicit information through splay and depression angles. An example of an explicit cue (for altitude) in the display is the vertical distance between the horizon line and the center of the box.

In their experiment, Negrin et al. compared the effectiveness of various display configurations using elements shown in the figure, as well as the extent to which pilots preferred either

implicit (perspective) or explicit cues [66]. Pilots only controlled altitude, with target height being at the level of the box's center; pitch attitude and fore-aft motion was commanded by the autopilot. The researchers argue that human pilots prefer explicit over implicit positional cues, as conditions in which only the hover cube was provided showed that the implicit cues were effective only when the box was either rather large, or viewed from nearby. Best performance, thus lowest altitude RMS error, was achieved for a configuration with the deck, horizon line, and a relatively small cube.

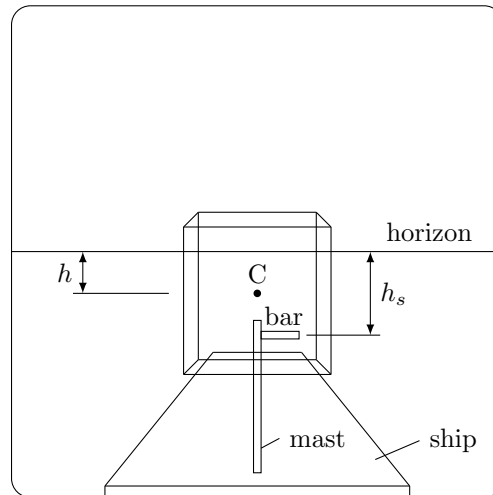


Figure 5-3: Display to aid hovering above a moving ship deck [66]

## 5-2 Display design considerations

Some important design considerations must be made from a human factors perspective, in order to optimize the effectiveness of the to-be-developed AR display. These considerations may provide indications of the limitations in current state-of-the-art hover displays. First, attention and the effect of cognitive tunneling will be introduced, followed by a brief discussion on visual clutter.

### 5-2-1 Cognitive tunneling

With superimposed symbology, be it on HUDs or HMDs, information is portrayed on top of the real-world view of the pilot. As such, AR displays hide a part of the external environment. The pilot thus needs to process and integrate the information from both the OTW view as well as the overlaid display. He or she may do so simultaneously with *divided attention*, or by alternating their *focused attention* between either channel of information [67].

However, in either case, the synthetic overlay on the HUD or HMD may be so compelling that it completely captures the pilot's attention, thereby substantially deteriorating their awareness of other displays or important external events [68]. Evidently, this effect, known as *cognitive tunneling*, can lead to perilous situations when unexpected events are not detected in a timely manner. Failure to notice such a stimulus due to a lack of attention is known

as *inattentional blindness* [69]. The tunneling effect is much more substantial for displays with non-conformal elements such as head-up depictions of 2D flight instruments [67], which remains a common design choice in current-day hover displays as discussed in Section 3-3. Conformal symbology, instead, may allow for more successful division of attention.

### 5-2-2 Visual clutter

One reason for the cognitive tunneling effect is visual cluttering. In a cluttered display, the amount of information shown is excessive (i.e., it obscures too much of the OTW environment) or the displayed information is not integrated in an appropriate way (e.g., through mixed 2D non-conformal and 3D conformal imagery), causing the pilot to have more difficulty and require more time interpreting the display [70]. Indeed, visual clutter can cause pilot confusion and thus adversely affect task performance [71].

Clearly, these effects are more pronounced for displays with a higher level of clutter, as more of the environmental information is obscured by the superimposed elements. With this knowledge in mind, it can be argued that a considerable number of the displays introduced in Section 3-3 are cluttered and may be more effective when part of the depicted data is omitted, so as to preserve only the absolutely essential information for the task at hand.

# Identification of Visual Cue Usage

Once a display to support helicopter pilots hovering in brownout conditions is developed, its effectiveness will need to be investigated. An interesting tool that may prove useful for such analysis is the Visual Cue Control Model (VCCM). It is a promising model for three reasons [72]; it can help to

1. identify what cues the pilot used,
2. demonstrate whether implemented cues were used as expected, and
3. indicate whether an implemented cue was ineffective.

The VCCM is an extension for perspective scene viewing of the crossover model introduced by McRuer, therefore first a brief introduction of McRuer's work will be provided before further examining the VCCM.

### 6-1 Crossover model

McRuer and his colleagues investigated ways to better understand and model human manual control. Due to the highly non-linear nature of the human controllers, modeling the behavior is no simple task. McRuer's approach resulted in the quasi-linear model shown in Figure 6-1 [73], in which the output of the pilot  $c$  is composed of two parts. The first part is through describing function  $Y_p(s)$ , the output of which ( $u$ ) is linearly related to input  $e$ . The second part is the difference between  $u$  and the measured pilot output  $c$ .

The principle of the crossover model is that the human controllers adjust their response  $Y_p(s)$  depending on the system dynamics  $Y_c(s)$  such that the open-loop transfer function for the region around crossover frequency  $\omega_c$  is given by Equation 6-1 [73]. The crossover frequency  $\omega_c$  is the frequency for which open-loop magnitude  $|Y_{OL}| = |Y_p Y_c| = 1$ .

$$Y_{OL}(j\omega) = Y_p(j\omega)Y_c(j\omega) = \frac{\omega_c e^{-j\omega\tau_e}}{j\omega} \quad (6-1)$$

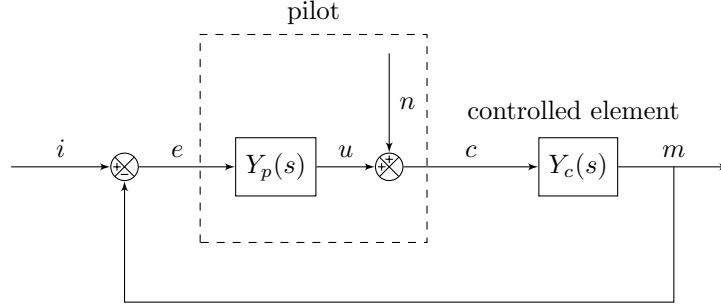


Figure 6-1: Control diagram for quasi-linear pilot model

## 6-2 Visual cue control model

The VCCM is developed based on the assumption that pilots select visual cues that correspond to certain aircraft states, and then directly control those cues rather than first mentally reconstructing the corresponding state variables [74]. Thus, in simulator environments this implies that the pilot selects a visual cue, or display element, of which the on-screen position is a function of one or more states. The VCCM entails developing a mathematical description of this visual cue in terms of states and then incorporating this into the crossover model.

Before a potential cue can be described as a function of states, first a mathematical description of the perspective projection transformation is needed. This transformation, given by Equation 6-2 [74], relates the image coordinates ( $I_h$ ,  $I_v$ ) to the inertial position and orientation of the pilot ( $x$ ,  $y$ ,  $z$ ,  $\phi$ ,  $\theta$ ,  $\psi$ ), the inertial location of a scene feature ( $D_x$ ,  $D_y$ ,  $D_z$ ) and focal length  $L$ . Thus, this transformation allows one to convert the position of an element in the (virtual) world to its display coordinates.

$$\begin{aligned}
 I_h = w & \left[ (D_x - x) (-\sin \psi \cos \phi + \cos \psi \sin \theta \cos \phi) \right. \\
 & \left. + (D_y - y) (\cos \psi \cos \phi + \sin \psi \sin \theta \sin \phi) + (D_z - z) \cos \theta \sin \phi \right] \\
 I_v = w & \left[ (D_x - x) (\sin \psi \sin \phi + \cos \psi \sin \theta \cos \phi) \right. \\
 & \left. + (D_y - y) (-\cos \psi \sin \phi + \sin \psi \sin \theta \cos \phi) + (D_z - z) \cos \theta \cos \phi \right]
 \end{aligned} \tag{6-2}$$

$$\text{with } w = \frac{L}{(D_x - x) \cos \phi \cos \theta + (D_y - y) \sin \phi \cos \theta - (D_z - z) \sin \theta}$$

Now, any visual cue (splay, depression, etc.) can be described as some function  $G$  in terms of image or (virtual) world coordinates. A general description of nonlinear cue  $\Lambda$  is

$$\Lambda = G_{image}(I_h, I_v) = G_{world}(L, x, y, z, \phi, \theta, \psi, D_x, D_y, D_z) \tag{6-3}$$

Evidently, the relation between aircraft states and display (image) coordinates are still nonlinear. In order to incorporate it into the quasi-linear crossover model, a linearized expression

for the visual cue is developed. For example, if a pilot wishes to control longitudinal position  $x$ , a linearized visual cue  $\lambda$  for state  $x$  is obtained by differentiating nonlinear cue  $\Lambda$  of Equation 6-3 with respect to each of the states and subsequently normalizing with  $\partial\Lambda/\partial x$ , see Equation 6-4 [74]. The resulting linear cue  $\lambda$  has a one-to-one relationship with and has the same units as longitudinal position  $x$ .

$$\lambda = \left. \frac{d\Lambda}{\partial\Lambda/\partial x} \right|_{x=x_0, y=y_0, z=z_0, \phi=\phi_0, \theta=\theta_0, \psi=\psi_0} \quad (6-4)$$

$$\text{where} \quad d\Lambda = \frac{\partial\Lambda}{\partial x} dx + \frac{\partial\Lambda}{\partial y} dy + \frac{\partial\Lambda}{\partial z} dz + \frac{\partial\Lambda}{\partial\phi} d\phi + \frac{\partial\Lambda}{\partial\theta} d\theta + \frac{\partial\Lambda}{\partial\psi} d\psi$$

This linearized cue can be written as a weighted linear combination of state variables, using a sensitivity parameter  $W$ , defined by Equation 6-5, for each of the remaining states [72].

$$W_{[\Lambda, y]} = \left. \frac{\partial\Lambda/\partial y}{\partial\Lambda/\partial x} \right|_{x=x_0, y=y_0, z=z_0, \phi=\phi_0, \theta=\theta_0, \psi=\psi_0} \quad (6-5)$$

Dropping the delta in the linearized states for sake of clarity (thus, from now on  $x = dx$ , etc.), any nonlinear cue  $\Lambda$  can now be linearized and described in terms of vehicle states. As an example, the previously defined cue for  $x$  is given in Equation 6-6 as a linear combination of state variables.

$$\lambda = x + W_{[\Lambda, y]}y + W_{[\Lambda, z]}z + W_{[\Lambda, \phi]}\phi + W_{[\Lambda, \theta]}\theta + W_{[\Lambda, \psi]}\psi \quad (6-6)$$

To illustrate how this can be incorporated into the crossover model, the previous example will be further simplified. Consider a system with forward position  $x$  and pitch angle  $\theta$  as the only degrees-of-freedom, with the pilot only able to control  $x$ . To do this, a pilot might use two visual cues;  $\gamma$  for position and  $\beta$  for velocity, each a function of  $x$  and  $\theta$  [72]:

$$\gamma(s) = x(s) + W_{[\Gamma, \theta]}\theta(s) \quad (6-7)$$

$$\beta(s) = \dot{x}(s) + W_{[B, \theta]}\theta(s)$$

This description of the visual cue can be incorporated into the crossover model. Figure 6-2 shows the control diagrams for a pilot performing the task with a compensatory display and a perspective display, where controlled dynamics are  $Y_c = 1/s(s + 0.2)$  and pilot dynamics  $Y_p$  are predicted with the crossover model, see Equation 6-1. Note how with the VCCM, the pilot is assumed to directly control the visual cues  $\gamma$  and  $\beta$ .

In order to now use the VCCM to identify whether the pilot in fact used a certain cue provided on the perspective display, a potential candidate visual cue for this task still needs to be selected and described mathematically. The choice of this candidate cue can be based on

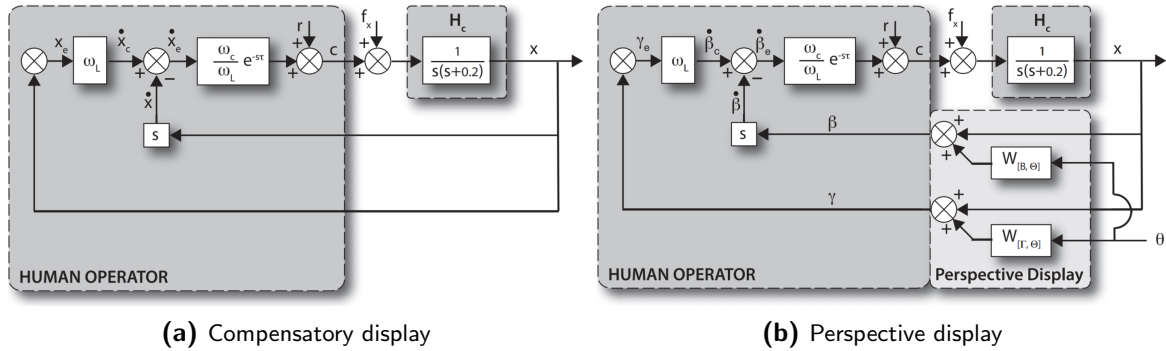


**Figure 6-2:** Block diagrams illustrating incorporation of VCCM into crossover model [72]

the theory covered in Section 4-2. For the example situation with two degrees-of-freedom introduced here, the pilot may use the vertical location of a depression line on the display as a cue for controlling forward position [72]. Then, this nonlinear cue can be expressed with Equation 6-8.

$$\Gamma = I_v = \frac{L[(D_x - x) \sin \theta + \cos \theta]}{(D_x - x) \cos \theta - \sin \theta} \quad (6-8)$$

Note that the limited number of degrees-of-freedom has simplified the expression for  $I_v$  (cf. Equation 6-2). Taking the partial derivatives as in Equation 6-5 and evaluating at  $x_0 = \theta_0 = 0$ , the sensitivity parameter for this cue is

$$W_{[\Gamma, \theta]} = D_x^2 + 1 \quad (6-9)$$

The same method outlined here for a simple two degree-of-freedom task can be applied to any arbitrary control task and any visual cue that can be described mathematically in terms of display coordinates. Experimental validation of the model for this example case showed close correspondence between the model and measurements [72].

---

## Chapter 7

---

# Research Proposal

The preceding literature review aimed at answering the research questions stated in Section 1-1. Based on the findings so far, two AR displays will be developed with the aim of incorporating only those visual cues that are absolutely essential for pilots to be able to successfully perform a hover maneuver. Whether the proposed displays indeed allow pilots to accurately hover will be investigated in a human-in-the-loop experiment.

In this chapter, first the two displays are introduced and the rationale behind them is detailed. Then, the set-up of the human-in-the-loop experiment is introduced. Finally, the anticipated outcome and results from the experiment are described.

### 7-1 Configuration of proposed displays

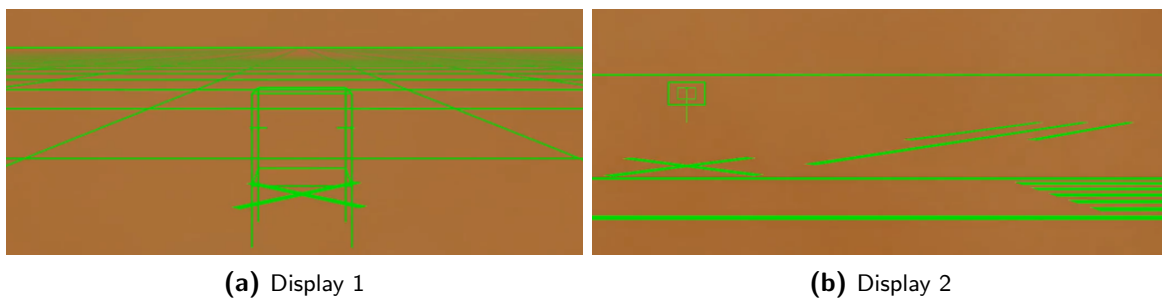
The survey presented in Section 3-3 showed that many current hover displays contain a plethora of information, often resulting in fairly cluttered displays. The common procedure of combining 2D flight information with 3D conformal symbology further adds to the clutter, and may invoke cognitive tunneling. Therefore, the displays proposed here contain exclusively 3D conformal elements to avoid such adverse effects and, moreover, allow for thorough investigation into the effectiveness of those visual cues.

Analyzing the control diagrams showed that a pilot performing a hover maneuver must have sufficiently accurate knowledge of the helicopter state variables  $x$ ,  $y$ ,  $z$ ,  $u$ ,  $v$ ,  $w$ ,  $\theta$ ,  $\psi$ ,  $\phi$ ,  $p$ ,  $q$ , and  $r$ . A minimalistic display, that is, one that portrays only the absolutely essential visual cues, must therefore convey information on each of these states. Developing such a display is not a straight-forward task; the previous chapters have shown that a multitude of options exist for providing such cues with conformal symbology.

The displays, as well as the brownout cloud simulation, are developed in the open-source 3D graphics library OSG in C++ and incorporated into the Delft University Environment for Communication and Activation (DUECA) architecture of the SRS at TU Delft. The proposed displays are shown in Figure 7-1. Table 7-1 lists the visual cues that are available in

**Table 7-1:** Available visual cues in each of the displays

	Outside view (ADS-33)	Display 1	Display 2
$x$	Longitudinal cone position	Depression lines, hover box and cross	Longitudinal lines (cones), hover cross
$u$	Optical flow, edge rate	Depression lines	Hover course (depression) lines
$\theta$	Hover board pitch position	Horizon position	Horizon position, hover board pitch position
$q$	Optical flow	Horizon vertical speed	Horizon vertical speed
$y$	Hover board lateral indicator	Hover box and cross	Hover board lateral indicator
$v$	Optical flow, edge rate	Splay lines	Hover course movement, diagonal lines (cones)
$\phi$	Horizon bank position	Horizon bank position	Horizon bank position
$p$	Optical flow	Horizon rotational speed	Horizon rotational speed
$z$	Hover board	Splay and depression lines, hover box and ticks	Hover board and reference marker
$w$	Optical flow, edge rate	Splay and depression lines	Hover course (depression) lines
$\psi$	Diagonal cones and hover board yaw position	Hover box position, grid lines	Diagonal lines (cones) and hover board yaw position
$r$	Optical flow	Grid lines	Diagonal lines and hover board rotational speed

**Figure 7-1:** Configuration of proposed displays

the displays for each of the helicopter states. The baseline condition in good visibility shows the ADS-33 hover course introduced in Section 3-2-2, see Figure 7-2.

The first proposed display, depicted in Figure 7-1a, contains splay and depression lines (i.e., a grid ground texture), a horizon line and a hover box. The cube is somewhat similar to

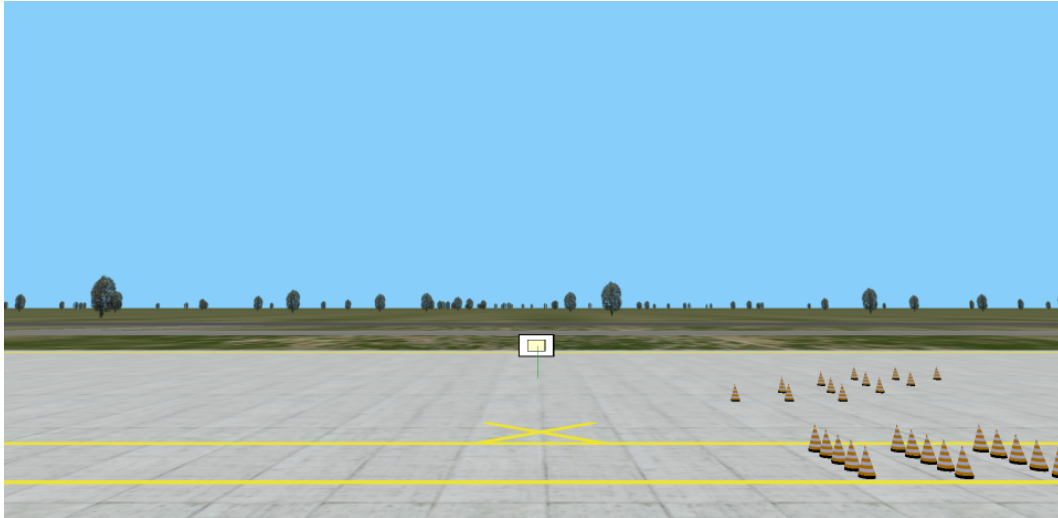


**Figure 7-2:** Baseline condition with good visibility

the one used by Negrin et al. in Figure 5-3, with the important distinction that the target position here is not in front of the box but in the center of the box. Once inside the box, the hover cross (also part of the ADS-33 course) is visible for longitudinal positioning, and tick lines on the rear edges of the cube can be used for reference of vertical position. The second display, shown in Figure 7-1b, is based on the ADS-33 course visible in GVE. It bears resemblance to the PHS display developed at TU Munich of Figure 3-7, albeit with some important differences. The display proposed here is less cluttered and exclusively contains 3D conformal symbology, whereas the PHS also includes 2D imagery. The cones present in the ADS-33 course are replaced by lines. Furthermore, the PHS was tested on a HMD with a small FOV. The displays developed here will instead be projected as overlays on the outside view (effectively a full cockpit HUD), thereby avoiding limiting the usefulness of certain visual cues due to a restricted FOV and image resolution.

## 7-2 Experimental set-up

The set-up for the human-in-the-loop experiment that will be conducted in the SRS at the Faculty of Aerospace Engineering at TU Delft is described here.

### Aim

The goal of the human-in-the-loop experiment is to investigate the effectiveness of the developed displays. An effective display is one that allows pilots to perform an accurate hover maneuver in brownout conditions, using their natural control strategy (i.e., which they use in GVE). In other words, the question that should be answered is:

**What are the effects on pilot performance, control strategy and situational awareness during a hover maneuver in brownout conditions using the developed displays?**

## Control task

The task for the pilot is based on the ADS-33 hover maneuver described in Section 3-2-2, and is the same as the control task of another experiment conducted in the SRS at TU Delft [34]:

“Approach the hover target point with the initial forward speed of the helicopter at the beginning of the run. At a distance you deem appropriate, initiate a deceleration maneuver to smoothly and precisely come to a stop at the hover point. After reaching the hover point, maintain a stabilized hover, minimizing deviations from the hover target point, for thirty seconds. Please avoid accomplishing most of the deceleration maneuver well before the hover point and then creeping up to the final hover position.”

The initial velocity will be 10 m/s in all experiment conditions. The starting position quasi-randomized (in order to avoid pilots remembering the exact trajectory) around the point 100 m directly in front of the hover target location, which is at an height of 10 ft.

## Independent variables

The independent, dependent and control variables of the proposed experiment are listed in Table 7-2.

**Table 7-2:** Experiment variables

Independent variables	vari-	Dependent variables	Control variables
Visibility / display		Task performance	Control task
Vehicle dynamics		Control strategy	Simulator set-up
		Control activity	Basic instrument panel
		Workload	
		Situational awareness	
		Pilot opinion	

The variable **visibility / display** describes the availability of OTW visuals (good or brownout) and, in brownout conditions, which of the two designed hover displays are provided as overlays on top of the outside view of the pilot. The proposed displays and visibility conditions are shown in Figures 7-1 and 7-2. The first display contains splay and depression lines, a horizon line, a hover box, and a hover cross. The second display consists of an ADS33-like hover course and a horizon line. In the experiment conditions with good visuals, no hover display is shown.

The variable **vehicle dynamics** describes the flight dynamics model used for the helicopter. Two different models will be used. One is a non-linear Bo105 model with six degrees-of-freedom [75], which was also used in an experiment on hover HDDs conducted in the SRS at TU Delft [34]. The other is a linearized, decoupled version of that model. The linearized

version of the model is included predominantly because linear systems are much easier to analyze with the models introduced in Chapter 6. Therefore, if the present research shows sufficiently similar results and control strategy with both vehicle models, it may be beneficial for future experiments to be conducted with the linear version rather than the more complex non-linear model.

A complete list of all six resulting experiment conditions can be found in Table 7-3. Prior to the experiment, participants will conduct training runs with each condition in order to get acquainted with both the simulator as well as the conditions. A run will be aborted in case the helicopter collides with the ground.

**Table 7-3:** Experiment conditions

Visibility / Interface	Model	
	non-linear	linear
Good visibility, no hover display	A	B
Brownout, display 1	C	D
Brownout, display 2	E	F

### Dependent variables

**Task performance** will be measured via the RMS error between the hover target and the horizontal and vertical helicopter position. The measurements thereof will start once the pilot first reaches an adequate distance from the target, and they will end 30 s later. Adequate performance targets according to the ADS-33 manual are indicated in Table 7-4. **Control activity** and **strategy** will be evaluated based on analysis of the measured experiment data. **Pilot workload** estimates will be collected after each experiment condition via the Rating Scale Mental Effort (RMSE) [76]. The Situation Awareness Rating Scale (SART) will be used to obtain subjective pilot judgments on **situational awareness** [77]. Any additional comments the pilots make after an experiment condition will be noted down as **pilot opinion** on the displays.

**Table 7-4:** Adequate performance bounds from the ADS-33

Parameter	Boundary
Longitudinal deviation	$\pm 6$ ft
Lateral deviation	$\pm 6$ ft
Altitude deviation	$\pm 4$ ft

### Control variables

During all experiment conditions, the head-down basic instrument panel depicted in Figure 7-3 will be available continuously. The control task described before will be the same for each condition. No wind will be present during the experiment, nor will the motion cueing system of the simulator be used.



Figure 7-3: Basic instrument panel

## Participants

As the aim of the display is to support helicopter pilots in performing a hover maneuver, the participants invited for the experiment will be licensed helicopter pilots. Using participants without experience in flying helicopters might add confounds, as they do not yet have a natural control strategy in performing a hover maneuver. Furthermore, the complexity of the helicopter model used would need to be substantially downgraded when using novice pilots. Thus, eligible participants are private, commercial or military helicopter pilots. A minimum number of two participants is needed, provided that there is enough time available for them to do 6 – 10 runs for every condition.

## Hypotheses

The hypotheses are listed in Table 7-5. The first hypothesis is based on the expectation that the lack of available OTW visuals and the potential false motion cues caused by the brownout simulation will decrease the pilot SA. Reduced SA in turn is assumed to lead to increased activity and workload, possibly resulting in worse hover performance.

The reasoning for the second hypothesis is that the invited participants are experienced helicopter pilots. The non-linear model most realistically simulates the behavior of a real helicopter, therefore the linearized model might lead to increased control activity and workload as the behavior may be somewhat unexpected for the pilots. Expected heading changes will be minimal in the experiment, since the starting position is directly in front of the target location. This should lower the difference experienced between the models by the pilots, leading to the expectation that performance will be comparable with both models.

Finally, the third hypothesis concerns a comparison of the two display configurations. Unlike the first one, the second display has no grid ground texture. This will result in a lower amount of optical flow, potentially leading to a decreased SA and requiring more control input from the pilots. However, the explicit cues present in the synthetic ADS-33 course might compensate for the reduced optical flow. Therefore, it is expected that performance will be only slightly worse with the second display configuration.

Table 7-5: Hypotheses

#	Comparison	Expected difference
1	A → C, E	Performance decreased
	B → D, F	Control activity increased
		Situational awareness decreased
		Workload increased
2	A → B	Similar performance
	C → D	Control activity increased
	E → F	Similar situational awareness
		Workload increased
3	C → E	Performance slightly decreased
	D → F	Control activity increased
		Situational awareness slightly decreased
		Workload increased

### 7-3 Results, outcome and relevance

The results of the experiment will consist of the recorded time traces of the relevant aircraft states and the pilot control input, as well as the subjective pilot judgments on situational awareness and workload and pilot opinions for each of the display configurations. The recorded aircraft states and the control input can then be plotted against time, resulting in approach-to-hover trajectories. Once a stable hover is reached, the positional RMS error (with respect to the hover target) should be as small as possible and the velocities in all axes should be as close to zero as possible.

An effective display adequately compensates for the loss of SA, thereby allowing pilots to perform a hover maneuver in brownout conditions with similar precision and control strategy as in GVE. The baseline condition in good visibility thus provides important comparison data to judge the effectiveness of the display configurations. Further reference trajectories may also be generated with the crossover model described in Section 6-1. Despite the fact that this model was validated only for compensatory displays with single-axis disturbance-rejection tasks, the generated trajectories can still serve as useful comparison material. Finally, the experimental data from the conditions with the linearized vehicle dynamics will be analyzed with the VCCM introduced in Section 6-2, with the aim of identifying what cues the pilots used and whether the implemented cues were used as expected.

The tested display configurations will not be equally effective in supporting hover performance. The results of the research will indicate which of the display conditions was most effective. The outcome will point in the direction of what cues need to *at least* be present in such a display, and based on this, recommendations for new hover aid displays as well as future research can be made.



---

# Bibliography

- [1] Syal, M. and Leishman, J. G., “Modeling of bombardment ejections in the rotorcraft brownout problem,” *AIAA Journal*, vol. 51, no. 4, pp. 849–866, 2013.
- [2] Benson, A. J. and Stott, J. R. R., “Spatial Disorientation in Flight,” in *Ernsting’s Aviation Medicine* (Rainford, D. J. and Gradwell, D. P., eds.), ch. 28, pp. 433–458, London, United Kingdom: Hodder Arnold, 4 ed., 2006.
- [3] Federal Aviation Administration, “Basic Flight Maneuvers,” in *Helicopter Flying Handbook*, ch. 9, pp. 9.1–9.20, Oklahoma City, OK, United States: U.S. Department of Transportation, FAA-H-8083-21B ed., 2019.
- [4] Couch, M. and Lindell, D., “Study on Rotorcraft Safety and Survivability,” in *Proceedings of the 66th American Helicopter Society Forum*, (Phoenix, AZ, United States), May 10–13, 2010.
- [5] Task Group HFM-162, “Rotary-Wing Brownout Mitigation: Technologies and Training,” tech. rep., (RTO-TR-HFM-162), Brussels, Belgium: NATO, 2012.
- [6] Wagtendonk, W. J., *Principles of Helicopter Flight*. Newcastle, WA, United States: Aviation Supplies & Academics, 2 ed., 2011.
- [7] Griffiths, D. A., Ananthan, S., and Leishman, J. G., “Predictions of rotor performance in ground effect using a free-vortex wake model,” *Journal of the American Helicopter Society*, vol. 50, no. 4, pp. 302–314, 2005.
- [8] Jasion, G. and Shrimpton, J., “Prediction of Brownout Inception Beneath a Full-Scale Helicopter Downwash,” *Journal of the American Helicopter Society*, vol. 57, no. 4, pp. 1–13, 2012.
- [9] Phillips, C. and Brown, R. E., “Eulerian Simulation of the Fluid Dynamics of Helicopter Brownout,” *Journal of Aircraft*, vol. 46, no. 4, pp. 1416–1429, 2009.
- [10] Tritschler, J. K., Celi, R., and Leishman, J. G., “Methodology for rotorcraft brownout mitigation through flight path optimization,” *Journal of Guidance, Control, and Dynamics*, vol. 37, no. 5, pp. 1524–1553, 2014.

- [11] Phillips, C. and Brown, R. E., “The Effect of Helicopter Configuration on the Fluid Dynamics of Brownout,” in *34th European Rotorcraft Forum*, (Liverpool, United Kingdom), September 16–19, 2008.
- [12] Cowherd, C., “Sandblaster 2 Support of See-Through Technologies for Particulate Brownout Task 5 Final Technical Report,” tech. rep., Kansas City, MO, United States: Midwest Research Institute, 2007.
- [13] Milluzzo, J. and Leishman, J. G., “Assessment of rotorcraft brownout severity in terms of rotor design parameters,” *Journal of the American Helicopter Society*, vol. 55, no. 3, pp. 1–9, 2010.
- [14] Tritschler, J. K., Syal, M., Celi, R., and Leishman, J. G., “A Methodology for Rotorcraft Brownout Mitigation Using Rotor Design Optimization,” in *66th Annual Forum of the American Helicopter Society*, (Phoenix, AZ, United States), May 10–13, 2010.
- [15] Phillips, C., Kim, H. W., and Brown, R. E., “The Effect of Rotor Design on the Fluid Dynamics of Helicopter Brownout,” in *35th European Rotorcraft Forum*, (Hamburg, Germany), September 22–25, 2009.
- [16] Whitehouse, G. R., Wachspress, D. A., and Quackenbush, T. R., “Aerodynamic Design of Helicopter Rotors for Reduced Brownout,” in *International Powered Lift Conference*, (Philadelphia, PA, United States), October 5–7, 2010.
- [17] Jansen, C., Wennemers, A., Vos, W., and Groen, E., “FlyTact: A Tactile Display Improves a Helicopter Pilot’s Landing Performance in Degraded Visual Environments,” in *6th International Conference on Haptics: Perception, Devices and Scenarios (EuroHaptics 2008)*, (Madrid, Spain), pp. 867–875, June 10–13, 2008.
- [18] Wachspress, D. A., Whitehouse, G. R., Keller, J. D., Yu, K., Gilmore, P., Dorsett, M., and McClure, K., “A High Fidelity Brownout Model for Real-Time Flight Simulations and Trainers,” in *65th Annual Forum of the American Helicopter Society*, (Grapevine, TX, United States), May 27–29, 2009.
- [19] Syal, M. and Leishman, J. G., “Predictions of brownout dust clouds compared to photogrammetry measurements,” *Journal of the American Helicopter Society*, vol. 58, no. 2, pp. 1–18, 2013.
- [20] Gerlach, T., “Visualisation of the brownout phenomenon, integration and test on a helicopter flight simulator,” *The Aeronautical Journal*, vol. 115, no. 1163, pp. 57–63, 2011.
- [21] Cheung, B., “Nonvisual Spatial Orientation Mechanisms,” in *Spatial Disorientation in Aviation* (Previc, F. H. and Ercoline, W. R., eds.), ch. 7, pp. 37–94, Reston, VA, United States: American Institute of Aeronautics and Astronautics, 2004.
- [22] Parmet, A. J. and Ercoline, W. R., “Spatial Orientation in Flight,” in *Fundamentals of Aerospace Medicine* (Davis, J. R., Johnson, R., Stepanek, J., and Fogarty, J. A., eds.), ch. 6, pp. 142–205, Philadelphia, PA, United States: Lippincott Williams & Wilkins, 4 ed., 2008.

- [23] Benson, A. J., "Spatial Orientation in Flight," in *Ernsting's Aviation Medicine* (Rainford, D. J. and Gradwell, D. P., eds.), ch. 18, pp. 293–306, London, United Kingdom: Hodder Arnold, 4 ed., 2006.
- [24] Previc, F. H., "Visual Illusions in Flight," in *Spatial Disorientation in Aviation* (Previc, F. H. and Ercoline, W. R., eds.), ch. 7, pp. 283–321, Reston, VA, United States: American Institute of Aeronautics and Astronautics, 2004.
- [25] Baskett, B. J., "Aeronautical Design Standard, Performance Specification: Handling Qualities Requirements for Military Rotorcraft," tech. rep., (ADS-33E-PRF), Redstone Arsenal, AL, United States: U.S. Army Aviation and Missile Command, 2000.
- [26] Hoh, R. H., Baillie, S. W., and Morgan, J. M., "Flight Investigation of the Tradeoff Between Augmentation and Displays for the NOE Flight in Low Visibility," in *American Helicopter Society National Specialists' Meeting on Flight Controls and Avionics*, (Cherry Hill, NJ, United States), pp. 1–13, October 13–15, 1987.
- [27] Hart, S. G., "Helicopter Human Factors," in *Human Factors in Aviation* (Wiener, E. L. and Nagel, D. C., eds.), ch. 18, pp. 591–638, San Diego, CA, United States: Academic Press, 1 ed., 1988.
- [28] Heffley, R. K., "A Model for Manual Decelerating Approaches to Hover," in *Proceedings of the 15th Annual Conference on Manual Control*, (Dayton, OH, United States), pp. 545–554, March 20–22, 1979.
- [29] Moen, G. C., DiCarlo, D. J., and Yenni, K. R., "A Parametric Analysis of Visual Approaches for Helicopters," tech. rep., (NASA-TN-D-8275), Hampton, VA, United States: NASA Langley Research Center, 1976.
- [30] Rotaru, C. and Todorov, M., "Helicopter Flight Physics," in *Flight Physics: Models, Techniques and Technologies* (Volkov, K., ed.), ch. 2, pp. 19–48, London, United Kingdom: IntechOpen, 1 ed., 2018.
- [31] Padfield, G. D., *Helicopter Flight Dynamics: The Theory and Application of Flying Qualities and Simulation Modelling*. Oxford, United Kingdom: Blackwell Publishing, 2 ed., 2007.
- [32] Hess, R. A. and Gorder, P. J., "Design and evaluation of a cockpit display for hovering flight," *Journal of Guidance, Control, and Dynamics*, vol. 13, no. 3, pp. 450–457, 1990.
- [33] Eshow, M. M. and Schroeder, J. A., "Improvements in Hover Display Dynamics for a Combat Helicopter," *Journal of the American Helicopter Society*, vol. 38, no. 1, pp. 17–28, 1993.
- [34] Friesen, D., Pavel, M. D., Borst, C., Masarati, P., and Mulder, M., "Pilot Model Development and Human Manual Control Considerations for Helicopter Hover Displays," in *45th European Rotorcraft Forum*, (Warsaw, Poland), September 17–19, 2019.
- [35] Doehler, H.-U., Knabl, P. M., Schmerwitz, S., Eger, T. W., and Klein, O., "Evaluation of DVE Landing Display Formats," in *Proceedings of SPIE 8360, Airborne Intelligence, Surveillance, Reconnaissance (ISR) Systems and Applications IX*, (Baltimore, MD, United States), April 23–27, 2012.

- [36] Viertler, F. X., *Visual Augmentation for Rotorcraft Pilots in Degraded Visual Environment*. Ph.D. dissertation, Fakultät für Maschinenwesen, Technische Universität München, Munich, Germany, 2017.
- [37] Stanton, N. A., Plant, K. L., Roberts, A. P., Allison, C. K., and Harvey, C., “The virtual landing pad: facilitating rotary-wing landing operations in degraded visual environments,” *Cognition, Technology and Work*, vol. 20, no. 2, pp. 219–232, 2018.
- [38] Bachelder, E., McRuer, D., and Hansman, R. J., “Experimental Study of 3-D Synthetic Cues on Rotorcraft Hover Performance,” in *AIAA Atmospheric Flight Mechanics Conference*, (Monterey, CA, United States), August 5–8, 2002.
- [39] Doehler, H.-U., Schmerwitz, S., and Lueken, T., “Visual-conformal display format for helicopter guidance,” in *Proceedings of SPIE 9087, Degraded Visual Environments: Enhanced, Synthetic, and External Vision Solutions 2014*, (Baltimore, MD, United States), May 5–9, 2014.
- [40] Feltman, K. A., Curry, I., Bernhardt, K., Hayes, A., Kirby, S., Davis, B., Sapp, J., Durbin, D., and Hartnett, G., “Integrated Cueing Environment: Simulation Event Four,” tech. rep., (ARL-TR-8538), Fort Rucker, AL, United States: U.S. Army Aeromedical Research Laboratory, 2018.
- [41] Münsterer, T., Kress, M., and Klasen, S., “Sensor based 3D conformal cueing for safe and reliable HC operation specifically for landing in DVE,” in *Proceedings of SPIE 8737, Degraded Visual Environments: Enhanced, Synthetic, and External Vision Solutions 2013*, (Baltimore, MD, United States), April 29–May 3, 2013.
- [42] Jagacinski, R. J. and Flach, J. M., *Control Theory for Humans*. Mahwah, NJ, United States: Lawrence Erlbaum Associates, 2003.
- [43] Wickens, C. D., Lee, J. D., Liu, Y., and Gordon-Becker, S. E., *An Introduction to Human Factors Engineering*. Harlow, United Kingdom: Pearson Education Limited, 2 ed., 2014.
- [44] Gibson, J. J., *The Perception of the Visual World*. Cambridge, MA, United States: The Riverside Press, 1950.
- [45] Koenderink, J. J., “Optic Flow,” *Vision Research*, vol. 26, no. 1, pp. 161–180, 1986.
- [46] Perrone, J. A., “The Perception of Surface Layout During Low Level Flight,” tech. rep., (NASA CP-3118), Moffett Field, CA, United States: NASA Ames Research Center, 1991.
- [47] Warren, W. H., Morris, M. W., and Kalish, M., “Perception of Translational Heading From Optical Flow,” *Journal of Experimental Psychology: Human Perception and Performance*, vol. 14, no. 4, pp. 646–660, 1988.
- [48] Li, L. and Chen, J., “Relative contributions of optic flow, bearing, and splay angle information to lane keeping,” *Journal of Vision*, vol. 10, no. 11, pp. 1–14, 2010.
- [49] Warren, W. H. and Hannon, D. J., “Eye movements and optical flow,” *Journal of the Optical Society of America A*, vol. 7, no. 1, pp. 160–169, 1990.

- [50] Warren, W. H. and Hannon, D. J., "Direction of self-motion is perceived from optical flow," *Nature*, vol. 336, no. 6195, pp. 162–163, 1988.
- [51] Dyre, B. P. and Andersen, G. J., "Image Velocity Magnitudes and Perception of Heading," *Journal of Experimental Psychology: Human Perception and Performance*, vol. 23, no. 2, pp. 546–565, 1997.
- [52] Rogers, B. and Graham, M., "Similarities between motion parallax and stereopsis in human depth perception," *Vision Research*, vol. 22, no. 2, pp. 261–270, 1982.
- [53] Gibson, J. J., Olum, P., and Rosenblatt, F., "Parallax and perspective during aircraft landings," *American Journal of Psychology*, vol. 68, no. 3, pp. 372–385, 1955.
- [54] Warren, R., "Optical transformation during movement: Review of the optical concomitants of egomotion," tech. rep., (AFOSR-TR-82-1028), Columbus, OH, United States: Ohio State University, Department of Psychology, Aviation Psychology Laboratory, 1982.
- [55] Larish, J. F. and Flach, J. M., "Sources of Optical Information Useful for Perception of Speed of Rectilinear Self-Motion," *Journal of Experimental Psychology: Human Perception and Performance*, vol. 16, no. 2, pp. 295–302, 1990.
- [56] Padfield, G. D., Lee, D. N., and Bradley, R., "How Do Helicopter Pilots Know When to Stop, Turn or Pull Up? (Developing Guidelines for Vision Aids)," *Journal of the American Helicopter Society*, vol. 48, no. 2, p. 108, 2010.
- [57] Flach, J. M., Warren, R., Garness, S. A., Kelly, L., and Stanard, T., "Perception and Control of Altitude: Splay and Depression Angles," *Journal of Experimental Psychology: Human Perception and Performance*, vol. 23, no. 6, pp. 1764–1782, 1997.
- [58] Flach, J. M., Hagen, B. A., and Larish, J. F., "Active regulation of altitude as a function of optical texture," *Perception & Psychophysics*, vol. 51, no. 6, pp. 557–568, 1992.
- [59] Denton, G. G., "The Influence of Visual Pattern on Perceived Speed," *Perception*, vol. 9, no. 4, pp. 393–402, 1980.
- [60] Lee, D. N., "A theory of visual control of braking based on information about time-to-collision," *Perception*, vol. 5, no. 4, pp. 437–459, 1976.
- [61] Kaiser, M. K. and Mowafy, L., "Optical Specification of Time-to-Passage: Observers' Sensitivity to Global Tau," *Journal of Experimental Psychology: Human Perception and Performance*, vol. 19, no. 5, pp. 1028–1040, 1993.
- [62] Szoboszlay, Z. P., McKinley, R. A., Braddom, S. R., Harrington, W. W., Burns, H. N., and Savage, J. C., "Landing an H-60 Helicopter in Brownout Conditions Using 3D-LZ Displays," in *Proceedings of the 66th Annual American Helicopter Society Forum*, (Phoenix, AZ, United States), May 11–13, 2010.
- [63] Sykora, B., "BAE Systems Brownout landing aid system technology (BLAST) system overview and flight test results," in *Proceedings of SPIE 8360, Airborne Intelligence, Surveillance, Reconnaissance (ISR) Systems and Applications IX*, (Baltimore, MD, United States), April 23–27, 2012.

- [64] Anonymous, “Synthetic Vision EFIS for Helicopters,” tech. rep., Mineral Wells, TX, United States: Cobham Avionics, Integrated Systems, 2009.
- [65] Johnson, W. W. and Phatak, A. V., “Optical Variables and Control Strategy Used in a Visual Hover Task,” in *IEEE International Conference on Systems, Man and Cybernetics*, pp. 719–724, 1989.
- [66] Negrin, M., Grunwald, A. J., and Rosen, A., “Superimposed Perspective Visual Cues for Helicopter Hovering Above a Moving Ship Deck,” *Journal of Guidance, Control, and Dynamics*, vol. 14, no. 3, pp. 652–660, 1991.
- [67] Prinzel, L. J. and Risser, M., “Head-Up Displays and Attention Capture,” tech. rep., (NASA TM-2004-213000), Hampton, VA, United States: NASA Langley Research Center, 2004.
- [68] Crawford, J. and Neal, A., “A Review of the Perceptual and Cognitive Issues Associated With the Use of Head-Up Displays in Commercial Aviation,” *The International Journal of Aviation Psychology*, vol. 16, no. 1, pp. 1–19, 2006.
- [69] Wickens, C. D. and Alexander, A. L., “Attentional Tunneling and Task Management in Synthetic Vision Displays,” *The International Journal of Aviation Psychology*, vol. 19, no. 2, pp. 182–199, 2011.
- [70] Newman, R. L. and Greeley, K. W., “Helmet-Mounted Display Design Guide,” tech. rep., (NASA CR-97-206824), San Marcos, TX, United States: Crew Systems, 1997.
- [71] Curtis, M. T., Jentsch, F., and Wise, J. A., “Aviation Displays,” in *Human Factors in Aviation*, pp. 439–478, Burlington, MA, United States: Elsevier, 2010.
- [72] Sweet, B. T., “A Model of Manual Control with Perspective Scene Viewing,” in *Proceedings of the AIAA Modeling and Simulation Technologies Conference*, (Boston, MA, United States), pp. 1–20, August 19–22, 2013.
- [73] McRuer, D. T. and Jex, H. R., “A Review of Quasi-Linear Pilot Models,” *IEEE Transactions on Human Factors in Electronics*, vol. HFE-8, no. 3, pp. 231–249, 1967.
- [74] Sweet, B. T., *The Identification and Modeling of Visual Cue Usage in Manual Control Task Experiments*. Ph.D. dissertation, Department of Aeronautics and Astronautics, Stanford University, Stanford, CA, United States, 1999.
- [75] Miletović, I., Pool, D. M., Stroosma, O., Pavel, M. D., Wentink, M., and Mulder, M., “The Use of Pilot Ratings in Rotorcraft Flight Simulation Fidelity Assessment,” in *Proceedings of the 73rd American Helicopter Society Forum*, (Fort Worth, TX, United States), May 9–11, 2017.
- [76] de Waard, D., *The Measurement of Drivers’ Mental Workload*. Ph.D. dissertation, Rijksuniversiteit Groningen, Groningen, Netherlands, 1996.
- [77] Curtis, M. T., Jentsch, F., and Wise, J. A., “Situational Awareness Rating Technique (SART): The development of a tool for aircrew systems design,” in *Situational Awareness in Aerospace Operations*, pp. 3.1–3.17, Neuilly-Sur-Seine, France: NATO Advisory Group for Aerospace Research and Development, 1990.

# **Part III**

# **Appendices**



---

# Appendix A

---

## Software Architecture

This chapter provides a summary of the software developed for the experiment, aimed at helping future users of the project. Appendix A-1 describes the various modules and channels included in the DUECA project. Appendix A-2 provides further details on the module responsible for the creation of the outside visuals and the displays.

### A-1 DUECA Architecture

The project can be found in the repository under the name **MeimaHoverBrownout**. The diagram in Figure A-1 portrays the most important modules (rectangles) and channels (rounded rectangles) in the DUECA project. Color-coding was used to improve clarity: blue modules and channels are involved in the development of visuals or displays, red relates to the implementation of vehicle dynamics, green is for the graphical user interfaces, yellow refers to the hover performance score communicated to the pilots during the experiment, and gray shows logging-related components. Arrows pointing toward a module indicate that the module reads data from the channel; arrows pointing away indicate that the module writes data to the channel. A brief summary of the main modules is given below, separated by functionality.

Modules related to visuals and displays:

- **ExperimentOSGViewer** uses the OpenSceneGraph library for C++ to create the outside visuals and the displays. More information is provided in the next section.
- **ExperimentOSGOverlay** contains two-dimensional HUD elements, such as a flight-path marker and altitude or speed tapes. These were not used during the experiment.

Modules related to vehicle dynamics:

- **InputAdapter** prepares the raw pilot control inputs for use in the two vehicle models.
- **LinearDynamics** simulates the response of the linear model used in the experiment.

- **DraftSim/Model** is a borrowed module responsible for the implementation of the non-linear vehicle dynamics.
- **OutputAdapter** uses the output of the vehicle models to calculate the new helicopter position in the virtual world.

Graphical user interfaces:

- **ExperimentOSGViewerGUI** allows the user to switch between good visibility and brownout conditions, and to change the display configuration without the need to restart the project. Furthermore, it is used to set the initial conditions of the linear model.
- **DraftSim/ECI** is a borrowed module that is responsible for initialization of the non-linear model.

Miscellaneous modules:

- **HoverPerformanceScore** starts calculating the RMS position error relative to the hover target when the helicopter enters the adequate performance bounds described in the ADS-33 for the first time. Both the score and a timer (to note when the 30-second hover phase is over) are shown on the ExperimentOSGViewerGUI.
- **Logger** is responsible for logging all control inputs and state variables throughout the experiment.

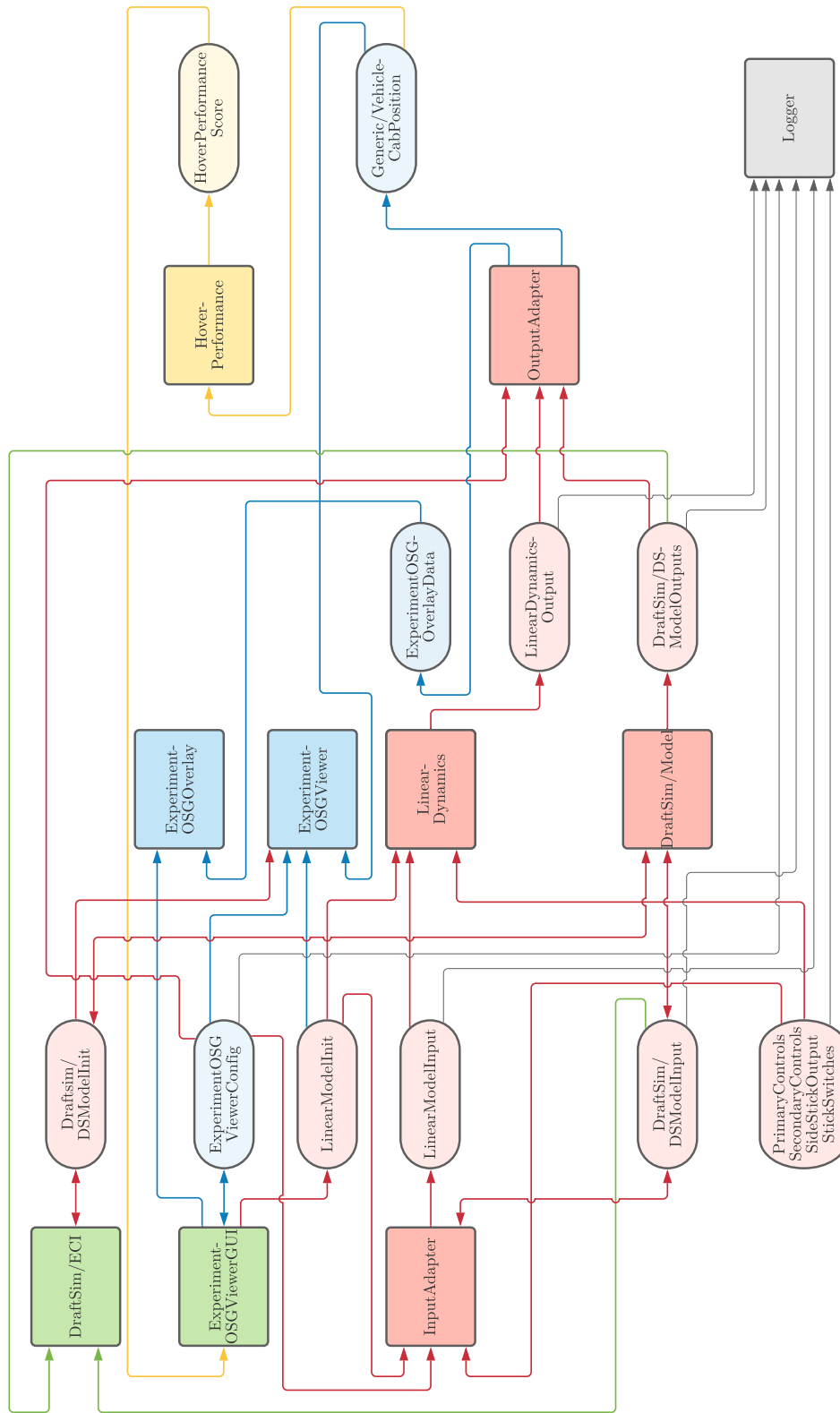


Figure A-1: Software architecture of the DUECA project

## A-2 OpenSceneGraph Implementation

This section describes the **ExperimentOSGViewer** module in more detail. The visuals were predominantly implemented using OpenSceneGraph. Some nodes (mainly those for outside visuals in clear conditions) were designed using the 3D rendering program 3ds Max.

A basic overview of the scene graph structure and a description of the various shapes used in the diagrams is shown in Figure A-2. Figure A-3 summarizes the structure of the implementation of the outside visuals in good visibility. The structure of the displays and brownout are provided in Figure A-4.

The module makes extensive use of switches in OpenSceneGraph, which, when linked to the graphical user interface, can be used to hide or show various display elements without the need to restart the program. Matrix transforms are used to dynamically update the drawing of the horizon, splay and depression lines. The latter two were designed to fade out (using alpha values) further away in the scene, in order to avoid clutter in the far field. To achieve this throughout the experiment, the transform matrices effectively shift the entire grid by one cell size whenever the helicopter passes over a grid line, such that the lines close to the pilot are clearly visible at all times.

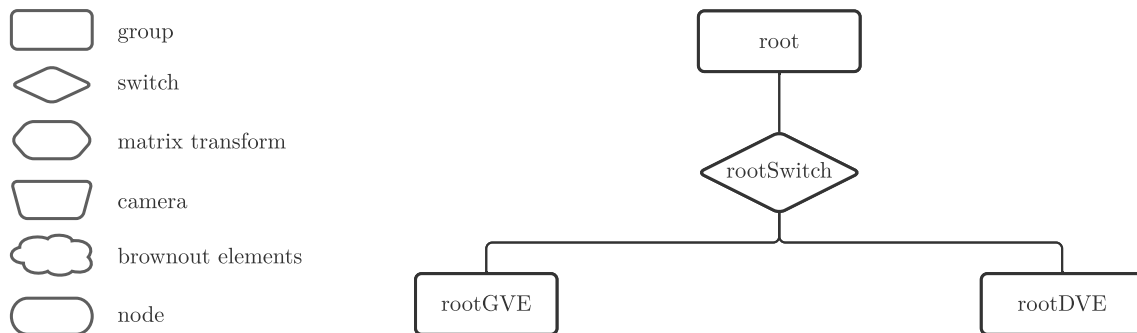


Figure A-2: Basic overview of scene graph structure

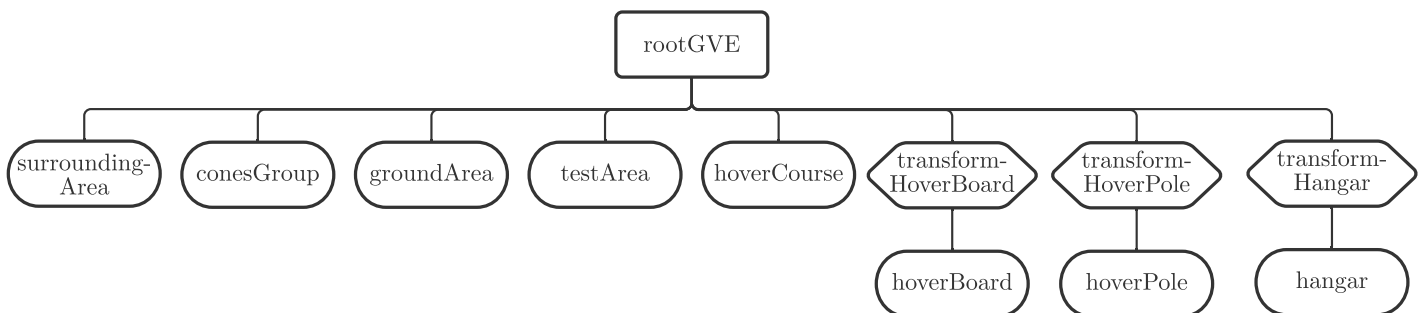


Figure A-3: Detailed overview of the implementation of good visuals

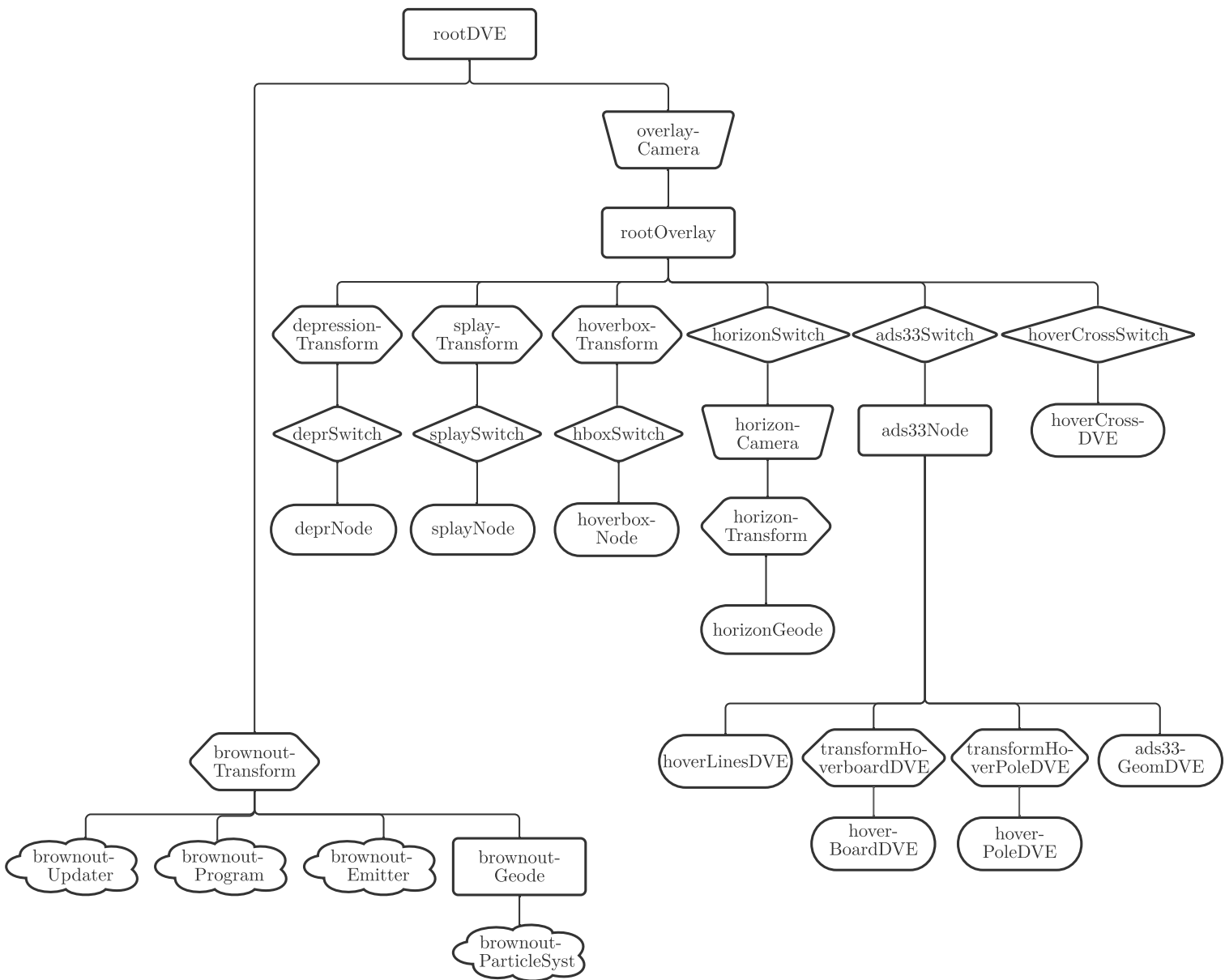


Figure A-4: Detailed overview of the implementation of displays and brownout



---

# Appendix B

---

## Experiment Briefing

### Superimposed visual cues for helicopters hovering in brownout conditions

Experiment participant briefing, 04-07-2020, Niek Meima

#### Introduction

Thank you very much for participating in this scientific experiment. Your participation and input is essential to be able to connect theoretical research with its practical implications. This experiment has the goal of investigating the effect of two different helicopter displays that are superimposed on the out-the-window view of a pilot flying in brownout conditions.

This document provides the most important information to prepare you for the experiment. Apart from reading this document, no further preparation is needed on your part. After covering organizational topics, this document summarizes the purpose of the research project and this specific experiment. Afterwards, the experiment procedure and your task as participant is described. The last section explains what data will be collected during the experiment and how it will be processed afterwards.

## Organizational

---

<b>Name of researcher:</b>	Niek Meima
<b>Contact information:</b>	n.v.meima@student.tudelft.nl +31 6 23 25 96 79
<b>Location:</b>	SIMONA Research Simulator, Faculty of Aerospace Engineering, Delft University of Technology, Kluyverweg 1, 2629 HS Delft
<b>Date of experiment:</b>	15 July 2020
<b>Meeting time and place:</b>	10:00h at the service desk in the main entry hall
<b>Duration:</b>	Approximately three hours, including breaks

---

Special regulations are in place at TU Delft due to the current COVID-19 situation. Upon arrival, you will be provided with detailed safety instructions to ensure your participation to the experiment will be in line with current RIVM COVID-19 regulations at all times.

Before the experiment starts, a form will be handed to you with which you can request to be reimbursed for your travel costs from inside the Netherlands. If you traveled by car and want to claim travel cost reimbursement, please note down your point of origin on the form. **Due to COVID-19 safety regulations at TU Delft, we kindly ask you not to travel to the experiment location by public transport.**

## Purpose of the research

Brownouts are one of the leading causes of helicopter accidents in dry climates. A brownout occurs when the downwash of the rotor blades causes loose particles in the environment to be stirred up, forming a cloud of sand or dust around the helicopter. The outside view of the pilot is obscured and the motion of the particles in the cloud can give the pilot incorrect motion cues, significantly impairing their situational awareness. With the emergence of affordable high-performance helmet-mounted displays, the use of augmented reality has become a promising means to compensate for the loss of visual information and reduce the risks associated with flying in brownout conditions.

This experiment focuses on the hover maneuver, and its aim is to investigate what visual cues should be provided on a display such that the pilot can successfully perform the maneuver in case of a brownout. Two displays were developed, which will be provided as overlays on top of the outside view of the simulator. You will have the opportunity to accustom yourself with the displays before the experiment. Performance, control strategy, workload, and situational awareness will be compared between runs with good visuals and experiment runs in brownout conditions, where one of the two displays will be provided. Each condition will be flown with a non-linear helicopter model and a linear model. There are a total of six experiment conditions, see Table B-1. The order of the conditions will be randomized and for each condition multiple runs will be conducted. One experiment run contains the elements of

1. approaching a predefined hover point with a set velocity from a certain horizontal distance,

2. decelerating towards the hover point in a smooth maneuver, and
3. hovering at the point as precisely as possible for thirty seconds.

**Table B-1:** Experiment conditions

Visibility / Interface	Model	
	non-linear	linear
Good visibility, no hover display	A	B
Brownout, display 1	C	D
Brownout, display 2	E	F

## Experiment procedure

**Timetable:** The experiment will take approximately three hours to complete. This includes an introduction and time to get acclimated with the simulator, six experiment conditions of about twenty minutes each, and a final debriefing. A longer coffee break is scheduled halfway the experiment, between the third and fourth experiment condition. Smaller breaks can be held at any time, preferably before or after an experiment condition is completed.

**Simulator:** For this experiment, the motion system of the SIMONA Research Simulator will be deactivated. The simulator will not move while you are inside. You will receive a simulator safety briefing before the experiment.

**Experiment conditions:** Each experiment condition will take approximately twenty minutes to complete and contains the following steps:

1. You are seated in the right-hand seat of the simulator, the door is closed, and you are connected with the researcher through the audio system
2. You can conduct multiple practice runs for the condition to familiarize yourself with the situation
3. You conduct a specific number of recorded experiment runs
4. You fill out questionnaires pertaining to this experiment condition

**Experiment run:** One experiment run consists of the following steps:

1. The researcher sets the correct condition, starting position and velocity
2. You can utilize a separate trim-display to place the helicopter controls in approximate trim-position for this flight state
3. When you are ready, the researcher will count down from three to one, afterwards calling out "your controls" and releasing the simulator controls to you, starting the run

4. You conduct the experiment task (as described in the next section). The researcher will inform you via intercom when you reached adequate performance, and when the thirty seconds of hovering are over
5. The researcher will call out “my controls”, stop the simulation, and reports a performance score for this run
6. The researcher asks you to indicate a MISC score

**Motion sickness:** It is possible that operating the simulator with moving visuals, but no actual body movement, can induce symptoms of motion sickness. Therefore, you will be asked to indicate a score on the so-called Misery Scale (MISC) after each run. The MISC scale is provided in Table B-2.

**Table B-2:** Misery Scale

Symptom		Score
No problems		0
Slight discomfort but no specific symptoms		1
Dizziness, warm, headache, stomach awareness, sweating, etc.	Vague	2
	Some	3
	Medium	4
	Severe	5
Nausea	Vague	6
	Some	7
	Medium	8
	Severe	9
Vomiting		10

**Withdrawal:** Your participation in this experiment is voluntary. You can, at any time, decide to stop participating in the experiment. There will be no repercussions for doing so, and you do not have to provide a reason.

## Experiment task

At the beginning of each experiment run, the helicopter you are flying will be placed at a fixed distance from the target hover point, traveling straight towards it with a predetermined forward velocity. In every experiment run, your task as a pilot is:

“Approach the hover target point with the initial forward speed of the helicopter at the beginning of the run. At a distance you deem appropriate, initiate a

deceleration maneuver to smoothly and precisely come to a stop at the hover point. After reaching the hover point, maintain a stabilized hover, minimizing deviations from the hover target point, for thirty seconds. Please avoid accomplishing most of the deceleration maneuver well before the hover point and then creeping up to the final hover position.”

After each run, an aggregated measure of your deviation from the hover point (after reaching adequate boundaries for the first time, see Table B-3) will be communicated to you. This allows you to judge your performance and to aim for improvements in hover precision. The target hover altitude is 7 ft. If you hit the ground during an experiment run, this run will be stopped.

**Table B-3:** Adequate performance bounds

Parameter	Boundary
Longitudinal deviation	$\pm 6$ ft
Lateral deviation	$\pm 6$ ft
Altitude deviation	$\pm 4$ ft

## Data management

Your privacy is important to us. Therefore, we want to inform you about how we will treat your personal data, and how we will treat the data we will collect during the experiment. If you have any questions or complaints, please feel free to contact the researcher of this experiment **Niek Meima**, [N.V.Meima@student.tudelft.nl](mailto:N.V.Meima@student.tudelft.nl), and/or the data steward of the Faculty of Aerospace Engineering at TU Delft: **Heather Andrews**, [H.E.AndrewsMancilla@tudelft.nl](mailto:H.E.AndrewsMancilla@tudelft.nl).

### Personal data collection

Personal data we collect from you, like your name and contact information, will only be used in two ways: 1) By the main researcher of this experiment to contact you, and 2) by the necessary university departments to reimburse your travel expenses. No personal information will ever be published or disclosed to third parties.

### Anonymous data collection

Before the experiment, some information about your experience as a helicopter pilot will be recorded anonymously, only linked to the anonymous experiment data. Flight data of the experiment runs, including manual control inputs, will be recorded during the experiment. It will be impossible to connect the data to the personal information of the participating pilot, except for a limited time for the main researcher of the experiment. The researcher will make all recorded data anonymous directly after the experiment. It will not be possible for other

members of the research group or third parties to link experiment data with your personal information at any time.

Data will only be published anonymously, with no connection to the personal information of the pilots. Publishing targets include: Scientific journals, scientific conference presentations, scientific and technical reports, public outreach material, education material and/or a MSc thesis.

---

## Professional experience information

To be able to put the results in relation to experience, you are asked to fill in this questionnaire.

1. Age: \_\_\_\_\_

2. Gender:

Male

Female

3. Based on your experience as a pilot, please provide the following information:

(a) Helicopter license type:

PPL

CPL

Other: \_\_\_\_\_

(b) Total helicopter flight hours: \_\_\_\_\_

4. Have you ever participated in a research experiment?

Yes

No

If yes, please elaborate on the type of experiment (handling qualities, motion cueing, ...):

---



---

Appendix C

---

## **Consent Forms**

**Participant Consent Form for  
“Experiment: Superimposed visual cues for helicopters hovering in brownout  
conditions”**

*Please tick the appropriate boxes*

Yes No

**Taking part in the experiment**

I have read and understood the experiment briefing dated 04-07-2020. I have been able to ask questions about the study and my questions have been answered to my satisfaction.  Yes  No

I consent voluntarily to be a participant in this study and understand that I can refuse to answer questions and that I can withdraw from the experiment at any time, without having to give a reason.  Yes  No

I understand that taking part in the experiment involves the recording of my manual control inputs while flying a helicopter model in the SIMONA Research Simulator, as well as filling out multiple survey questionnaires. I am aware that experience related pilot data such as licence type, flight hours, experiment experience and anonymous demographic information will be collected before the experiment.  Yes  No

**Risks associated with participating in the experiment**

I understand that taking part in the study involves the following risks: Possible physical discomfort while piloting the simulator due to motion sickness. I confirm that I am able to report my level of wellbeing to the researcher based on the “misery scale”, as explained in the briefing. The experiment will be paused or aborted if my self-reported sickness level reaches a certain misery-scale threshold, or at any time I don’t feel well enough to continue.  Yes  No

I understand that taking part in the experiment involves the following risks: Operating the SIMONA Research Simulator involves interacting with high-power equipment, which could be dangerous in the very unlikely situation of unexpected system behaviour. A detailed safety briefing, covering emergency shut-off and exit procedures, has been provided to me.  Yes  No

**Use of the information in the experiment**

I understand that the information I provide will be analysed in the research group (in anonymous form). I understand and consent that the anonymous data and the analysis results can be published in anonymous form in scientific journals, in scientific conference publications, PhD theses, public outreach material, technical reports or education material.  Yes  No

I understand that personal information collected about me that can identify me, such as my name or contact information, will not be shared beyond the research group.  Yes  No

I understand that my personal information will never be directly linked to the data collected during the experiment. I understand that the collected data will be anonymised by the researcher after the experiment, and before being analysed or shared with anyone in the research group.  Yes  No

**COVID-19 safety requirements**

I confirm that the researcher has provided me with detailed safety instructions to ensure my experiment session can be performed in line with current RIVM COVID-19 regulations *at all times* and that these instructions are fully clear to me.  Yes  No

I understand that also for my travel to/from the experiment session I should *at all times* adhere to current RIVM COVID-19 regulations. I confirm that I have travelled to TU Delft’s Faculty of Aerospace Engineering with either my own car, by bicycle, or on foot.  Yes  No

---

**Signatures**

---

Participant name (print letters)

---

Participant signature

---

Date

I, the researcher, have accurately discussed this sheet with the potential participant and, to the best of my ability, ensured that the participant understands to what they are freely consenting.

---

Researcher name (print letters)

---

Researcher signature

---

Date

**Participant Travel Reimbursement Form for  
“Experiment: Superimposed visual cues for helicopters hovering in brownout  
conditions”**

*Please tick the appropriate boxes*

**Travel cost reimbursement**

I would like to have my travel costs from within the Netherlands to TU Delft, to participate in this experiment, reimbursed.

**Yes No**

I used public transportation to travel to TU Delft.

*If yes: Please provide your transportation tickets (or an OV Chipcard log of the travel, detailing the travel cost) to the researcher.*

I used a car to travel to TU Delft.

*If yes: Your reimbursement will be based on the distance between TU Delft and the origin of travel, calculated with the ANWB route planner.*

If you want to claim travel reimbursement, please fill in the following information:

Name of participant \_\_\_\_\_

Bank account number \_\_\_\_\_

Postal address \_\_\_\_\_

\_\_\_\_\_

Travel origin address \_\_\_\_\_

(only if claiming car-allowance,  
and if different from postal address) \_\_\_\_\_

E-mail address \_\_\_\_\_

\_\_\_\_\_  
Participant name (print letters)

\_\_\_\_\_  
Participant signature

\_\_\_\_\_  
Date

---

# Appendix D

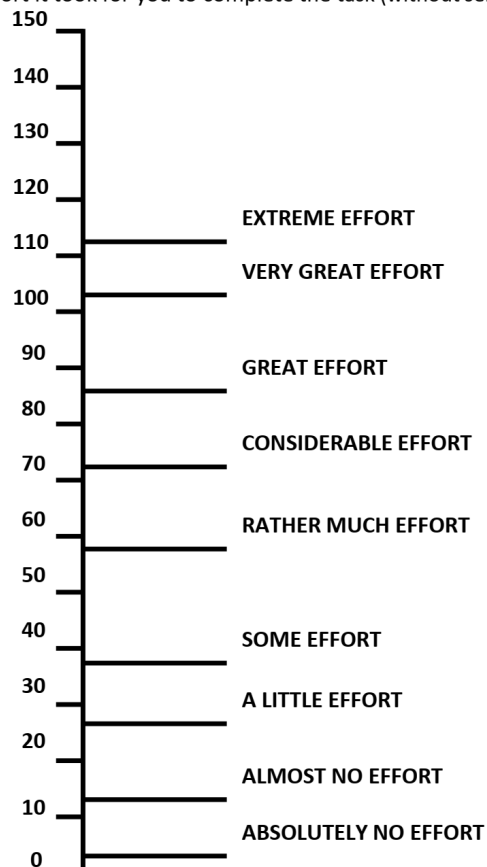
---

## Experiment Questionnaires

### D-1 RSME

#### RSME (Rating Scale Mental Effort)

Please indicate, by marking the vertical axis below, how much effort it took for you to complete the task (without sensor failure).



## D-2 SART

**SART (Situation Awareness Rating Scale)**

Please rate the level of each component of situation awareness that you had when you performed the task (without sensor failure) by circling the appropriate number for each component.

DEMAND									
Instability of situation									
Likeness of the situation to change suddenly	Low	1	2	3	4	5	6	7	High
Variability of situation									
Number of variables that require your attention during the task	Low	1	2	3	4	5	6	7	High
Complexity of situation									
Degree of complication (number of closely connected or coupled elements) of the situation	Low	1	2	3	4	5	6	7	High

SUPPLY									
Arousal									
Degree to which you are ready for activity; ability to anticipate and keep up with the flow of events	Low	1	2	3	4	5	6	7	High
Spare mental capacity									
Amount of free mental capacity available during the task to apply to new and different tasks	Low	1	2	3	4	5	6	7	High
Concentration									
Degree to which your thoughts are brought to bear on the situation; degree to which you focus on important elements and events	Low	1	2	3	4	5	6	7	High
Division of attention									
Ability to divide your attention among several key issues during the mission; ability to concern yourself with many aspects of current and future events simultaneously	Low	1	2	3	4	5	6	7	High

UNDERSTANDING									
Information quantity									
Amount of knowledge received and understood (e.g. attitude, aircraft & obstacle position, speed and direction of flight, information about future aircraft states)	Low	1	2	3	4	5	6	7	High
Information quality									
Degree of goodness, value, usefulness of information communicated	Low	1	2	3	4	5	6	7	High
Familiarity									
Degree of acquaintance with the situation	Low	1	2	3	4	5	6	7	High

## **D-3 Pilot opinion**

Code Tu

How confident did you feel in using the outside visuals to fulfil the task?	Low	1	2	3	4	5	6	7	High
Considering good visibility, how realistic were...									
...the helicopter handling characteristics with the non-linear model? (cond. 1, 4, 5)	*1 Low	1	2	3	4	5	6	7	High
...the helicopter handling characteristics with the linear model? (cond. 2, 3, 6)	*1 Low	1	2	3	4	5	6	7	High
...the outside visuals & visibility?	Low	1	2	3	4	5	6	7	High
...the cockpit control setup (cyclic, collective, pedals)?	Low	1	2	3	4	5	6	7	High
...the cockpit instrument setup (Primary flight instrument panel)?	Low	1	2	3	4	5	6	7	High
Do you have any additional comments on the simulation realism or the outside visuals?									
<p>The line of cones helps to visualise your position in the length path, however its not so clear which one to use.</p> <p>*1 There is a clear difference, model non-linear is a bit more difficult to fly</p>									
Considering the brownout conditions...									
...how realistic was the visual implementation of the brownout?	Low	1	2	3	4	5	6	7	High
Do you have any additional comments on the brownout implementation?									
no.									

Code TV

**Display 1:** grid, hover box, hover cross, horizon

How confident did you feel in using display 1 to fulfil the task?	Low	1	2	3	4	5	6	7	High
Considering bad visibility, how useful was display 1 in...									
...holding course and speed?	Low	1	2	3	4	5	6	7	High
...performing a smooth deceleration manoeuvre?	Low	1	2	3	4	5	6	7	High
...hovering precisely in place?	Low	1	2	3	4	5	6	7	High
To what intensity did display 1 change your control behaviour, compared to good visibility?	Low	1	2	3	4	5	6	7	High
If your rating is above 1, please elaborate how:									
<p>It clearly marks the 'safe' Area.                  The grid is of great help for view in distance</p>									
Do you have any additional comments on display 1?									
<p>When you slightly overshoot All references are gone.</p>									

Code Tu

## Display 2: ADS33, horizon line

How confident did you feel in using display 2 to fulfill the task?	Low 1 2 3 4 <u>5</u> 6 7 High
Considering bad visibility, how useful was display 2 in...	
...holding course and speed?	Low 1 2 3 4 5 <u>6</u> 7 High
...performing a smooth deceleration manoeuvre?	Low 1 2 3 4 <u>5</u> 6 7 High
...hovering precisely in place?	Low 1 2 3 4 5 <u>6</u> 7 High
To what intensity did display 2 change your control behaviour, compared to good visibility?	Low 1 2 3 4 <u>5</u> 6 7 High
If your rating is above 1, please elaborate how:	
Altitude/Height above terrain is difficult when not close to a marker line.	
To what intensity did display 2 change your control behaviour, compared to the display 1?	Low 1 2 3 <u>4</u> 5 6 7 High
If your rating is above 1, please elaborate how:	
Your inputs need to be less abrupt to maintain proper control.	
Do you have any additional comments on display 2?	
Same as <del>at</del> when using the cones, <del>it</del> it is difficult to determine the exact position in length.	

Code Tu

Do you have any additional comments that were not covered by the previous questions?



---

## Appendix E

---

# Additional Results

Some additional plots that were not included in the scientific paper are provided in this appendix. Time trajectories of the surge motion variables are presented for all runs in Appendix E-1. Subsequently, in Appendix E-2, the ground tracks during approach and during hover for all runs are plotted. Finally, additional boxplots of the state variables are included in Appendix E-3.

### **E-1 Time trajectories surge motion**

The time trajectories of the variables associated with surge motion are shown for all runs and conditions in Figures E-1 to E-12.

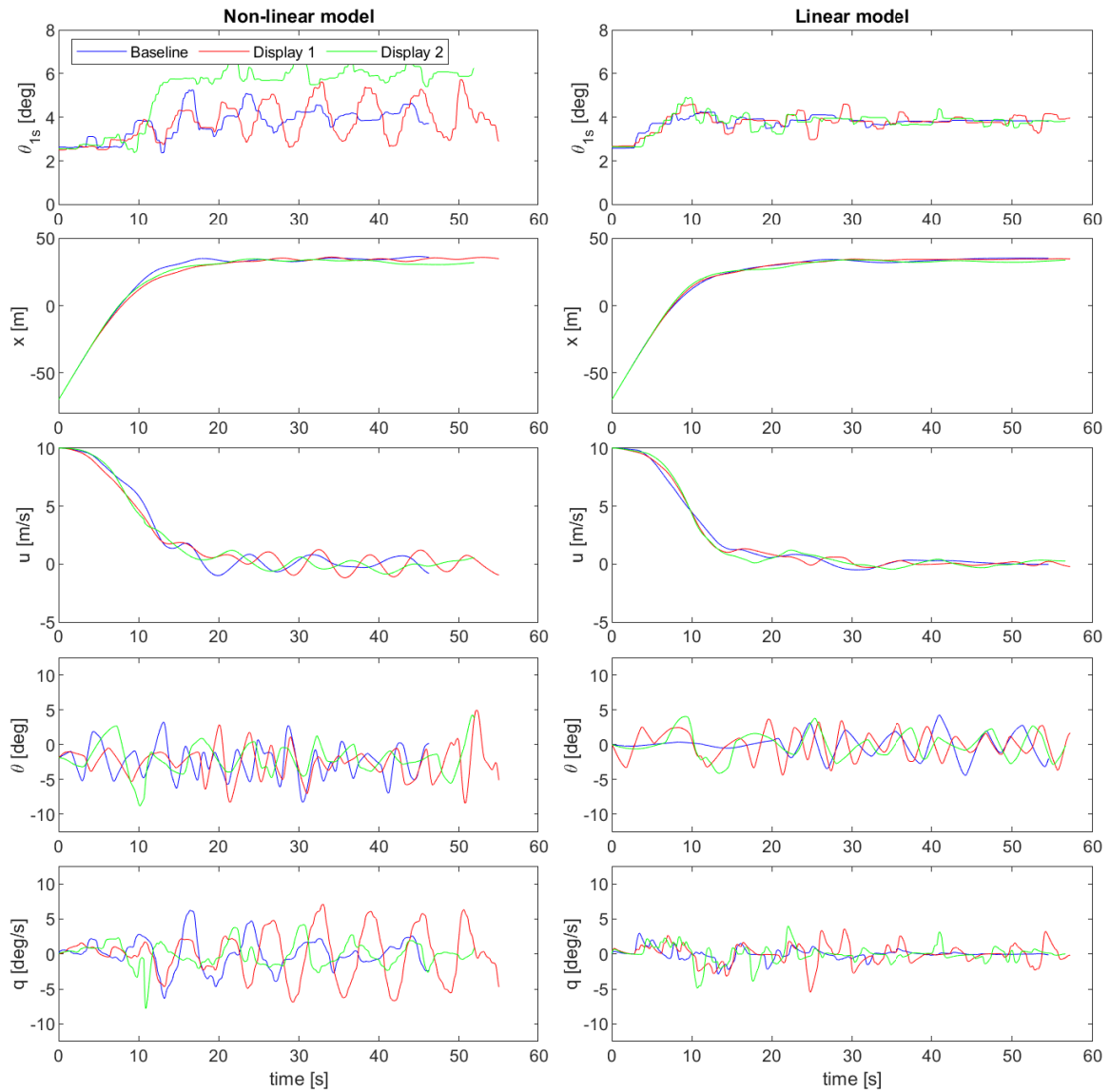


Figure E-1: Time trajectories of surge motion variables, pilot 1, run 1

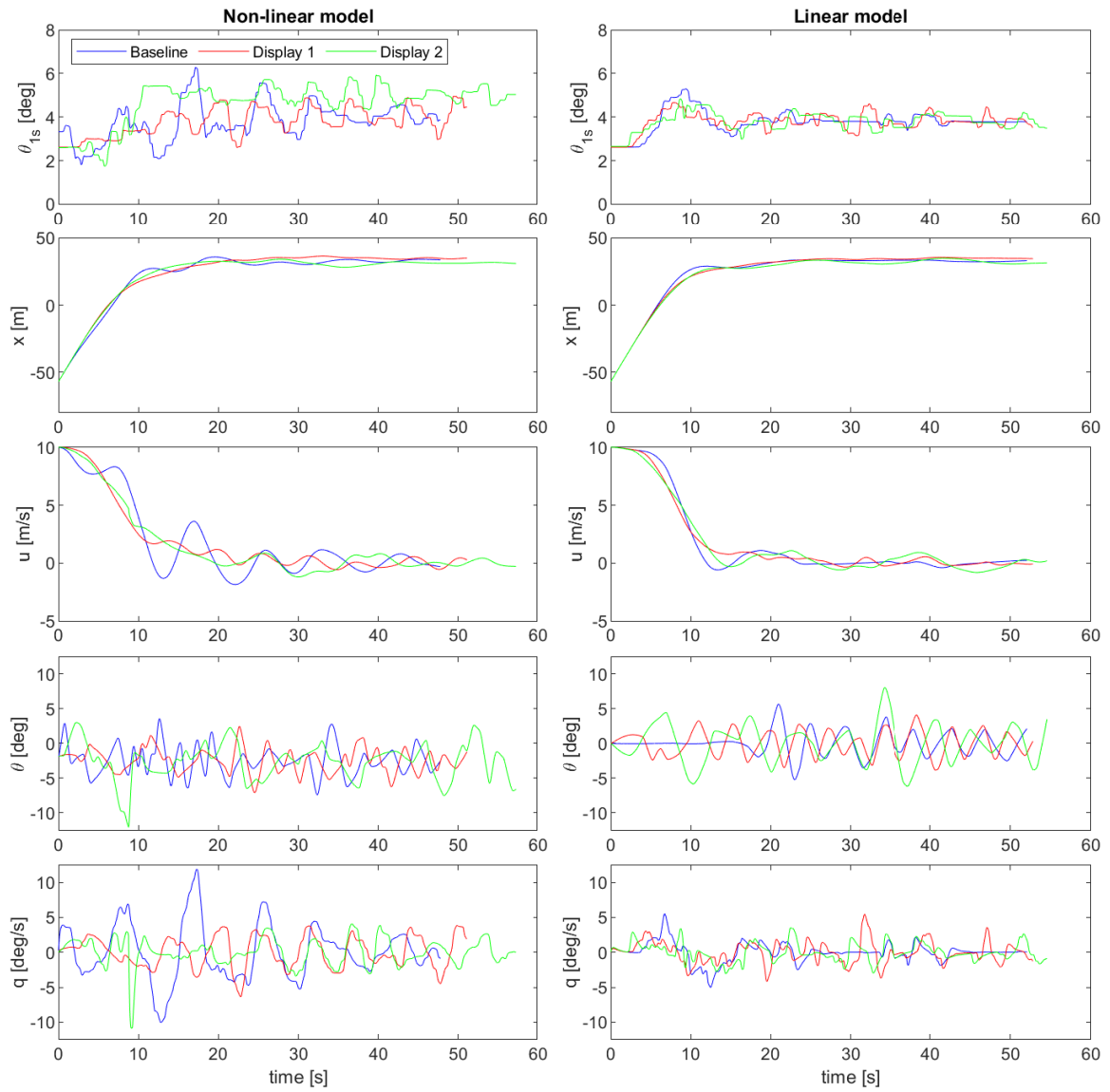


Figure E-2: Time trajectories of surge motion variables, pilot 1, run 2

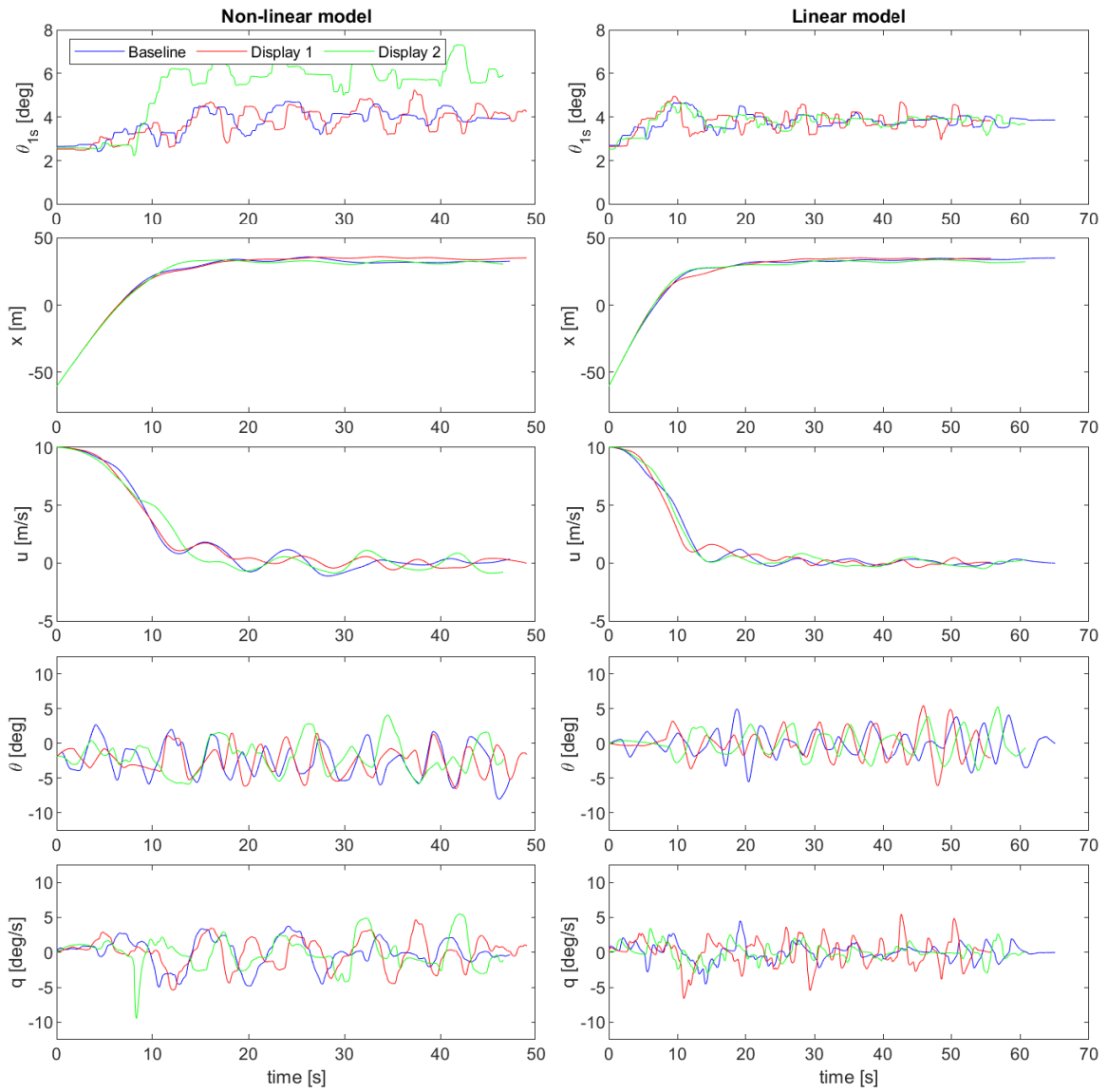


Figure E-3: Time trajectories of surge motion variables, pilot 1, run 3

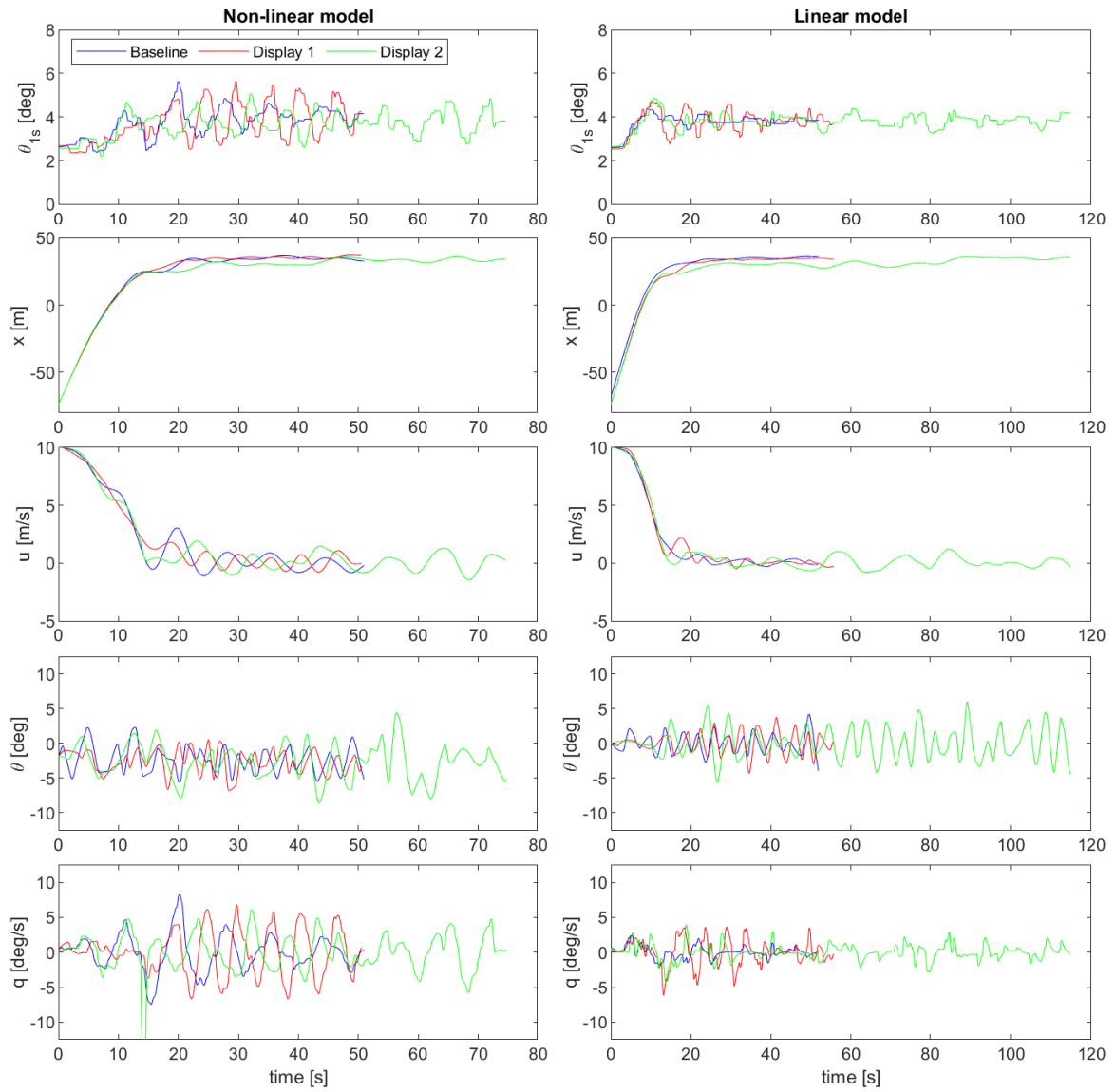
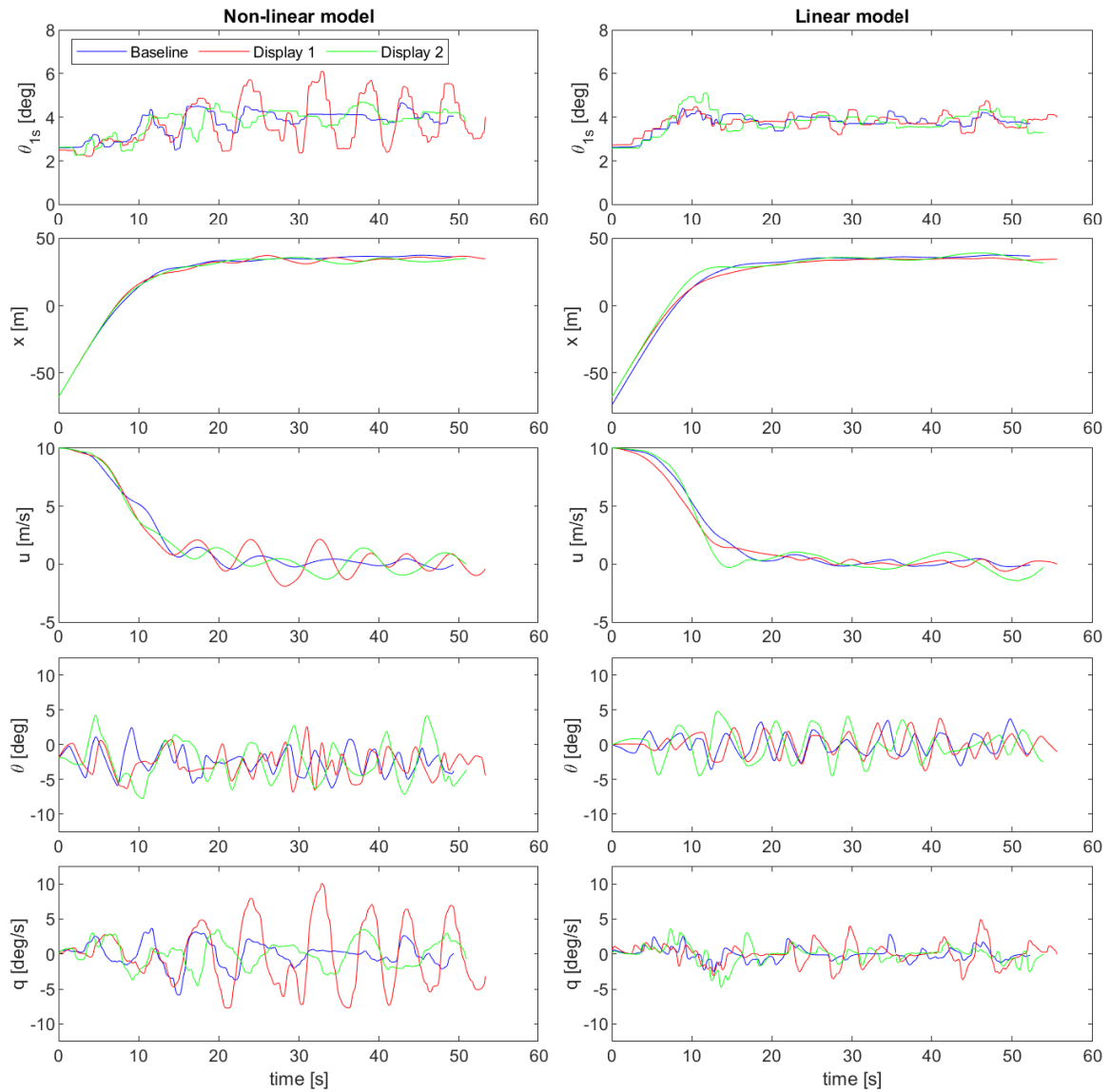


Figure E-4: Time trajectories of surge motion variables, pilot 1, run 4



**Figure E-5:** Time trajectories of surge motion variables, pilot 1, run 5

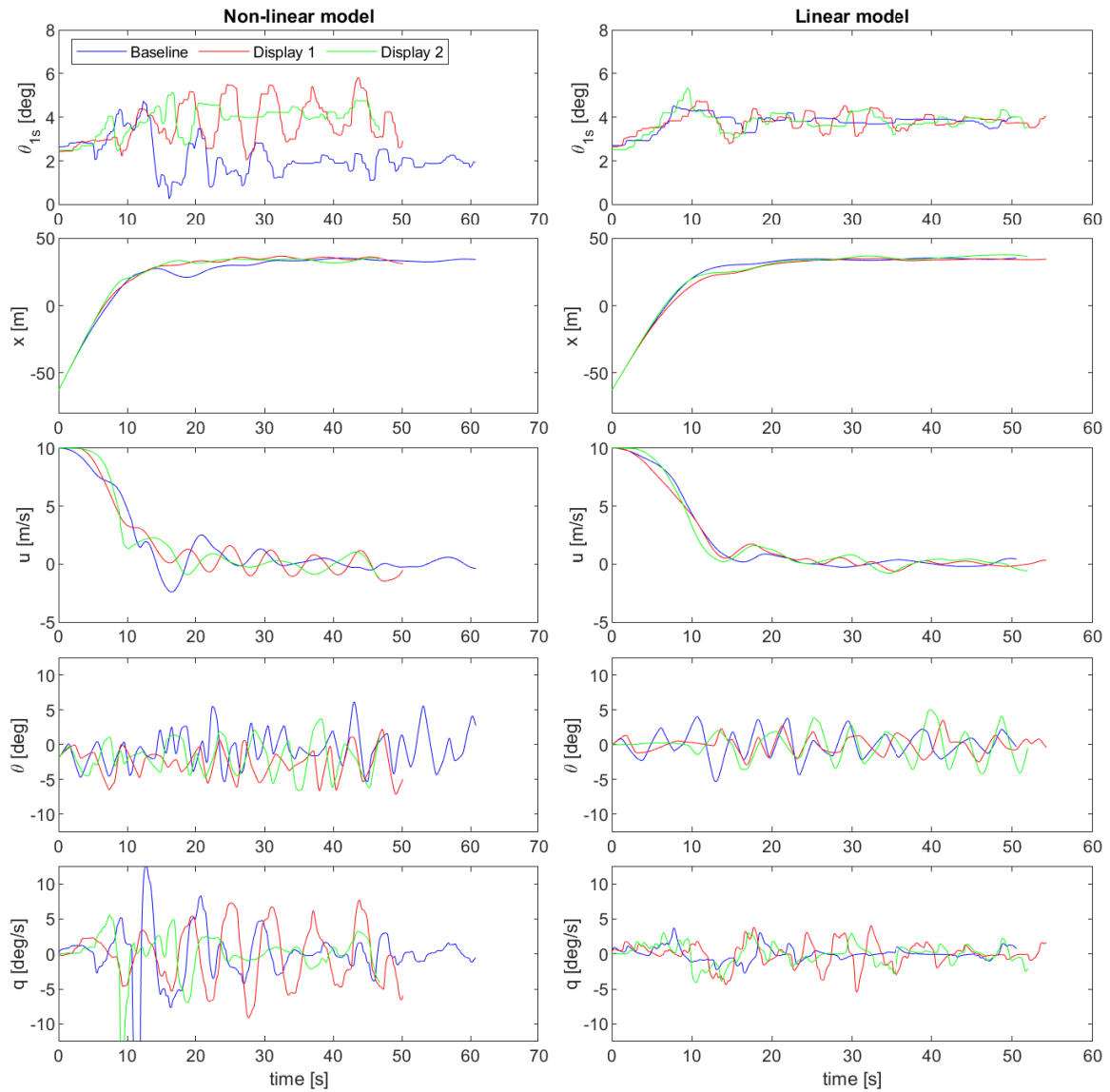


Figure E-6: Time trajectories of surge motion variables, pilot 1, run 6

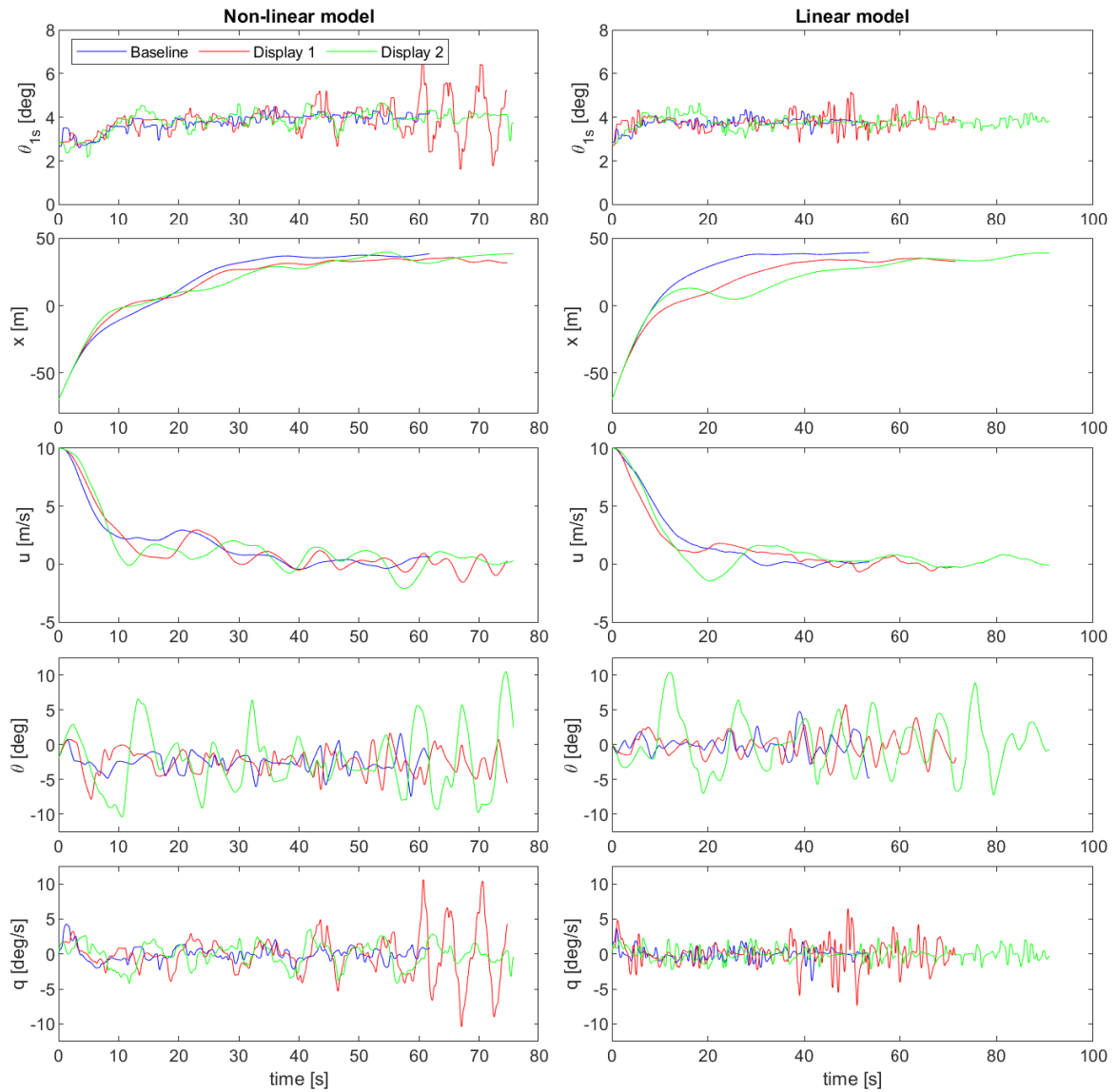


Figure E-7: Time trajectories of surge motion variables, pilot 2, run 1

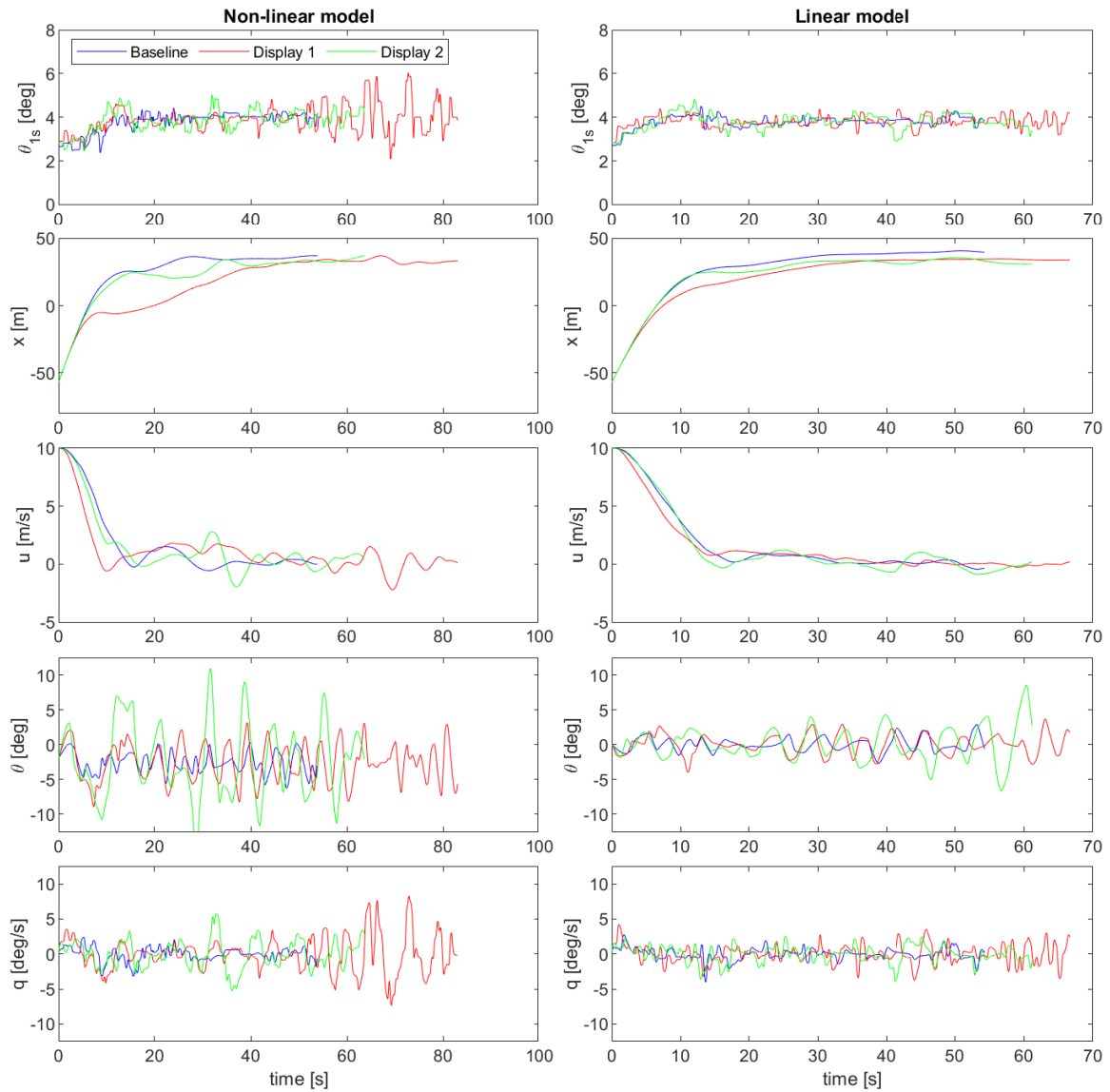


Figure E-8: Time trajectories of surge motion variables, pilot 2, run 2

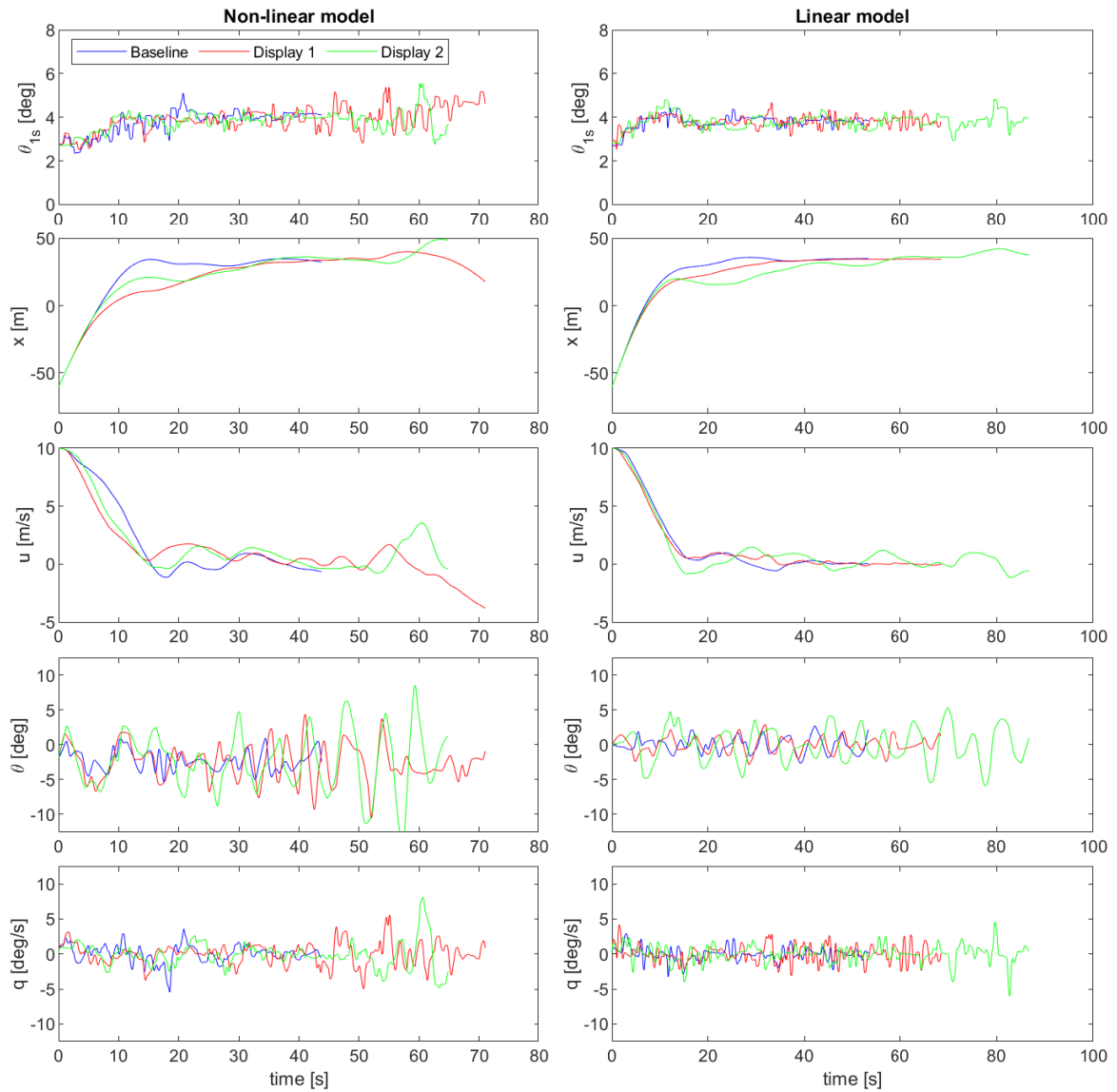


Figure E-9: Time trajectories of surge motion variables, pilot 2, run 3

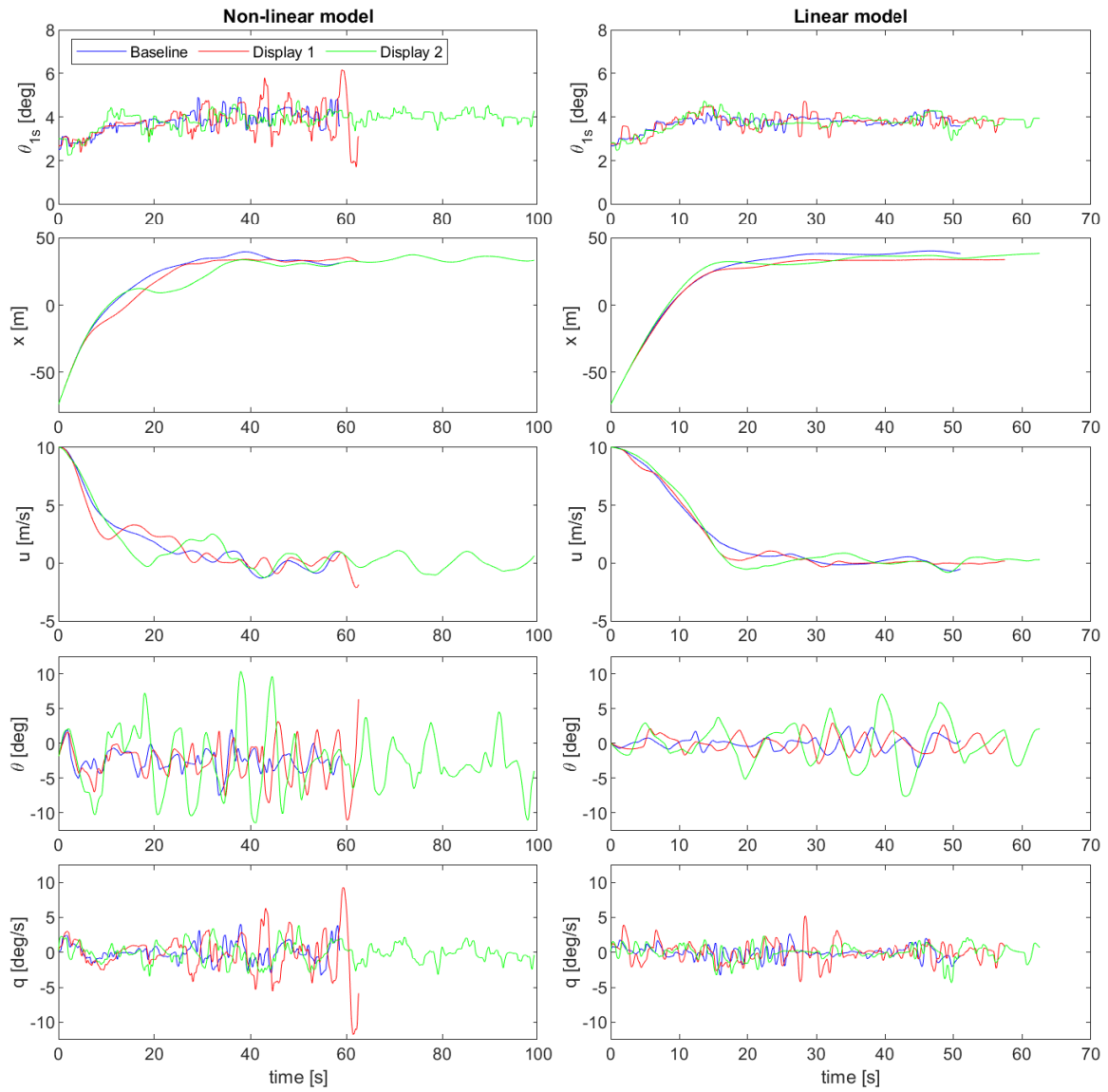


Figure E-10: Time trajectories of surge motion variables, pilot 2, run 4

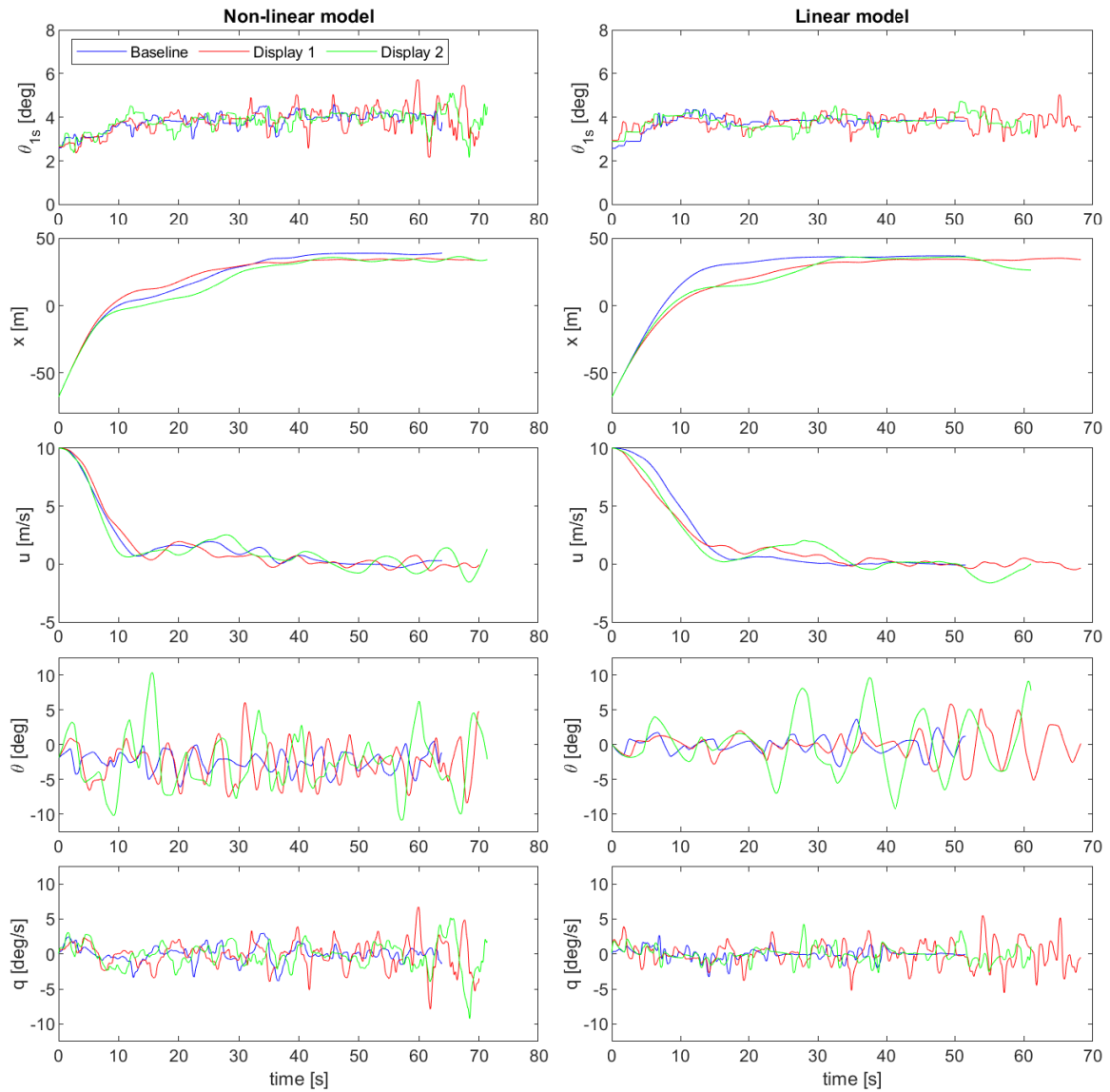


Figure E-11: Time trajectories of surge motion variables, pilot 2, run 5

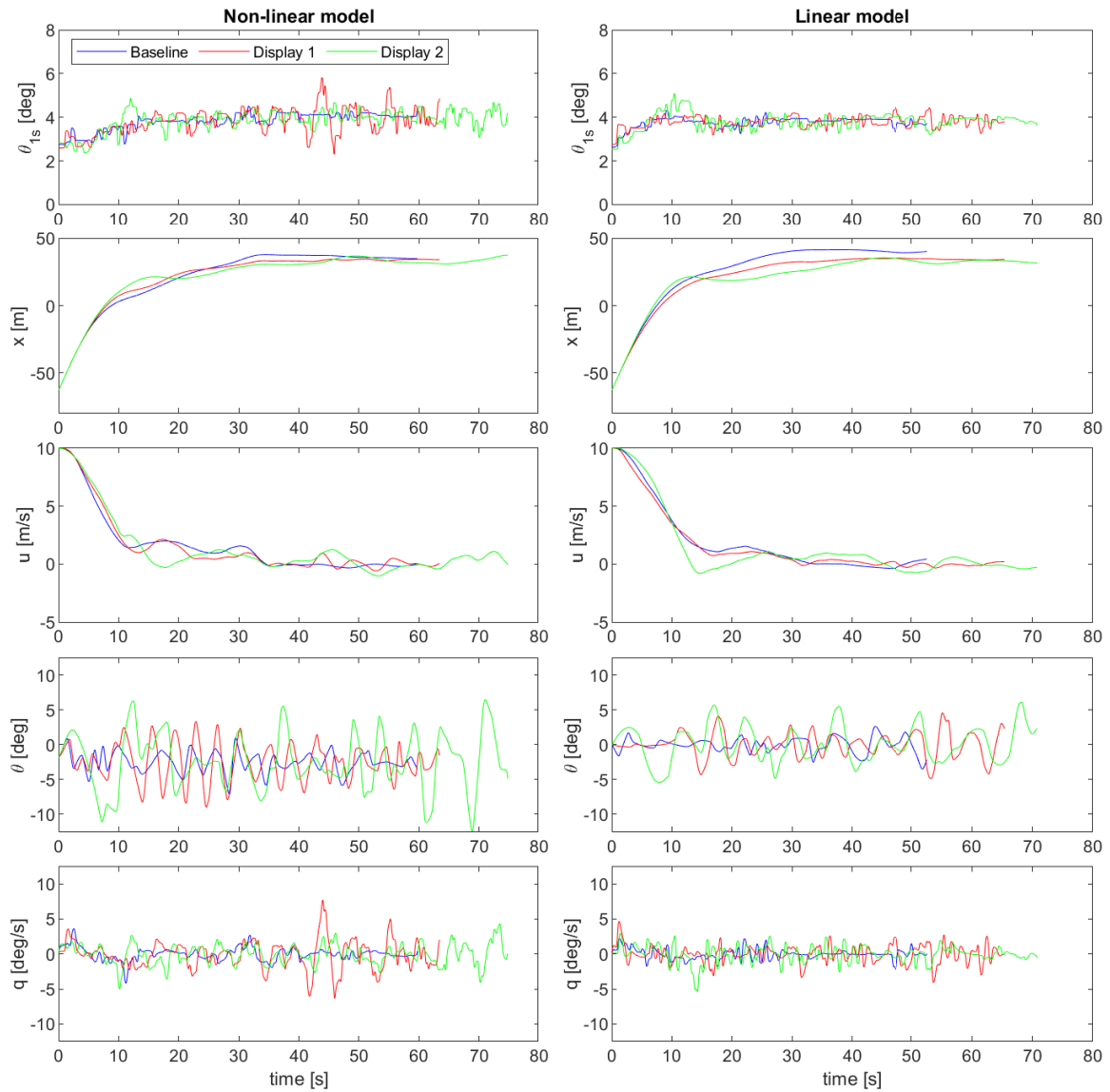
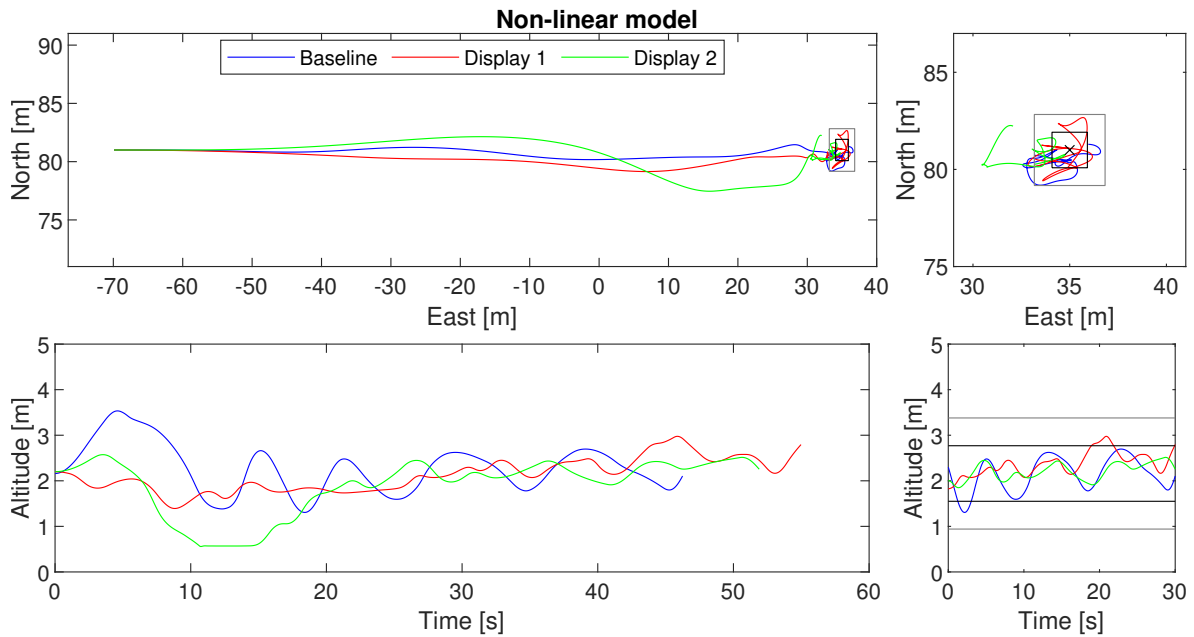


Figure E-12: Time trajectories of surge motion variables, pilot 2, run 6

## E-2 Ground tracks

The ground tracks for all runs and conditions are provided in this section. The first subsection covers all conditions with the non-linear model (Figures E-13 to E-24); the second one contains all conditions with the linear model (Figures E-25 to E-36). The run that was considered an outlier, as described in the paper, is shown in Figure E-21 (Display 1).

### E-2-1 Non-linear model



**Figure E-13:** Position trajectories during full run (left) and during hover (right), pilot 1, run 1

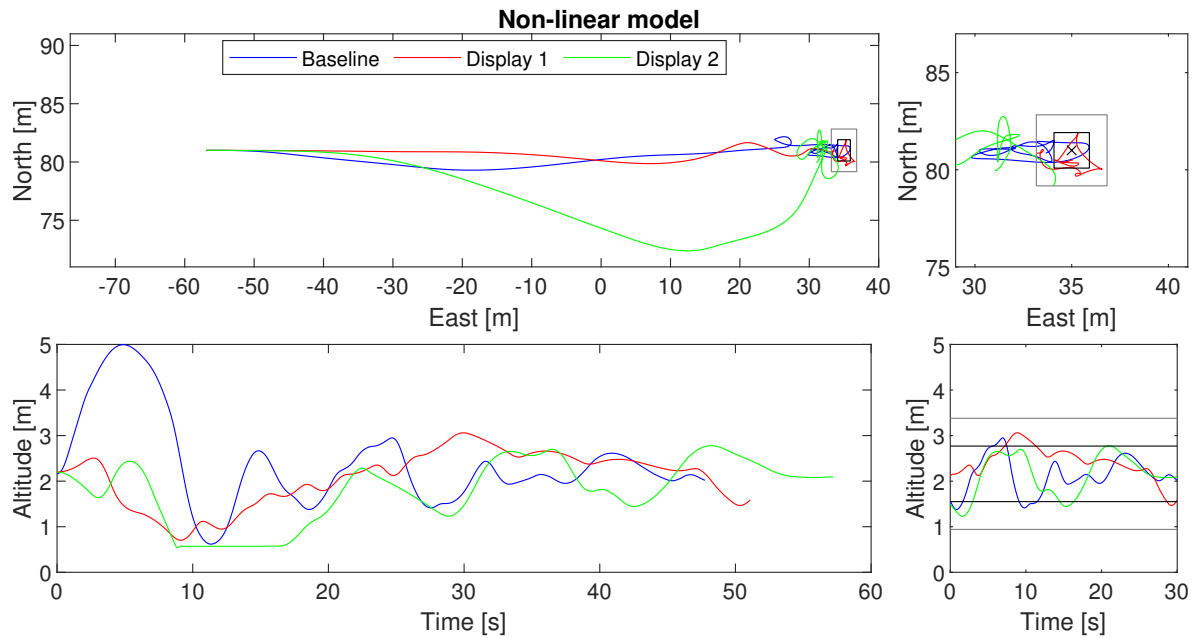


Figure E-14: Position trajectories during full run (left) and during hover (right), pilot 1, run 2

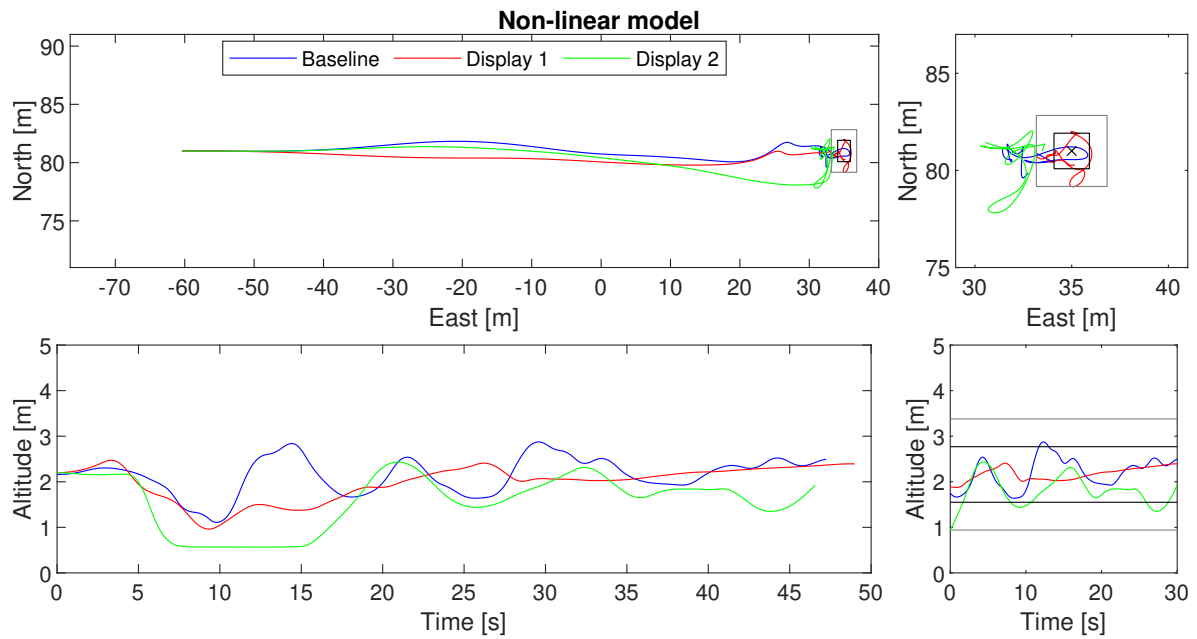


Figure E-15: Position trajectories during full run (left) and during hover (right), pilot 1, run 3

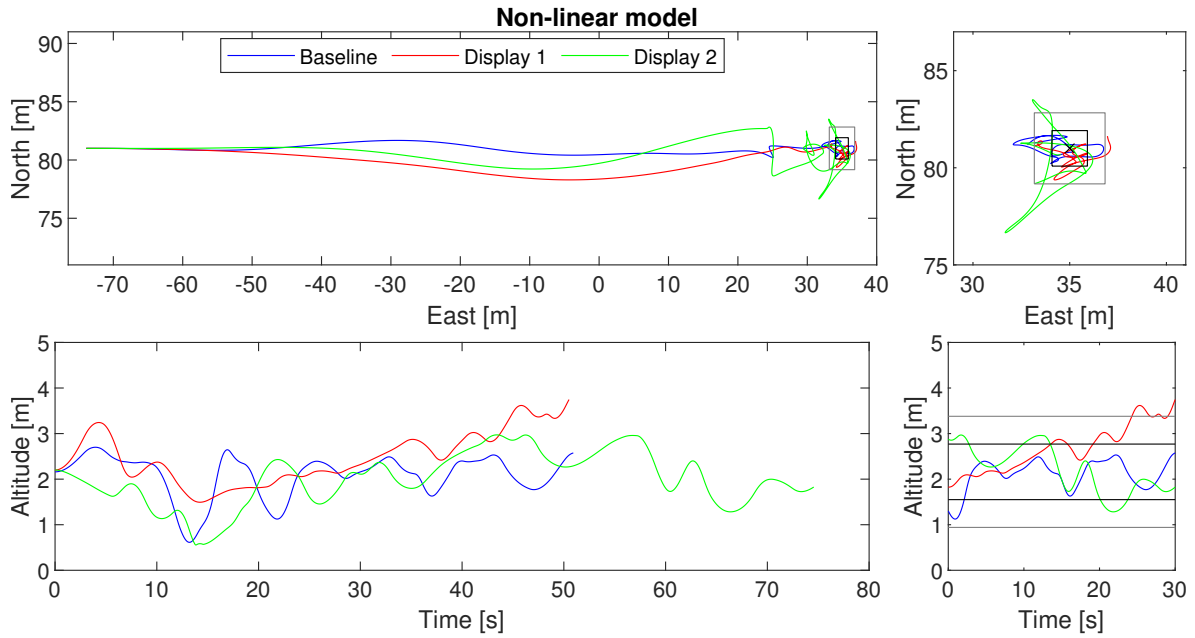


Figure E-16: Position trajectories during full run (left) and during hover (right), pilot 1, run 4

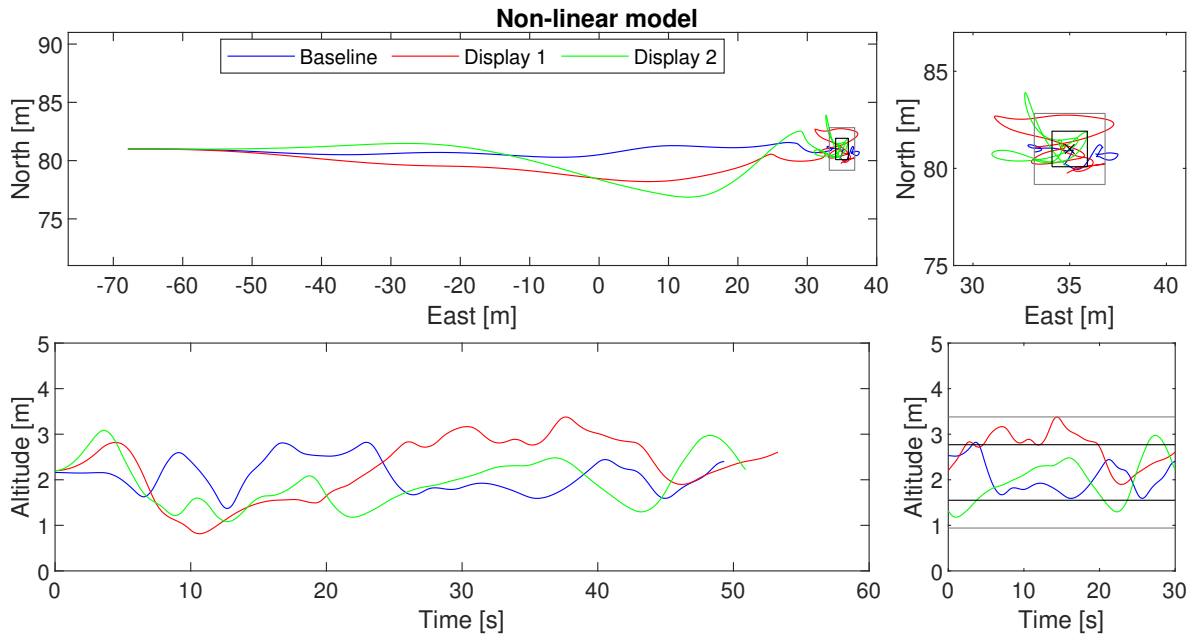


Figure E-17: Position trajectories during full run (left) and during hover (right), pilot 1, run 5

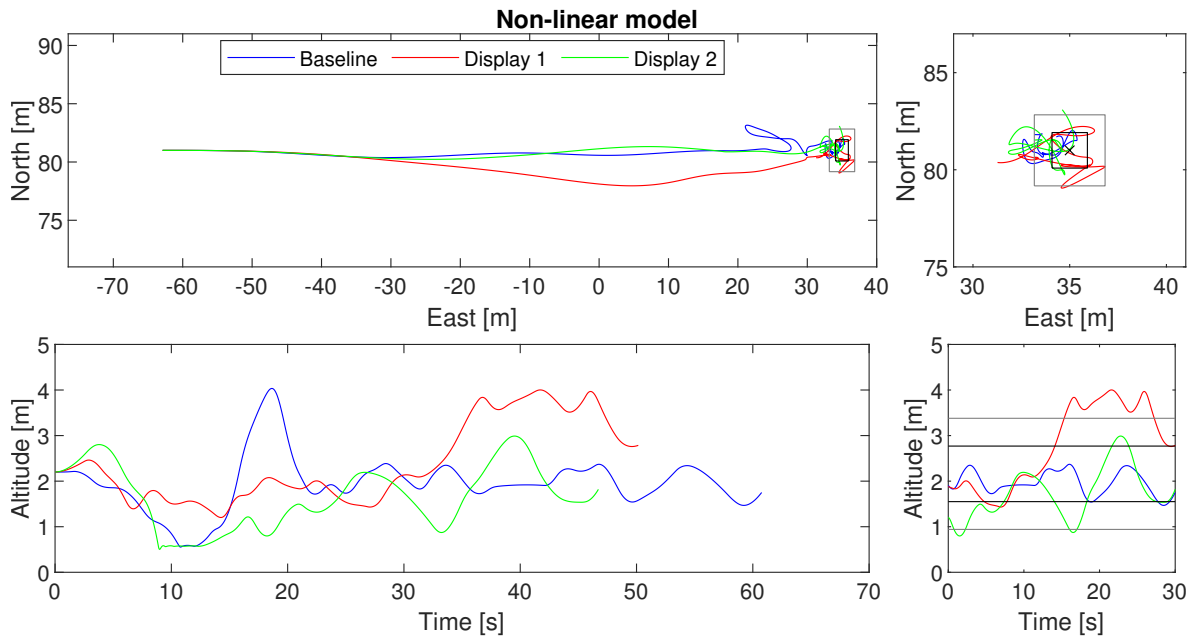


Figure E-18: Position trajectories during full run (left) and during hover (right), pilot 1, run 6

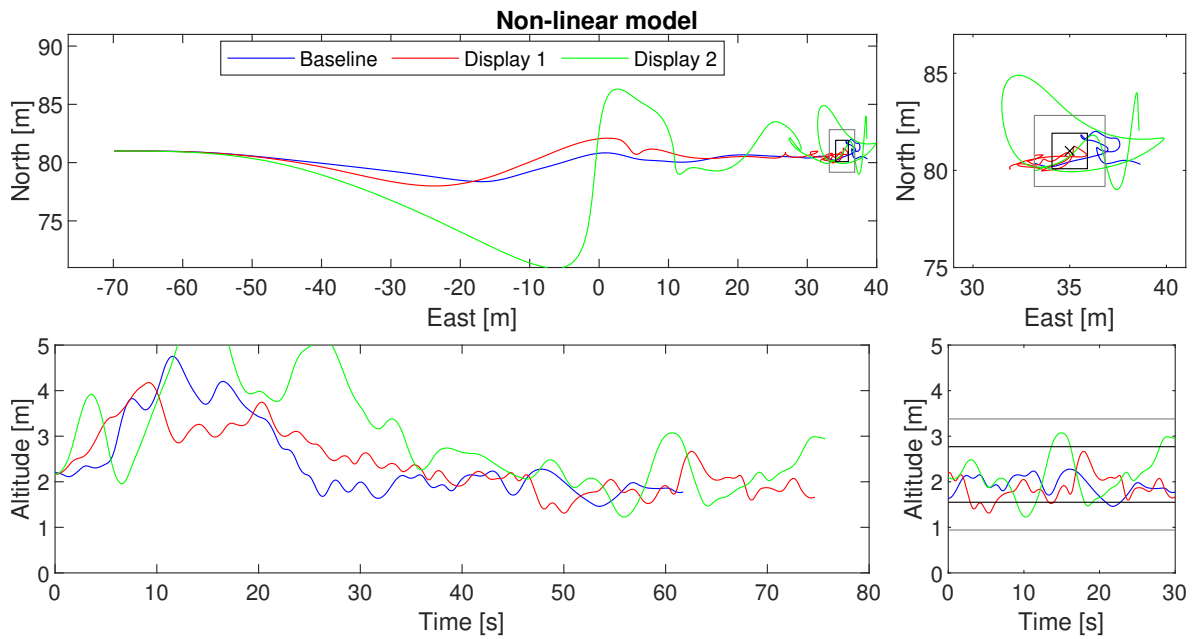


Figure E-19: Position trajectories during full run (left) and during hover (right), pilot 2, run 1

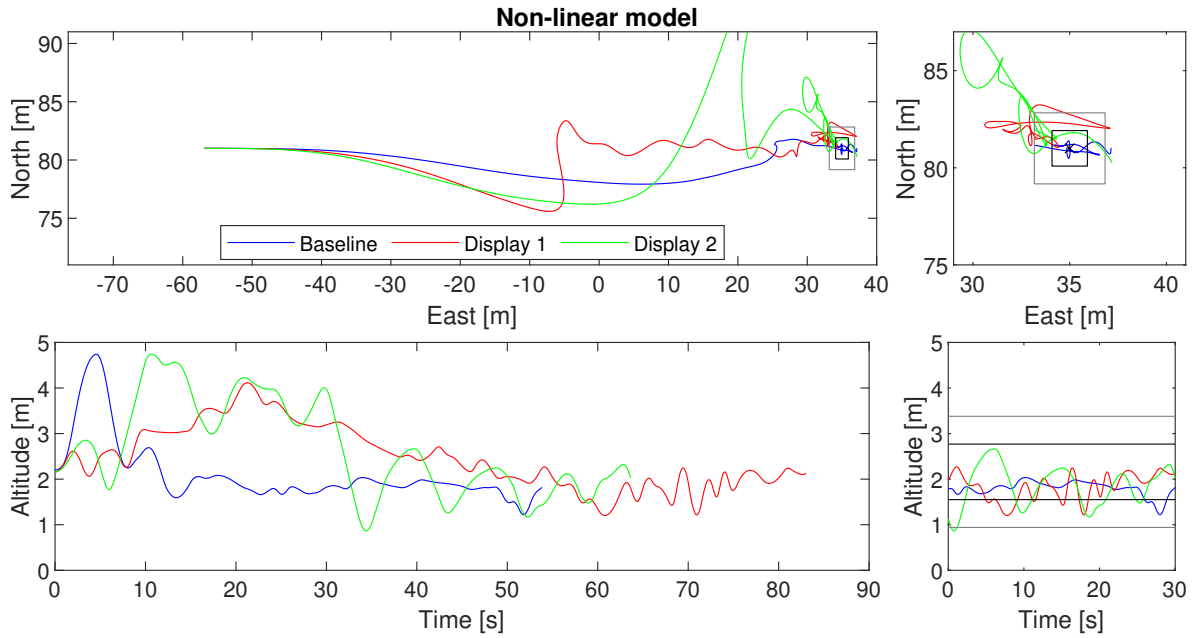


Figure E-20: Position trajectories during full run (left) and during hover (right), pilot 2, run 2

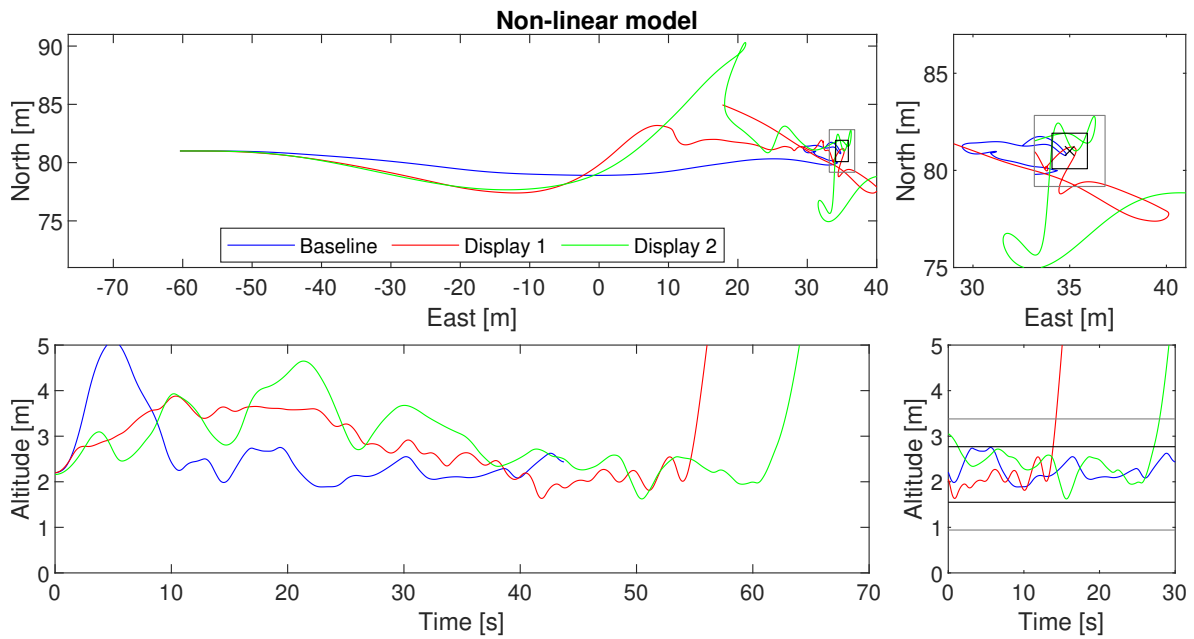


Figure E-21: Position trajectories during full run (left) and during hover (right), pilot 2, run 3

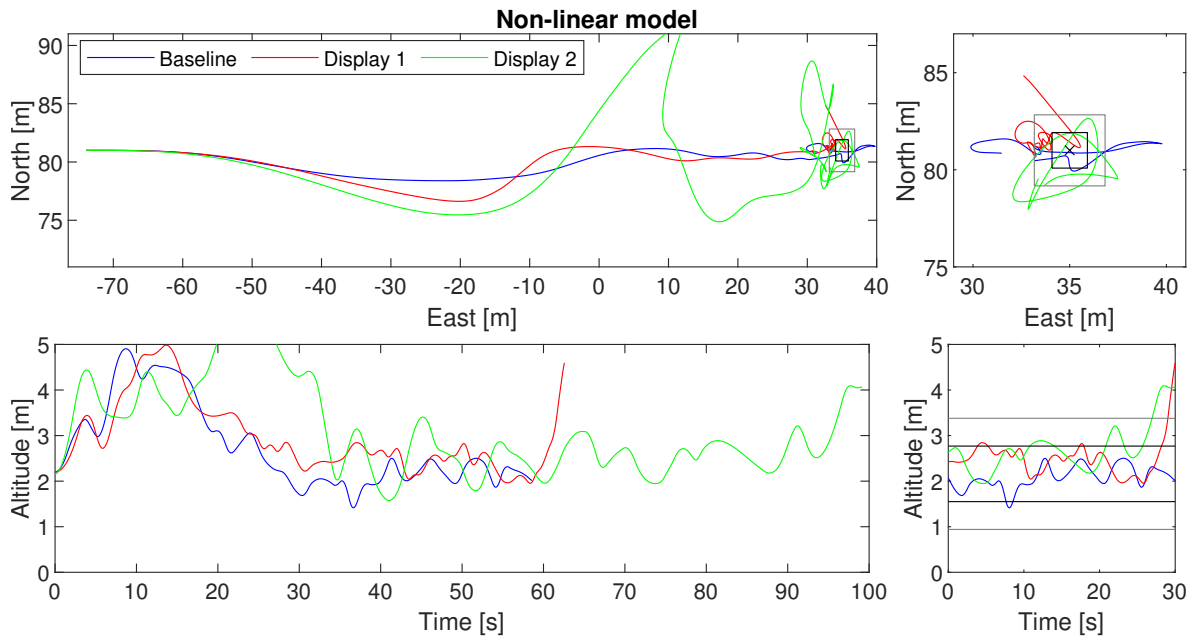


Figure E-22: Position trajectories during full run (left) and during hover (right), pilot 2, run 4

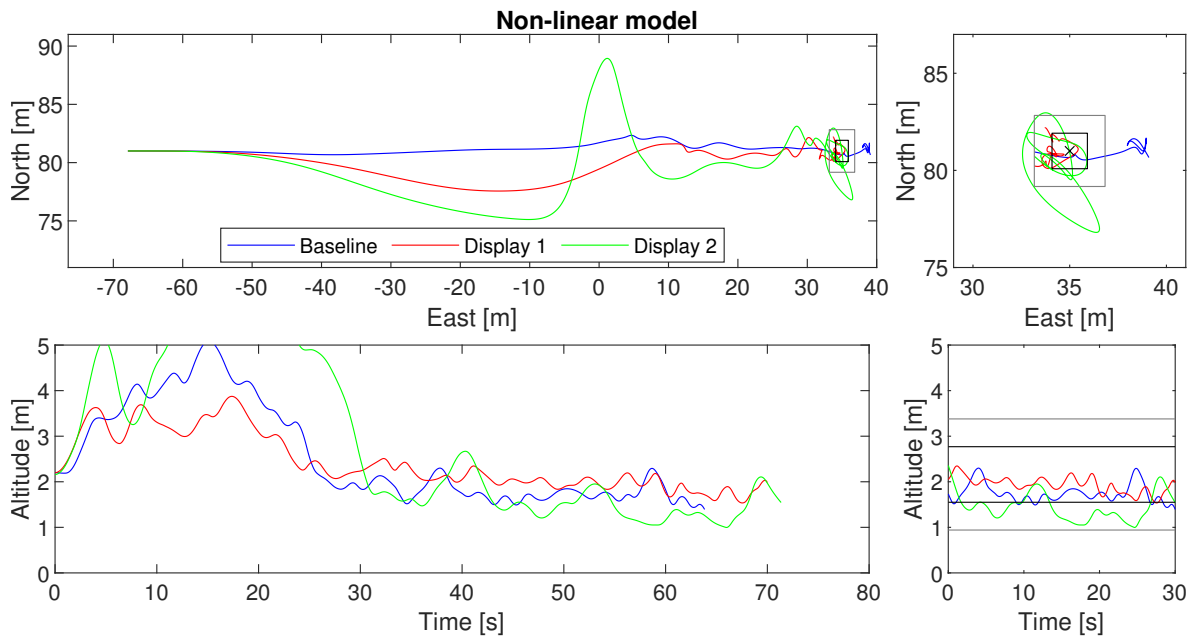
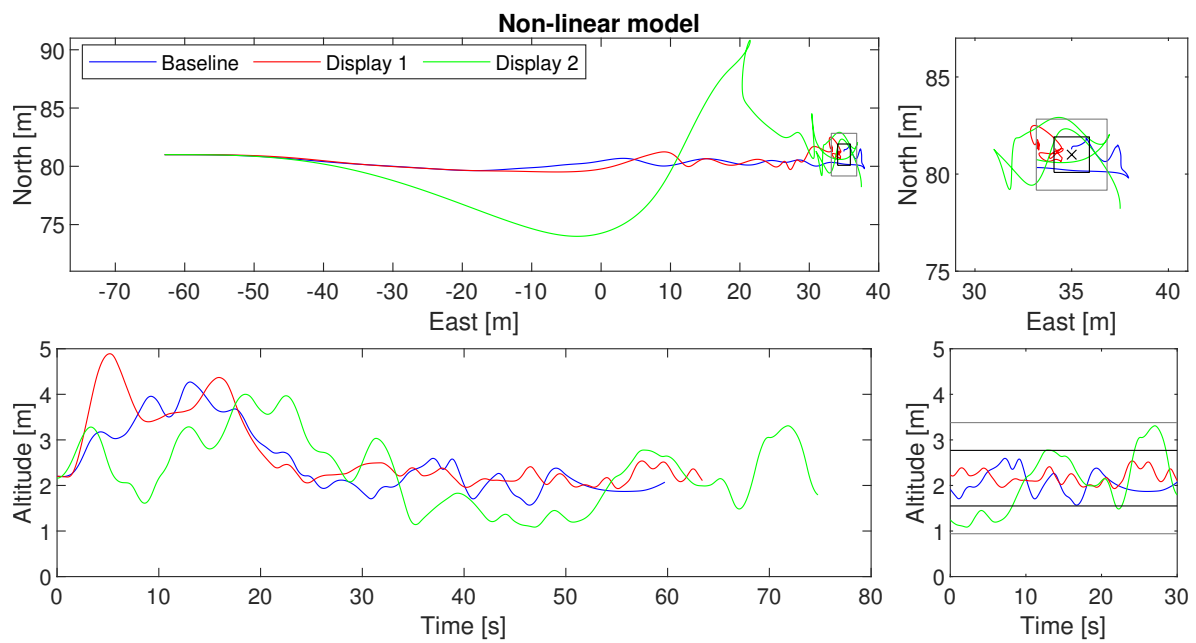


Figure E-23: Position trajectories during full run (left) and during hover (right), pilot 2, run 5



**Figure E-24:** Position trajectories during full run (left) and during hover (right), pilot 2, run 6

E-2-2 Linear model

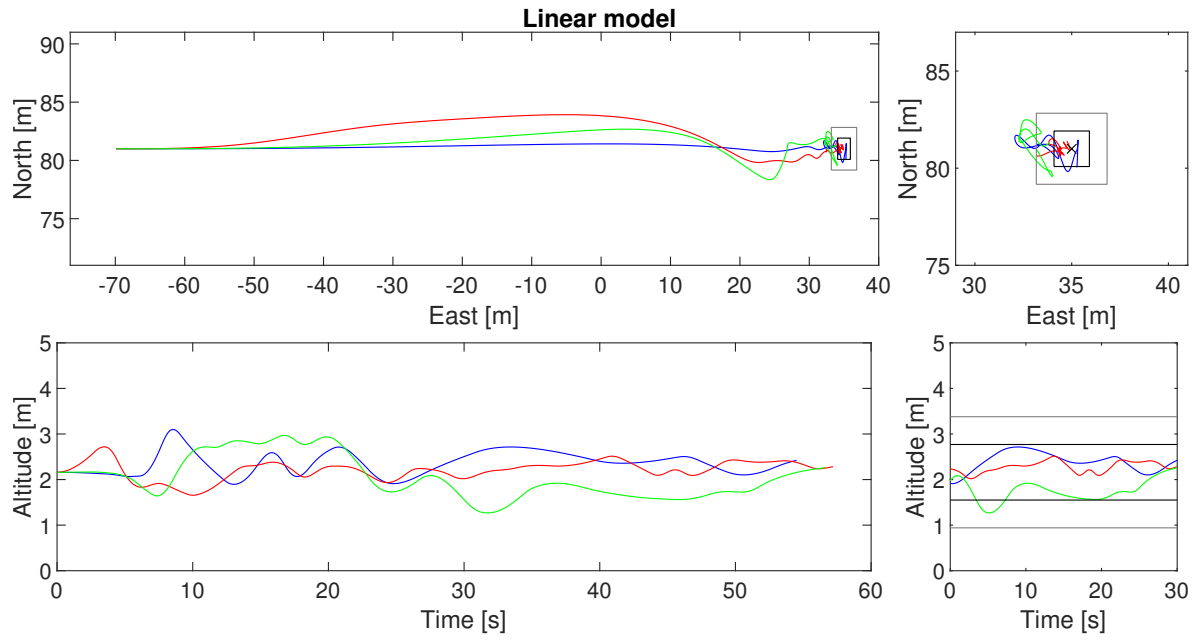


Figure E-25: Position trajectories during full run (left) and during hover (right), pilot 1, run 1

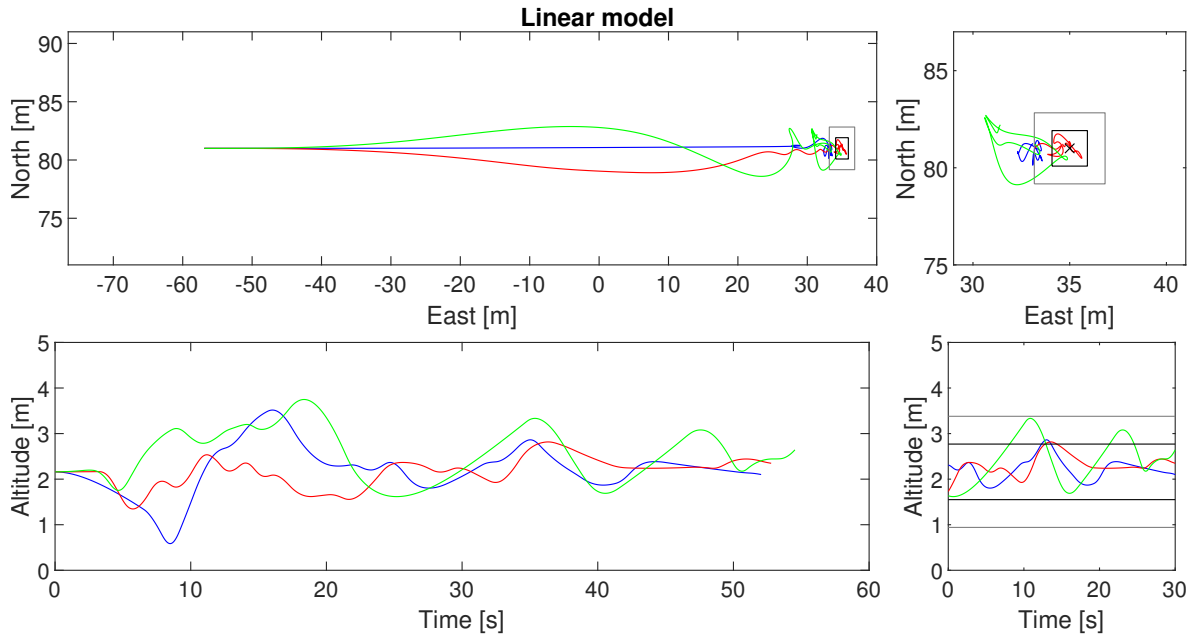


Figure E-26: Position trajectories during full run (left) and during hover (right), pilot 1, run 2

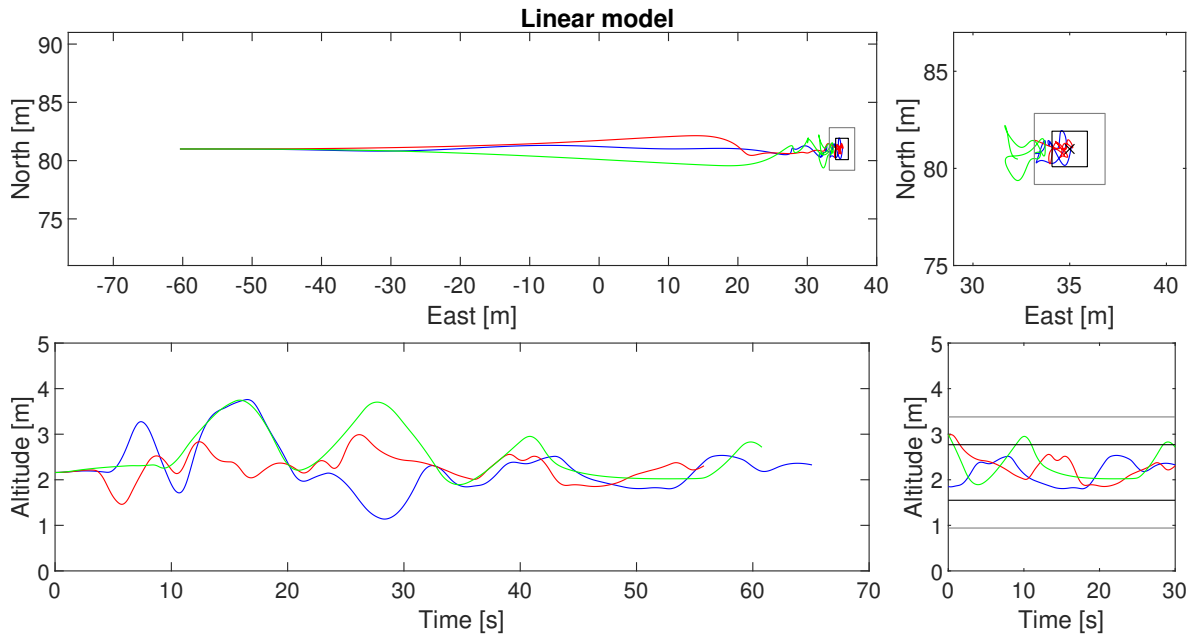


Figure E-27: Position trajectories during full run (left) and during hover (right), pilot 1, run 3

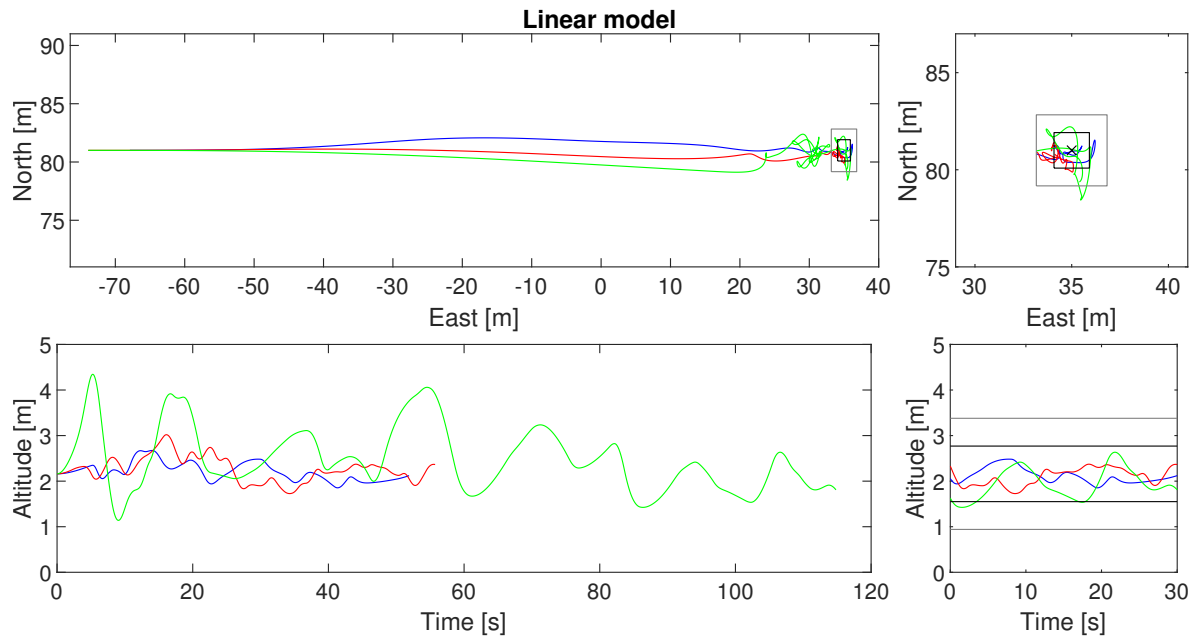


Figure E-28: Position trajectories during full run (left) and during hover (right), pilot 1, run 4

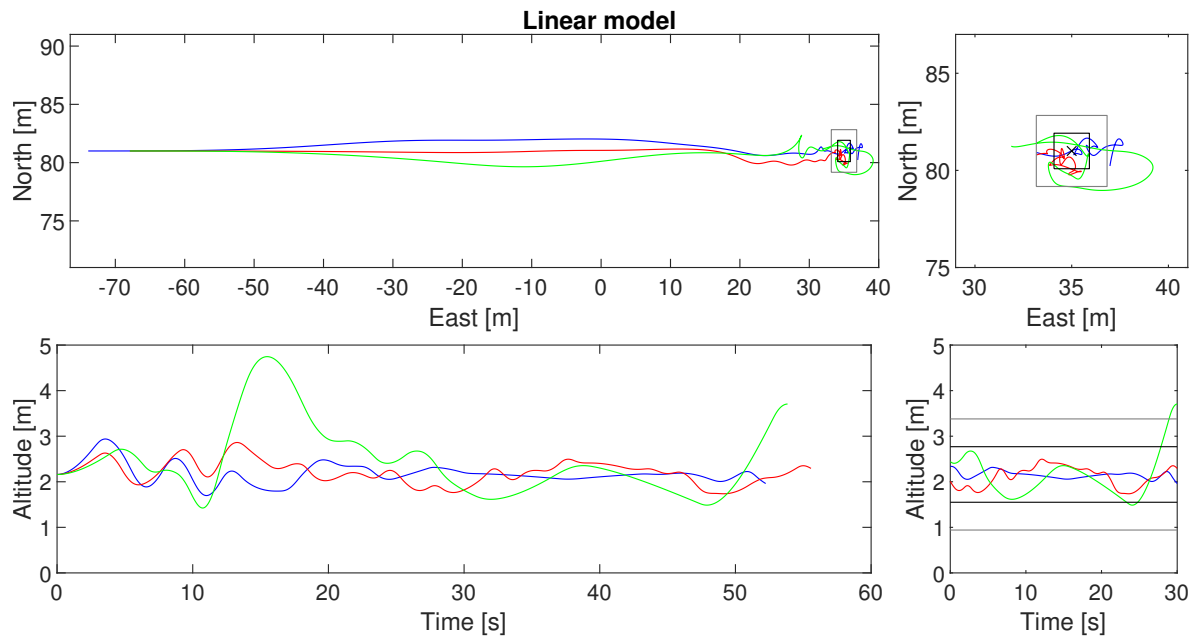


Figure E-29: Position trajectories during full run (left) and during hover (right), pilot 1, run 5

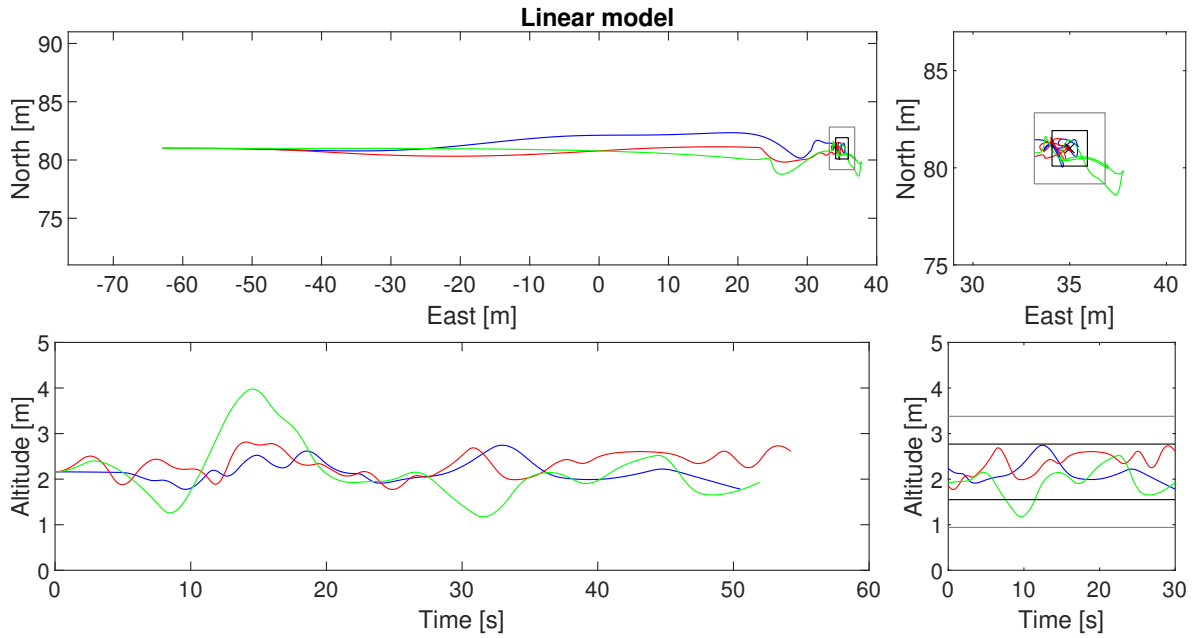


Figure E-30: Position trajectories during full run (left) and during hover (right), pilot 1, run 6

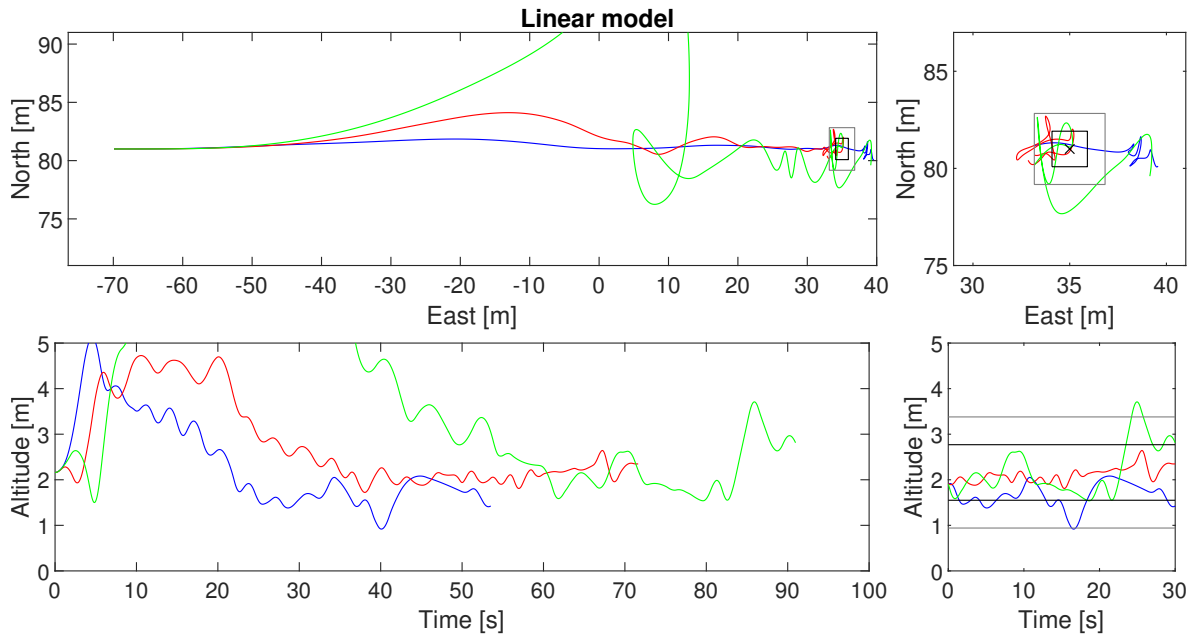


Figure E-31: Position trajectories during full run (left) and during hover (right), pilot 2, run 1

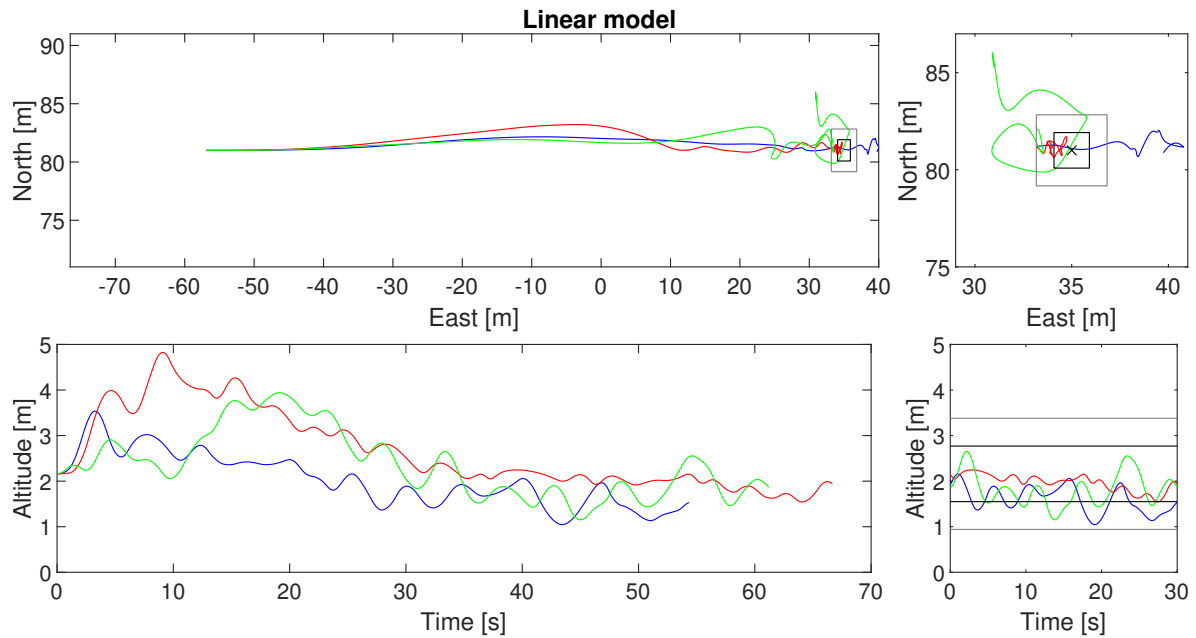


Figure E-32: Position trajectories during full run (left) and during hover (right), pilot 2, run 2

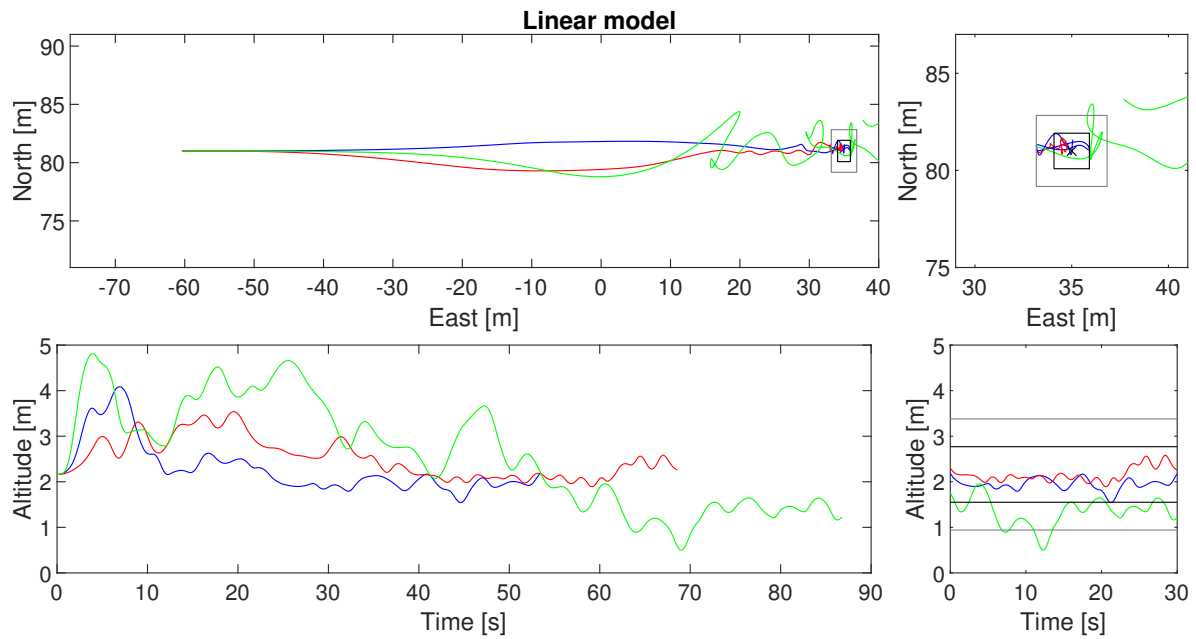


Figure E-33: Position trajectories during full run (left) and during hover (right), pilot 2, run 3

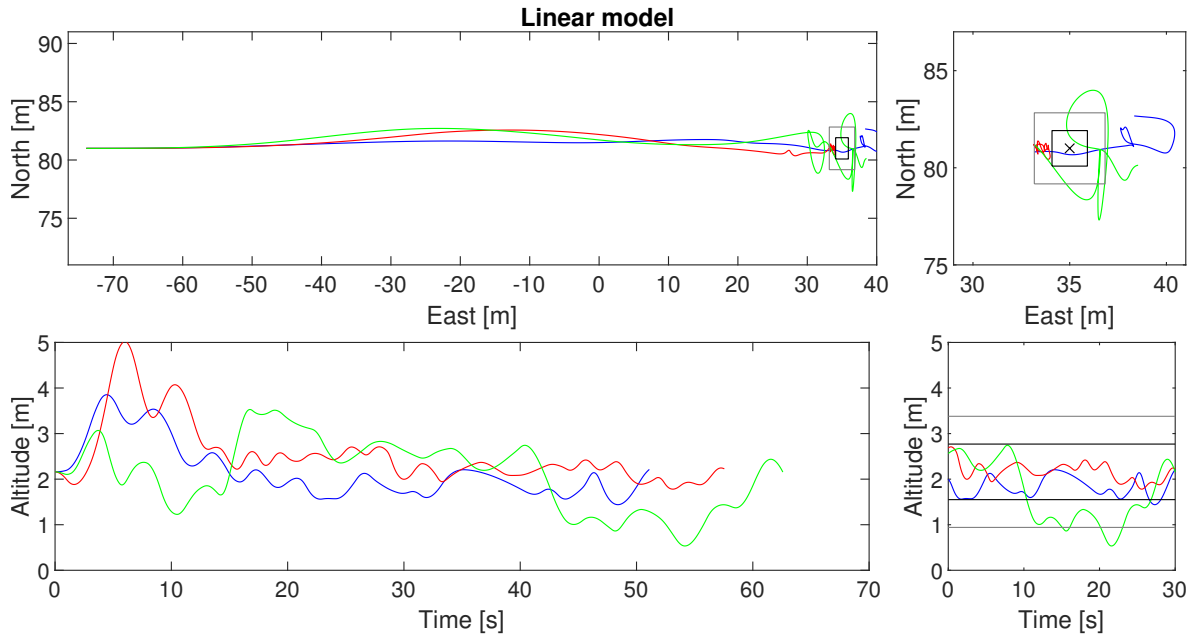


Figure E-34: Position trajectories during full run (left) and during hover (right), pilot 2, run 4

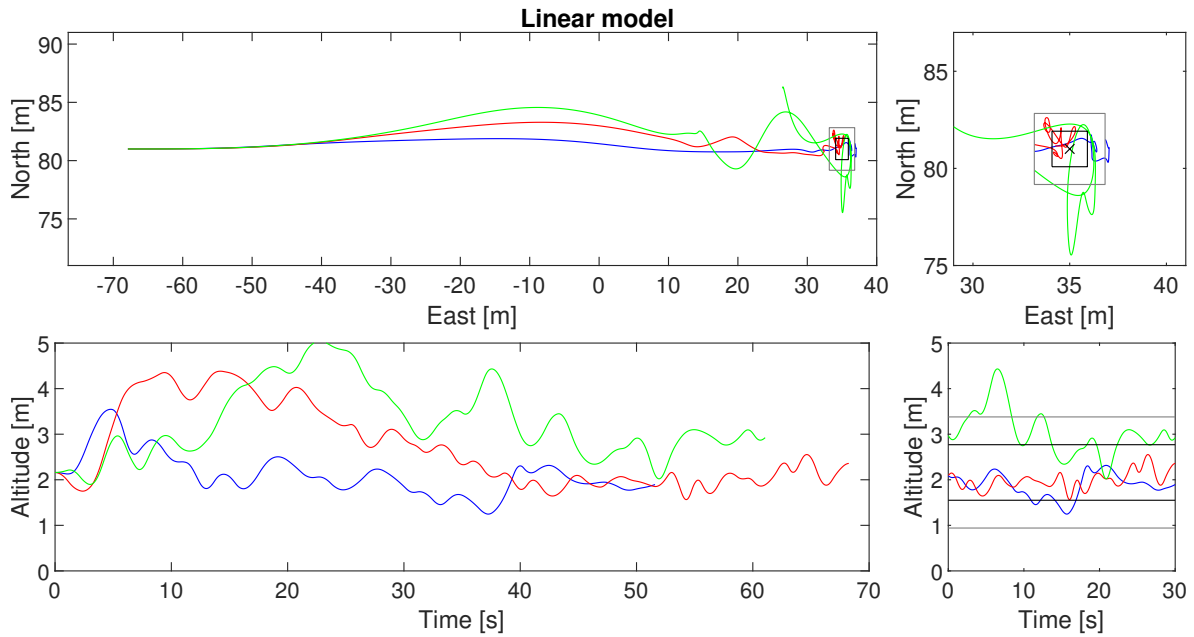
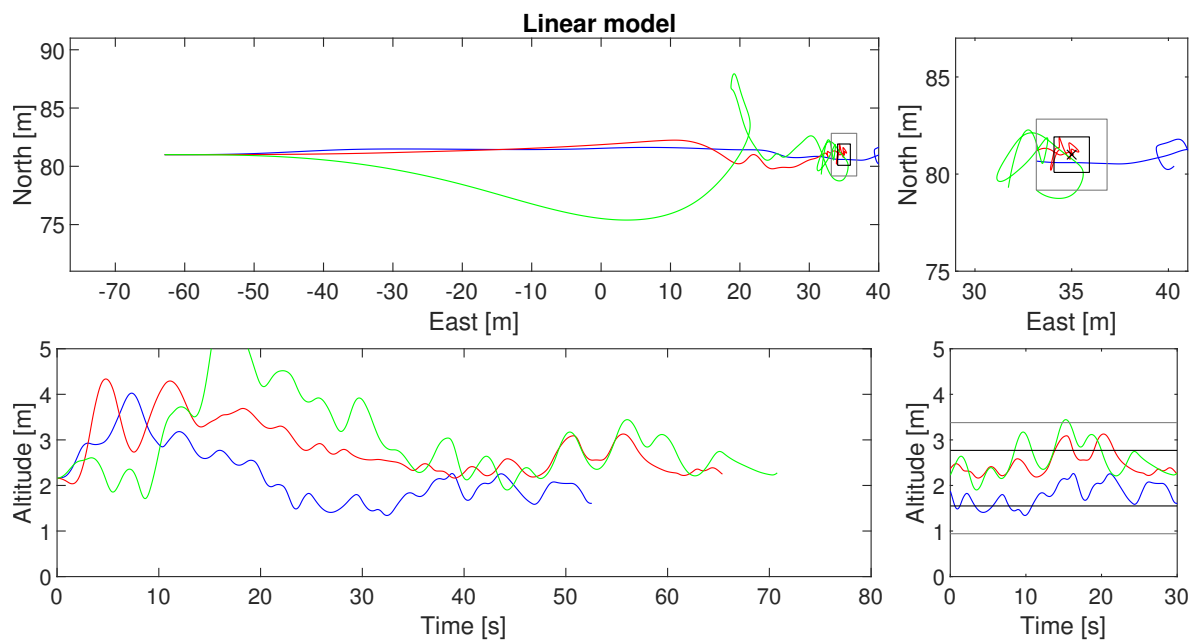


Figure E-35: Position trajectories during full run (left) and during hover (right), pilot 2, run 5



**Figure E-36:** Position trajectories during full run (left) and during hover (right), pilot 2, run 6

### E-3 Boxplots

This appendix provides additional boxplots that were omitted from the paper. Figure E-37 shows boxplots for the velocities in all three axes. The attitudes and attitude rates are shown in Figure E-38 and Figure E-39, respectively.

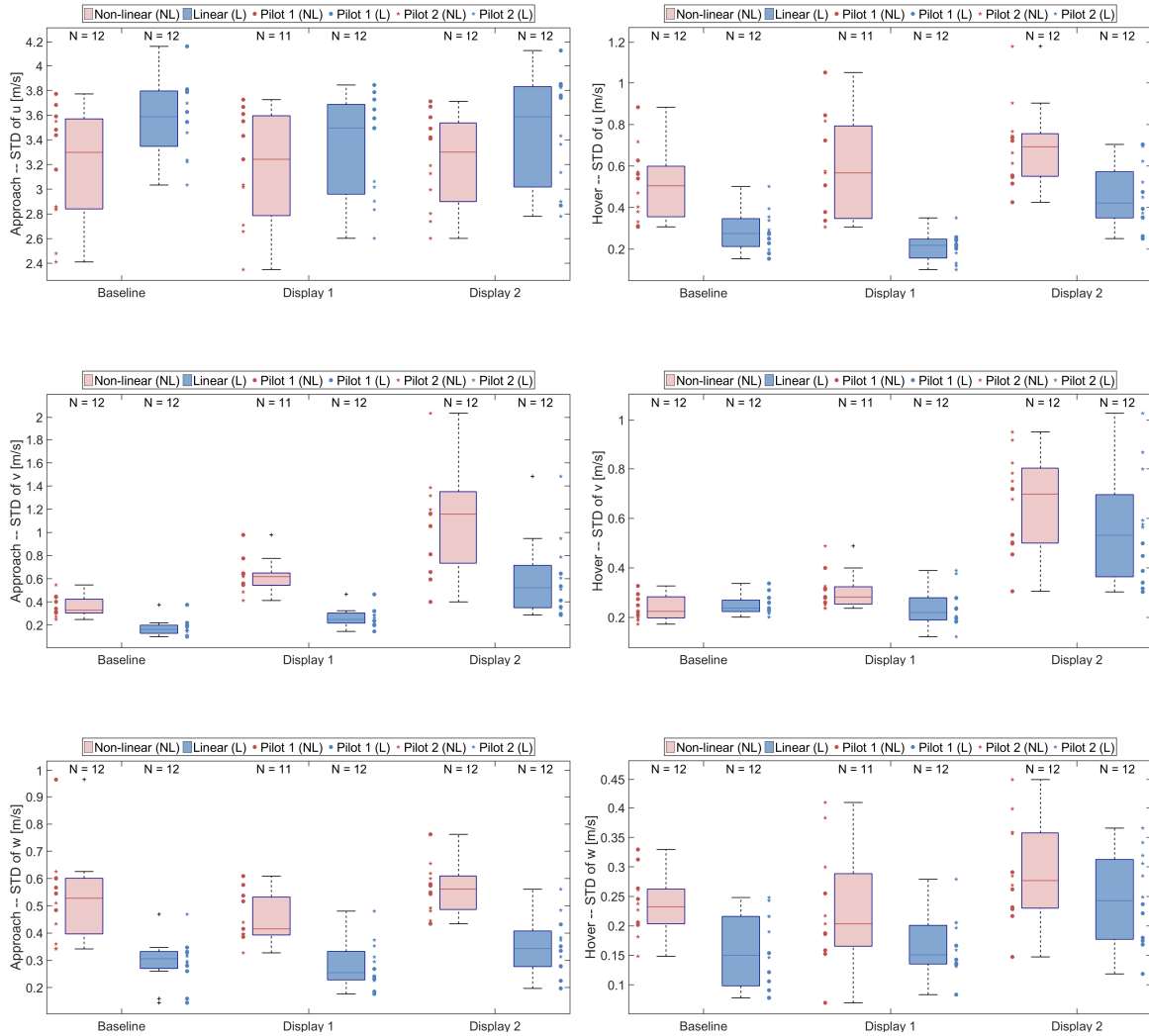


Figure E-37: Boxplots of velocities during approach (left) and hover (right)

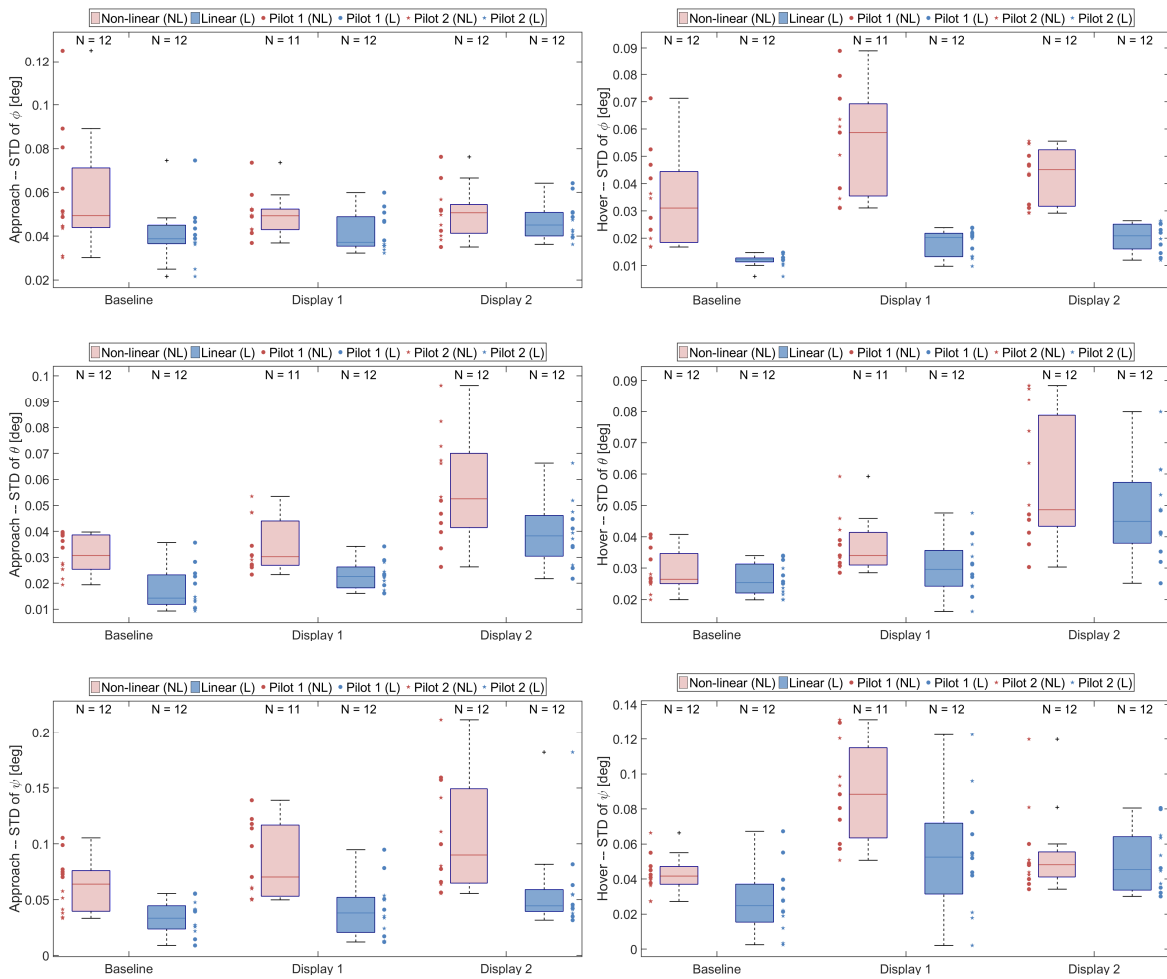


Figure E-38: Boxplots of attitudes during approach (left) and hover (right)

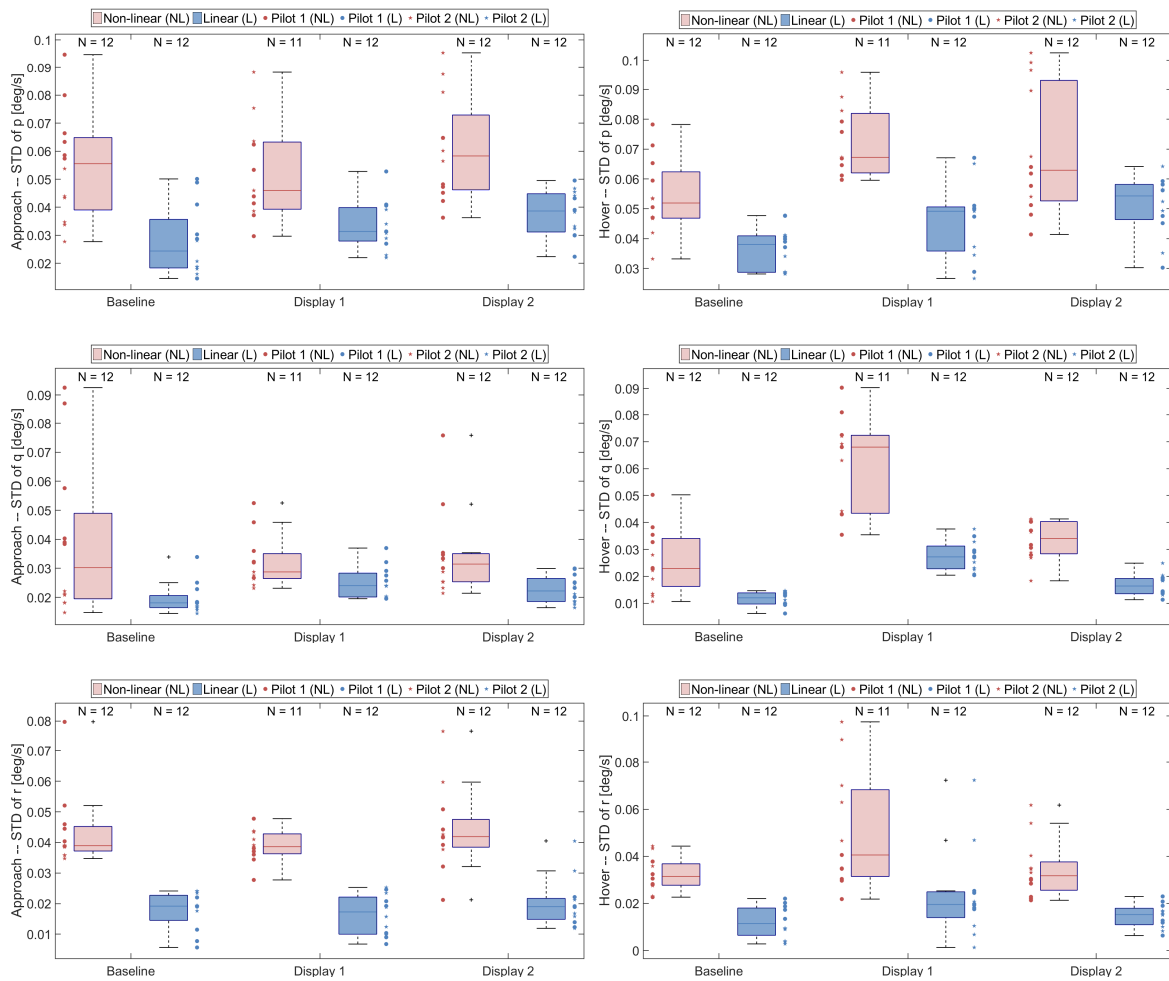


Figure E-39: Boxplots of rotational velocities during approach (left) and hover (right)